Ferdowsi University of Mashhad

Iranian Food Science and Technology Research Journal

Vol.12 No.6

2017

ISSN:1735-4161

Contents

نشریه علمی- پژوهشی پژوهشهای علوم و صنایع غذایی ایران جلد ۱۲ شماره ۶ سال ۱۳۹۶

Iranian Food Science and Technology Research Journal Vol.12 No.6 2017

Iranian Food Science and Technology Research Journal

Vol. 12 No. 6 2017

Published by: Department of Food Science and Technology, College of Agriculture, Ferdowsi University of Mashhad, Iran.

Executive Manager: Poorazarang, H.

Editor-in-Chief: Razavi, Seyed M. A.

Executive Director: Taghizadeh, M.

Printed by: Ferdowsi University of Mashhad Press, Iran.

Address: The Iranian Food Science & Technology Research Journal, Scientific Publication Office, Food Science and Technology Department, Agriculture Faculty, Ferdowsi University of Mashhad, Iran.

P.O.BOX: 91775- 1163

Phone: (98)511-8795618-20(321)

Fax: (98)511-8787430

E-Mail: ifstrj@um.ac.ir

Web Site: http://jm.um.ac.ir/index.php/food_tech/index

This journal is indexed in ISC, SID, and MAGIRAN.

Contents

Iranian Food Science and Technology Research Journal
Vol. 12, No. 6, Feb. Mrch. 2017, p. 716-729

نشریه پژوهشهای علوم و صنایع غذایی ایران
جلد 12، شماره 6، بهمن - اسفند 1395، ص. 729-716

Thin-layer convective air drying of lemon verbena (*lippia citriodora*) leaves

E. Naghavi[1*], S. Rigi[2]

Received: 2016.12.15
Accepted: 2017.04.22

Abstract

Lemon verbena leave is a flavoring food additive as well as a good source of valuable compounds such as essential oils, flavonoids and phenolic acids. However, similar to many other aromatic plants, lemon verbena leave is perishable due to its high moisture content. The aim of this work was to study the effect of air temperature (45, 55, and 65°C) on the quality attributes of lemon verbena leaves during hot-air drying (HAD). The drying kinetics were also modeled. The results showed that higher drying temperature led to a significant decrease ($p<0.05$) in the rehydration ratio due to a change in the structural features of the dried leaves. The essential oil content of dried samples was also significantly different ($p<0.05$) from that of the fresh leaves due to high loss of volatile components and ranged from 0.42 to 0.85. Moreover, a significant increase in the value of effective moisture diffusivity (D_{eff}) and color change was observed when the samples were dried at 65°C compared to 45°C. The value of D_{eff} varied from 1.140×10^{-10} to 2.280×10^{-9} m^2/s and the activation energy was found to be 31.04 kJ/mol. The greatest R^2 ($\geq$0.999) and the lowest RMSE and SSE were obtained for the Naghavi *et al*. model (proposed in this research)

Keywords: Color change, convective drying, effective moisture diffusivity, essential oil, modeling, lemon verbena leaves, rehydration ratio

Introduction

Lemon verbena (*Lippia citriodora*) is a type of herb which is widely raised in western South America. It is also cultivated in Iran and mainly consumed as a spice and a medicinal plant (Funes *et al.*, 2009). There is an increasing interest in using lemon verbena leave in the food industry, because it is generally considered as a flavoring food additive. The leaves of lemon verbena have compounds such as essential oils, flavonoids and phenolic acids, which possess antioxidant activity (Pereira *et al.*, 2007). They are mainly used to make herbal teas and refreshing sorbets as well as creating a lemon flavor in a number of food products such as fish and poultry dishes, jams, salad dressings, puddings, and beverages (Funes *et al.*, 2009). Moreover, the leaves have digestive, sedative, antispasmodic, stomachic, and antipyretic properties (Pereira *et al.*, 2007; Funes *et al.*, 2009). However, similar to many other aromatic plants and herbs, lemon verbena leaves are perishable to microbial growth, mainly due to their high moisture content (around 84-85% wet basis).

Drying is used to extend the shelf life of fruits, vegetables and aromatic plants as well as to reduce or suppress their enzymatic and microbial activities (Doymaz 2009; Doymaz 2012). Aromatic plants are dried in order to extract their valuable compounds by solvents. Among the drying methods, hot-air drying (HAD) is still the most popular method, which is being employed to decrease the moisture content of foods and plants. Although HAD is time and energy consuming (Erbay and Icier 2010), it has gained considerable attention by researchers due to its low capital cost compared to other drying techniques such as freeze-drying and infrared-drying. For this reason, it is still extensively employed by many researchers for long-term preservation of foods and herbs (Erbay and Icier 2010; Doymaz 2012; Lemus-Mondaca *et al.*, 2015;

1. Young Researchers and Elite Club, Tabriz Branch, Islamic Azad University, Tabriz, Iran.
2. Department of Food Science and Technology, Islamic Azad University, Sabzevar Branch, Sabzevar, Iran.
(Corresponding Author Email:E_naghavi@tabrizu.ac.ir)
DOI: 10.22067/ifstrj.v12i6.61049

Oberoi and Sogi 2015; Aral and Beşe 2016; Nozad *et al.*, 2016; Roshanak *et al.*, 2016; Salarikia *et al.*, 2016).

Effective moisture diffusivity (D_{eff}) and activation energy (E_a) are two important physical properties of dehydrated foods which represent the rate of moisture loss during HAD and the level of energy needed to initiate a chemical reaction and to activate moisture diffusion, respectively (Lemus-Mondaca *et al.*, 2015). D_{eff} can highly affect the drying kinetics and consequently the quality of dehydrated foodstuffs. Also, mathematical modeling of mass transfer during HAD requires the values of D_{eff}. On the other hand, rehydration ratio (RR) is a key physical characteristic of dried foods which can reflect the degree of textural damage (such as shrinkage and tissue collapse) to foodstuffs during HAD (Doymaz *et al.*, 2015).

Numerous research papers can be found on the determination of D_{eff}, E_a, and RR during HAD of various aromatic plants and herbs (Doymaz 2012; Tasirin *et al.*, 2014; Lemus-Mondaca *et al.*, 2015; Nozad *et al.*, 2016; Salarikia *et al.*, 2016). However, to the best of our knowledge, no study has been conducted on the determination of D_{eff}, E_a, RR, and color change for lemon verbena leaves under HAD conditions. The purpose of this research was to investigate the influence of hot-air temperature on the drying kinetics, color change, RR, and essential oil content of lemon verbena leaves under HAD and to calculate D_{eff} and E_a, as well as empirical modeling of the dimensionless moisture ratio as a function of drying time.

Materials and methods

Materials

Fresh lemon verbena leaves were collected every morning from a farm located in Tabriz (Iran), and immediately transferred to the laboratory. The leaves were sorted visually based on size, shape, color, and freshness and stored under refrigerated conditions (at 5°C) (Lemus-Mondaca *et al.*, 2015) until use. The initial moisture content of the leaves was measured using the AOAC method (AOAC 1984) and found to be equal to 84.72% (wet basis).

Hot-air drying

First, the leaves were removed from the refrigerator and arranged uniformly as a thin layer in a stainless steel basket. Then, they were dried using the HAD technique. The experiments were carried out in a pilot plant hot-air drier (UOP 8 Tray dryer, Armfield, UK, equipped with automatic data recording system and temperature and airflow velocity controller units) at 45, 55, and 65±1°C and the airflow rate of 1 m/s (Doymaz 2012; Lemus-Mondaca *et al.*, 2015). Moisture loss was calculated by measuring the mass loss of the samples at 15 min intervals (based on preliminary experiments) by a precision balance with an accuracy of ±0.01 g. Moisture content data were recorded throughout the drying experiments using a data logger connected to a PC. The experiments were continued until reaching a final moisture content of 10% (wet basis).

Modeling of drying curves

Eighteen different empirical and semi-empirical models were used to evaluate the kinetics of moisture loss during HAD of lemon verbena leaves (Table 1) (Ertekin and Heybeli 2014). The model parameters or drying constants (a, b, c, g, h, k, and n) were estimated by applying non-linear regression analysis using MATLAB software (Version 8.1.0.604 R2013a, The Math works, Inc., USA). The coefficient of determination (R^2), adjusted R^2, root mean squared error (RMSE), and sum of squared error (SSE) were used to evaluate the goodness of fit in order to select the suitable model(s) to predict the drying kinetics. These statistical criteria are as follows (Lemus-Mondaca *et al.*, 2015):

$$R^2 = 1 - \frac{\sum_{i=1}^{N} (MR_{exp,i} - MR_{pre,i})^2}{\sum_{i=1}^{N} (\overline{MR}_{exp} - MR_{pre,i})^2} \quad (1)$$

$$RMSE = \left(\frac{1}{N} \sum_{i=1}^{N} (MR_{exp,i} - MR_{pre,i})^2 \right)^{\frac{1}{2}} \quad (2)$$

$$SSE = \frac{1}{N} \sum_{i=1}^{N} (MR_{exp,i} - MR_{pre,i})^2 \quad (3)$$

Where $MR_{exp,i}$ is the i^{th} experimental moisture ratio, $MR_{pre,i}$ shows the ith predicted moisture ratio, $\overline{MR}_{exp}$ stands for the average experimental moisture ratio, and N denotes the number of observations or the number of data values.

Table 1. Kinetic models used to describe the drying of lemon verbena leaves*

Model number	Model equation	Model name
1	$MR = \exp(-kt)$	Lewis (Newton)
2	$MR = \exp(-kt^n)$	Page
3	$MR = \exp(-(kt)^n)$	Modified Page-I
4	$MR = a\exp(-kt)$	Henderson & Pabis
5	$MR = a\exp(-kt^n)$	Modified Page-II
6	$MR = a\exp(-kt^n) + bt$	Midilli et al.
7	$MR = a\exp(-kt)^n + b$	Demir et al.
8	$MR = (a-b)\exp(-kt^n)$	Weibull distribution-I
9	$MR = (a-b)\exp(-(kt)^n)$	Weibull distribution-II
10	$MR = \exp(\frac{-at}{1+bt})$	Aghlasho
11	$MR = \frac{a}{1+b\exp(kt)}$	Logistic
12	$MR = a\exp(-kt) + b\exp(-gt)$	Two-term
13	$MR = a\exp(-kt^n) + b\exp(-gt^n)$	Hii et al.
14	$MR = a\exp(-kt) + (1-a)\exp(-kat)$	Two-term exponential
15	$MR = a\exp(-kt) + (1-a)\exp(-bt)$	Modified two-term exponential
16	$MR = a\exp(-kt) + (1-a)\exp(-kbt)$	Diffusion approximation
17	$MR = (1-a)\exp(-kt) + (1-b)\exp(-gt^n) + c$	Naghavi et al. (present study)
18	$MR = a\exp(-kt) + b\exp(-gt) + c\exp(-ht)$	Modified Henderson & Pabis

*All models (except model-17) are available in the paper published by Ertekin and Heybeli (2014).
a, b, c, g, h, k, and n are model parameters (empirical constants).

Determination of the effective moisture diffusivity

The Fick's law-based model (Eq. 4) is often used to determine the effective moisture diffusivity (D_{eff}) of different food materials.

$$\frac{\partial M}{\partial t} = D_{eff} \frac{\partial^2 M}{\partial x} \quad (4)$$

The following initial and boundary conditions can be considered (Doymaz 2012):

$t = 0, \quad 0 < x < L, \quad M = M_0$

$t > 0, \quad x = L, \quad M = M_e$

$t > 0, \quad x = 0, \quad \frac{dM}{dx} = 0$

In the present study, the analytical solution of Fick's second law for an infinite slab (Eq. 5) was applied to calculate D_{eff} (Erbay and Icier 2010; Doymaz 2012):

$$MR = \frac{M_t - M_e}{M_0 - M_e} = \frac{8}{\pi^2} \sum_{n=0}^{\infty} \frac{1}{(2n+1)^2} \exp\left(-\frac{(2n+1)^2 \pi^2 D_{eff} t}{4L^2} \right) \quad (5)$$

where M is the moisture content (dry basis), D_{eff} represents the effective moisture diffusivity (m^2/s), L is the half thickness of the

slab (m), t stands for the time (s), MR is the moisture ratio (dimensionless), M_t shows the moisture content at any time (kg water/kg dry solid), M_0 is the initial moisture content (kg water/kg dry solid), M_e denotes the equilibrium moisture content (kg water/kg dry solid), and n is the number of the terms taken into consideration.

This method has also been used previously by several researchers (Doymaz 2012; Aral and Beşe 2016) and is based on the assumptions that shrinkage is negligible, D_{eff} remains constant and moisture loss occurs through the diffusion phenomenon (Crank 1975). For long drying times (M_e=0), the use of one-term approximation (n=1) to the series summation is reasonable and Eq. 5 reduces to (Doymaz 2012):

$$MR = \frac{M_t}{M_0} = \frac{8}{\pi^2}\exp\left(-\frac{\pi^2 D_{eff} t}{4L^2}\right) \quad (6)$$

By taking the natural logarithm, Eq. 6 can be further simplified to (Doymaz 2012; Oberoi and Sogi 2015):

$$\ln(MR) = \ln\left(\frac{8}{\pi^2}\right) - \left(\frac{\pi^2 D_{eff} t}{4L^2}\right) \quad (7)$$

A plot of the experimental data in terms of ln (MR) versus time gives a straight line with a slope of k_0 (Oberoi and Sogi 2015):

$$k_0 = \frac{-\pi^2 D_{eff}}{4L^2} \quad (8)$$

Determination of the activation energy

The Arrhenius model describes the relationship between D_{eff}, drying temperature (T), and the activation energy (E_a). Therefore, for quantifying E_a and investigating the effect of temperature on D_{eff}, the Arrhenius type equation (Eq. 9) was employed (Doymaz 2012):

$$D_{eff} = D_0 \exp\left(-\frac{E_a}{RT}\right) \quad (9)$$

Where E_a denotes the activation energy (kJ/mol), R is the universal gas constant [8.314 J/(mol K)], T is the absolute air temperature (K), and D_0 is the pre-exponential factor (constant) (m^2/s). This approach has been used by a number of researchers (Doymaz 2012; Aral and Beşe 2016).

Determination of the rehydration ratio

Measurement of the rehydration ratio (RR) of dried leaves was carried out according to the method described by Doymaz *et al.* (2015) and Nozad *et al.* (2016). Based on this method, 5 g of the dehydrated samples were poured into a glass beaker (750 mL) containing 500 mL of distilled water (25°C) and kept for 24 h. Next, the leaves were removed from the beaker and their surface water was blotted up using a tissue paper. Finally, the weight of the resulted sample was measured precisely using a digital balance. In all cases, the tests were triplicated for each sample and the mean values of the three replications ± standard deviation were reported. The RR calculation was carried out using Eq. 10 as employed by Doymaz *et al.* (2015), Nozad *et al.* (2016), and Salarikia *et al.* (2016):

$$RR = \frac{W_2 - W_1}{W_1} \quad (10)$$

Where RR denotes the rehydration ratio [kg water/kg dry matter (DM)], W_1 is the weight of the dried leaves (kg), and W_2 represents the weight of the rehydrated leaves (kg).

Color measurement

The color changes of leaves (fresh and hot-air dried) were quantified using image processing in MATLAB (Version 8.1.0.604 R2013a, The Math works, Inc., USA) (Nozad *et al.* 2016). The color test instrument was designed and constructed in the Department of Agricultural Machinery Engineering, University of Tabriz, Tabriz, Iran. It consists of a chamber with a trapezoidal cross section that was equipped by two D_{65} (daylight) lamps as the light source for illumination of sample. At first, a sample was put in the chamber. After zooming the lens and focusing, the images were taken by camera. A digital camera (Nikon, D3200, Japan) was used to capture images from leaf surfaces. The camera calibration was performed prior to each drying experiment.

In each experimental run, the color of the leaves (10 fresh and 10 dried samples) was measured as *L**, *a** and *b** values, which known as Hunter parameters. It is well known that the *L** value represents the degree of lightness/darkness, *a** stands for the degree of redness/greenness, and *b** shows the degree of yellowness/blueness. Changes in the color of the leaves were calculated as follows (Nozad *et al.*, 2016; Salarikia et al., 2016):

$$\Delta E = \sqrt{\Delta L^{*2} + \Delta a^{*2} + \Delta b^{*2}} \quad (11)$$

Where ΔE denotes the total color change of leaves and Δ*L**, Δ*a**, and Δ*b** represents the difference between the color parameters of initial samples (L_0*, a_0*, and b_0*) and final dried leaves (*L**, *a**, and *b**).

Determination of the essential oil content

The essential oil was extracted from the leaves using a flask connected to Clevenger hydro-distillation apparatus (Nozad *et al.*, 2016). Based on this method, a given amount of the samples (30 g) were put into a round-bottomed distillation flask filled with a given amount of distilled water (250 mL). Then, the heating was performed for 3 h and the distilled essential oil collected in the side arm was separated. The data of essential oil (%) were expressed on the basis of dry matter weight.

Statistical analysis

The experimental data were analyzed statistically by the analysis of variance (ANOVA) using Minitab statistical software (Minitab Release 14, Minitab Inc., USA). The significant difference between the means was determined using Tukey's honestly significant difference (HSD) test at the significance level of 5% ($p<0.05$). The data were expressed as the mean ± standard deviation and all experiments were carried out in triplicate.

Results and discussion

Drying kinetics

The effects of the drying temperature (45, 55, and 65°C) on the dimensionless moisture ratios of lemon verbena leaves are illustrated in Fig. 1.

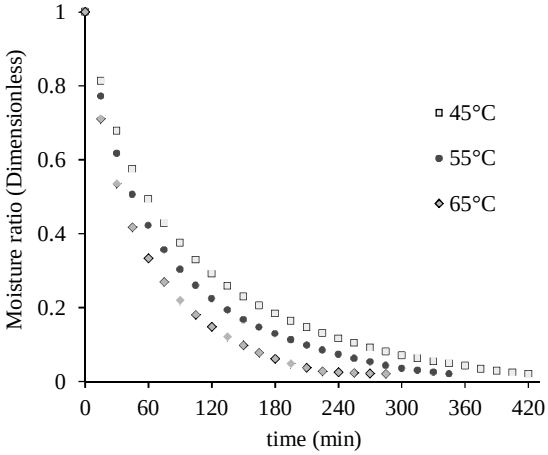

Fig. 1. Moisture ratios (dimensionless) as a function of the drying time at different temperatures during hot-air drying of lemon verbena leaves

It can be seen that the moisture ratio declined quickly in the initial period of HAD (almost up to 75-90 min) and was subsequently followed by a gradual non-linear decrease (almost exponential) with an increase in the process time. This result was similar to the findings of other researchers (Doymaz 2012; Lemus-Mondaca *et al.*, 2015; Said *et al.*, 2015; Aral and Beşe 2016).

Fig. 1 also shows that all drying temperatures exhibited a relatively similar behavior for the dried samples. Moreover, by increasing the drying temperature, the moisture ratios and consequently the drying

kinetics were altered. Based on ANOVA results, the drying time was significantly ($p<0.05$) lower in the case of the samples dried at 65°C than those dehydrated at lower temperatures (45 or 55°C). The total drying time was 420, 345, and 285 min for the leaves dried at 45, 55, and 65°C, respectively. This result indicates that a temperature increase of 20°C (i.e. from 45 to 65°C) caused a reduction of approximately 135 min in the total drying time ($p<0.05$). This might be due to the increased vapor pressure in lemon verbena leaves at higher drying temperatures, which in turn results in a faster moisture loss from the samples and thus, a shorter drying time (Aral and Beşe 2016). Other studies have reported similar findings (Ertekin and Heybeli 2014; Lemus-Mondaca *et al.*, 2015; Said *et al.*, 2015; Aral and Beşe 2016).

Modeling of the drying curves

In the literature, several empirical and semi-empirical models have been applied to describe the drying kinetics of food materials and plants under different drying conditions, which are based on the dimensionless moisture ratio as a function of drying time. In the present work, the experimental data of moisture loss in lemon verbena leaves during HAD at different drying temperatures (45, 55, and 65°C) were fitted to eighteen models summarized in Table 1 (Ertekin and Heybeli 2014), which allows of using and comparing different model correlations based on the fitting criteria (R^2, RMSE, and SSE) on a defined set of experimental data

Table 2. Statistical analysis of different kinetic models for different drying temperatures

Model number	T (°C)	R^2	Adjusted R^2	RMSE	SSE	Model number	T (°C)	R^2	Adjusted R^2	RMSE	SSE
1	45	0.9875	0.9875	0.0283	0.0225	10	45	0.9977	0.9976	0.0124	0.0041
	55	0.9870	0.9870	0.0294	0.0199		55	0.9981	0.9980	0.0116	0.0029
	65	0.9907	0.9907	0.0256	0.0125		65	0.9981	0.9980	0.0120	0.0026
2	45	0.9995	0.9995	0.0056	0.0008	11	45	0.9744	0.9735	0.0413	0.04611
	55	0.9996	0.9996	0.0050	0.0005		55	0.9723	0.9710	0.0439	0.04233
	65	0.9997	0.9997	0.0049	0.0004		65	0.9766	0.9753	0.0417	0.03132
3	45	0.9995	0.9995	0.0056	0.0008	12	45	0.9998	0.9998	0.0034	0.00028
	55	0.9996	0.9996	0.0050	0.0005		55	0.9998	0.9999	0.0032	0.00019
	65	0.9997	0.9997	0.0049	0.0004		65	0.9999	0.9998	0.0033	0.00017
4	45	0.9927	0.9924	0.0221	0.0131	13	45	0.9999	0.9999	0.0030	0.00021
	55	0.9916	0.9912	0.0241	0.0128		55	0.9997	0.9996	0.0051	0.00049
	65	0.9934	0.9931	0.0221	0.0088		65	0.9997	0.9996	0.0053	0.00042
5	45	0.9995	0.9995	0.0057	0.0008	14	45	0.9996	0.9996	0.0048	0.00063
	55	0.9996	0.9996	0.0051	0.0005		55	0.9995	0.9994	0.0061	0.00083
	65	0.9997	0.9996	0.0050	0.0004		65	0.9998	0.9998	0.0041	0.00030
6	45	0.9997	0.9997	0.0044	0.0005	15	45	0.9998	0.9998	0.0033	0.00029
	55	0.9997	0.9997	0.0046	0.0004		55	0.9999	0.9998	0.0032	0.00027
	65	0.9998	0.9997	0.0044	0.0003		65	0.9999	0.9998	0.0031	0.00026
7	45	0.9997	0.9997	0.0047	0.0005	16	45	0.9998	0.9998	0.0033	0.00030
	55	0.9997	0.9996	0.0048	0.0005		55	0.9999	0.9998	0.0030	0.00025
	65	0.9998	0.9997	0.0044	0.0003		65	0.9999	0.9999	0.0032	0.00017
8	45	0.9995	0.9995	0.0058	0.0008	**17**	**45**	**1**	**1**	**0.0007**	**0.000011**
	55	0.9996	0.9996	0.0052	0.0005		**55**	**1**	**0.9999**	**0.0013**	**0.000031**
	65	0.9997	0.9996	0.0052	0.0004		**65**	**0.9999**	**0.9999**	**0.0020**	**0.000056**
9	45	0.9995	0.9995	0.0058	0.0008	18	45	0.9998	0.9998	0.0035	0.00028
	55	0.9996	0.9996	0.0052	0.0005		55	0.9999	0.9998	0.0035	0.00022
	65	0.9997	0.9996	0.0052	0.0004		65	0.9997	0.9997	0.0049	0.00034

Table 3. Estimated coefficients of different kinetics models at different drying temperatures*

Model number	T (°C)	Coefficients		Model number	T (°C)	Coefficients	
1	45	a = 0.0102		10	45	a = 0.0124	b = 0.0014
	55	a = 0.0130			55	a = 0.0159	b = 0.0019
	65	a = 0.0177			65	a = 0.0212	b = 0.0022
2	45	a = 0.0230	n = 0.8315	11	45	a = 1.7520	k = 0.0128
	55	a = 0.0294	n = 0.8213		55	a = 1.7650	k = 0.0164
	65	a = 0.0360	n = 0.8346		65	a = 1.8030	k = 0.0229
3	45	a = 0.0107 n = 0.8315		12	45	a = 0.7404 b = 0.2604	g = 0.0350 k = 0.0078
	55	a = 0.0137 n = 0.8213			55	a = 0.7025 b = 0.2977	g = 0.0402 k = 0.0096
	65	a = 0.0186 n = 0.8346			65	a = 0.7515 b = 0.2490	g = 0.0625 k = 0.0138
4	45	a = 0.9339 k = 0.0095		13	45	a = 0.6834 b = 0.3152 g = 0.0268	k = 0.0051 n = 1.0690
	55	a = 0.9370 k = 0.0121			55	a = 1.0290 b = -0.0292 g = 3.1770	k = 0.0338 n = 0.7970
	65	a = 0.9500 k = 0.0168			65	a = 0.9833 b = 0.0168 g = 7.8360	k = 0.0334 n = 0.8485
5	45	a = 1.0020 k = 0.0233	n = 0.8298	14	45	a = 0.2325 k = 0.0349	
	55	a = 1.0020 k = 0.0298	n = 0.8195		55	a = 0.2449 k = 0.0417	
	65	a = 0.9993 k = 0.0359	n = 0.8352		65	a = 0.2307 k = 0.0612	
6	45	a = 1.0060 b = -3.089×10^{-5}	k = 0.0259 n = 0.8041	15	45	a = 0.2599 b = 0.0078	k = 0.0349
	55	a = 1.0040 b = -2.328×10^{-5}	k = 0.0317 n = 0.8036		55	a = 0.2977 b = 0.0096	k = 0.0401
	65	a = 1.0010 b = -2.562×10^{-5}	k = 0.0380 n = 0.8199		65	a = 0.2487 b = 0.0138	k = 0.0624
7	45	a = 1.0210 b = -0.0150	k = 0.0104 n = 0.8015	16	45	a = 0.2598 b = 0.2246	k = 0.0349
	55	a = 1.012 b = -0.0084	k = 0.0135 n = 0.8030		55	a = 0.2977 b = 0.2390	k = 0.0401
	65	a = 1.0100 b = -0.0087	k = 0.0183 n = 0.8154		65	a = 0.2490 b = 0.2214	k = 0.0623
8	45	a = 0.7216 b = -0.2803	k = 0.0232 n = 0.8298	17	45	a = 0.6936 b = 0.2731 c = -0.0333	g = 0.0114 k = 0.0256 n = 0.9001
	55	a = 1.1360 b = 0.1335	k = 0.0298 n = 0.8194		55	a = 0.6157 b = 1.9780 c = 0.6156	g = 6.0080 k = 0.0153 n = -0.4296
	65	a = 0.5534 b = -0.446	k = 0.0359 n = 0.8351		65	a = 0.3155 b = 0.6998 c = 0.0144	g = 0.0001 k = 0.0352 n = 1.8710
9	45	a = -6.0690 b = -7.0710	k = 0.0108 n = 0.8298	18	45	a = 0.7466 b = 0.2643 c = -0.0109	g = 0.0373 h = 10.300 k = 0.0079
	55	a = 1.3370 b = 0.3346	k = 0.0137 n = 0.8195		55	a = -0.1141 b = 0.4036 c = 0.7106	g = 0.0495 h = 0.0096 k = 0.0802
	65	a = 0.5256 b = -0.4736	k = 0.0186 n = 0.8352		65	a = 0.8052 b = -1.424 c = 1.6190	g = 1.4230 h = 0.2176 k = 0.0144

* a, b, c, g, h, k, and n are model parameters (empirical constants).

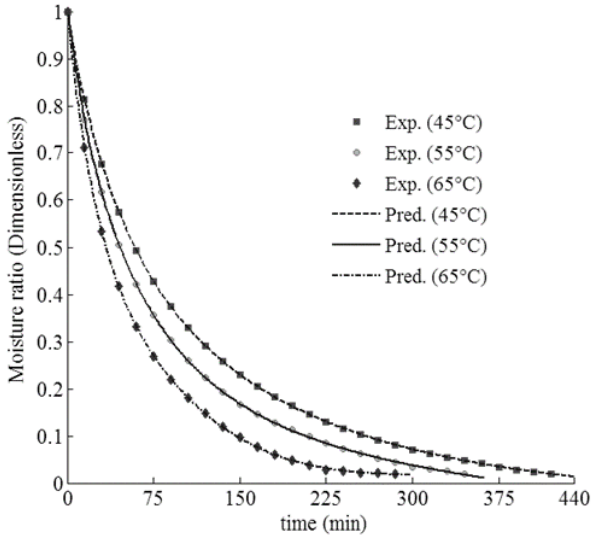

Fig. 2. Comparison of the experimental (exp.) and predicted (pred.) moisture ratios for lemon verbena leaves dehydrated at different drying temperatures

Table 2 indicates that for the most of tested models, R^2 and adjusted R^2 values were higher than 0.999, and RMSE and SSE values were between 0.0007-0.0413 and 0.000011-0.04611, respectively.

Genrally, the closer the experimental and predicted moisture ratios, the better they explain the adequacy of the regression model. As expected, the models with a larger number of coefficients (models 12, 13, 15-18 in Table 2) had higher R^2 and lower RMSE and SSE values. The data in Table 2 suggested that the employed models were suitable to describe the drying behavior of lemon verbena leaves. However, for plotting the predicted moisture ratios against the drying time, only the model presented in this research (model-17 in Table 1) was fitted to the experimental data (Fig. 2) which had greater R^2 (0.9999-1) and adjusted R^2 (0.9999-1) values and lower RMSE (0.0007-0.0020) and SSE (0.000011-0.000056) values than the other 17 models (Table 2). The models coefficients (constants) obtained at different drying temperatures are represented in Table 3. By increasing drying temperature, different coefficients did not follow a similar trend. As can be obtained from Table 3, drying rate constant (k) in the studied drying models increased with increasing drying temperatures. Thus, it may be assumed that this kinetic parameter would be directly proportional to drying temperature (Lemus-Mondaca *et al.*, 2015). Similar results were reported by other investigators (Vega-Gálvez *et al.*, 2012; Lemus-Mondaca *et al.*, 2015). Furthermore, there was no clear trend on the effect of drying temperature on the other constants (a, b, c, g, h, and n).

Rehydration ratio (RR)

Comparison of the RR results for the samples dried at different drying temperatures are presented in Fig. 3.

It can be seen that there was no significant change ($p>0.05$) in the RR of the dried leaves when the drying temperature changed from 45 to 55°C. However, RR reduced significantly ($p<0.05$) with an increase in the air temperature from 45 to 65°C. This was attributed to the fact that HAD at higher temperatures resulted in a change in the structural features of the leaves (such as tissue collapse, development of a surface hard layer and volumetric shrinkage), which in turn can cause significant damages to the textural quality of the dried samples and therefore a decrease in RR (Doymaz 2012; Nozad *et al.*, 2016; Salarikia *et al.*, 2016). The highest RR value of the dried samples (78.24%) was observed for the leaves dried at 45°C, followed by those dehydrated at 55 (76.12%) and 65°C (73.36%). These results are in

agreement with the results reported by f Doymaz (2012), who stated that the higher the drying temperature (40, 50, and 60 °C) resulted in a lower RR of the grape leaves, concluding that higher drying temperatures led to greater changes in the structural attributes and thus, lower RR values. Nozad *et al.*, (2016) also observed that in HAD of spearmint (*Mentha spicata* L.) leaves, an increase in the air temperature from 30 to 50°C had a considerable decreasing effect on RR. Similar findings were reported by other researchers (Jangam *et al.*, 2008; Vega-Gálvez *et al.*, 2012; Salarikia *et al.*, 2016).

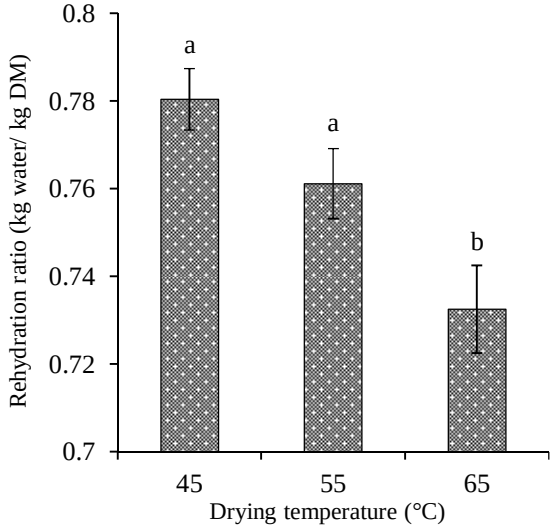

Fig. 3. Rehydration ratio of lemon verbena leaves at different drying temperatures. Error bars show one standard deviation from the mean and means with different letters are significantly different (p<0.05).

Effective moisture diffusivity (D_{eff})

In the present study, the value of D_{eff} at 45, 55, and 65°C was estimated by plotting ln(MR) versus the drying time (Eq. 4) (Oberoi and Sogi 2015). The slope of the corresponding line represents the value of D_{eff}. The D_{eff} values varied from 1.140×10^{-10} to 2.280×10^{-9} m^2/s (Table 4). Other researchers found similar values for the D_{eff} of dried foods (in particular leaf materials), which were in general in the range of 10^{-12} to 10^{-8} m^2/s (Zogzas *et al.*, 1996). D_{eff} values have been determined for other herbs as follows: mint leaves 3.067×10^{-9} to 1.941×10^{-8} m^2/s (Doymaz 2006), spinach leaves 6.590×10^{-10} to 1.927×10^{-9} m^2/s (Doymaz 2009), nettle leaves 1.744×10^{-9} to 4.992×10^{-9} m^2/s (Kaya and Aydın 2009), mint leaves 0.965×10^{-11} to 1.190×10^{-11} m^2/s (Therdthai and Zhou 2009), olive leaves 1.054×10^{-9} to 4.973×10^{-9} m^2/s (Erbay and Icier 2010), grape leaves 4.13×10^{-10} to 1.83×10^{-9} m^2/s (Doymaz 2012), kaffir lime leaves 2.61×10^{-11} to 9.24×10^{-11} m^2/s (Tasirin *et al.*, 2014), stevia leaves 4.67×10^{-10} to 14.90×10^{-10} m^2/s (Lemus-Mondaca *et al.*, 2015), and wild edible plant (*Allium roseum*) leaves 2.55×10^{-12} to 8.83×10^{-12} m^2/s (Said *et al.*, 2015).

Table 4. The values of effective moisture diffusivity (D_{eff}) for lemon verbena leaves at different drying temperatures

Drying temperature (°C)	D_{eff} (m^2/s)
45	$1.140 \times 10^{-10\ c}$
55	$1.710 \times 10^{-10\ b}$
65	$2.280 \times 10^{-9\ a}$

Different letters in the same column indicate significant differences (p<0.05)

As can be realized from Table 4, significant differences (p<0.05) of the D_{eff} values were

observed between the leaves dried at different drying temperatures. This indicates that hot-air temperature has a considerable effect on D_{eff} during HAD of plants and foods, as reported by numerous authors (Erbay and Icier 2010; Doymaz 2012; Lemus-Mondaca *et al.*, 2015; Said *et al.*, 2015; Aral and Beşe 2016). This may be related to the higher thermal energy transferring to the leaves at higher drying temperatures, which subsequently results in an increase in the kinetic energy of the water molecules (Aral and Beşe 2016). A higher D_{eff} value indicates the increasing rate of moisture loss with the rise of drying temperature (Fig. 1).

Activation energy (E_a)

The value of E_a in the drying of lemon verbena leaves was estimated from the slope of the linearized Arrhenius equation (Eq. 9) (Doymaz 2012) and was found to be 31.04 kJ/mol. The E_a value obtained in this research was in the range that reported for other aromatic plants and fruits. Experimentally-determined E_a values have been reported by several researchers, for example Ahmed *et al.* (2001) for coriander leaves (26.50 kJ/mol in the temperature range of 45-65°C), Doymaz (2006) for mint leaves (62.96 kJ/mol in the temperature range of 35-60°C), Doymaz (2009) for spinach leaves (34.35 kJ/mol in the temperature range of 50-80°C), Kaya and Aydın (2009) for nettle leaves (79.873-109.003 kJ/mol in the temperature range of 35-55°C and at airflow rates of 0.2-0.6 m/s), Erbay and Icier (2010) for olive leaves (60.97 kJ/mol in the temperature range of 50-70°C), Doymaz (2012) for grape leaves (64.56 kJ/mol in the temperature range of 40-60°C), Lemus-Mondaca *et al.* (2015) for stevia leaves (38.78 kJ/mol in the temperature range of 30-80°C), and Said *et al.* (2015) for wild edible plant (*Allium roseum*) leaves (46.80-52.68 kJ/mol in the temperature range of 30-80°C and 1 and l.5 m/s airflow velocity).

It has been reported that the value of E_a is influenced by several factors, including the drying air temperature, the moisture content of food or herb, and variations in the D_{eff} value with the drying temperature (Aghbashlo *et al.*, 2008), which makes it difficult to compare the E_a values for different foods and herbs dehydrated at different process conditions. However, from numerous conducted studies on the calculation of the E_a value, it can be concluded that long dehydration time, high initial moisture content, remarkable variation in the D_{eff} value with the drying temperature (at constant airflow rate) (Aghbashlo *et al.*, 2008) or with both temperature and airflow rate (Erbay and Icier 2010), low hot-air flow rate, low drying temperature, and textural changes in the sample due to the percentage of shrinkage and tissue collapse, are all the reasons for a considerable increase in the E_a value.

Color measurement

The value of color change (ΔE) represents the degree of total color change in dehydrated leaves compared to the color of fresh samples. The lower ΔE the better the quality of dried leaves (Salarikia *et al.*, 2016). The color of aromatic plants and herbs are very sensitive to heat damage during HAD. Fig. 4 shows the value of ΔE for dried samples. It can be seen that the value of ΔE increase significantly ($p<0.05$) with increasing of hot-air temperature from 45 to 65°C. Chlorophyll a and chlorophyll b are responsible for natural green color of leaves. The increase in ΔE is due to the increase in substitution of magnesium with hydrogen in chlorophyll with drying temperature. Under this condition, chlorophylls are converted to pheophytins (Therdthai and Zhou 2009). This finding confirmed the previous observations obtained by Therdthai and Zhou (2009) for mint leaves (*Mentha cordifolia* Opiz ex Fresen), Chenarbon *et al.* (2012) for St. John's wort (*Hypericum perforatum* L.) leaves, Akbudak and Akbudak (2013) for parsley, and Salarikia *et al.* (2016) for peppermint leaves.

Determination of the essential oil content

Essential oil content of lemon verbena leaves before (fresh sample) and after drying is shown in Fig. 5. The fresh samples had the

highest value of essential oil (1.10%) between the treatments. Furthermore, no significant difference ($p>0.05$) of essential oil content was observed between the leaves dried at different temperatures, while significant difference ($p<0.05$) of essential oil content was observed between fresh leaves and samples dehydrated at 55 and 65°C. The reduction in essential oil content with increasing drying temperature ($p>0.05$) might be explained by the fact that the relatively high temperature of hot-air result in an increase in rupture of oil glands and as a consequence, rapid evaporation or higher loss of volatile components (Argyropoulos and Müller 2014). This result is consistent with those obtained in previous studies, for example *Laurus nobilis* L. leaves (Sellami *et al.*, 2011), *Thymys daenensis* subsp. *daenensis.* Celak leaves (Rahimmalek and Goli, 2013), Lemon verbena (Shahhoseini *et al.*, 2013), and peppermint leaves (Salarikia *et al*., 2016).

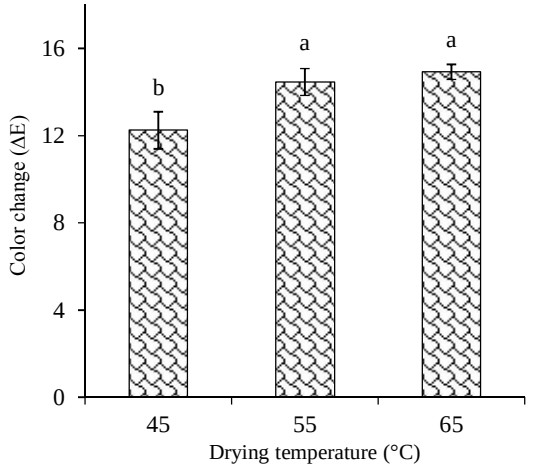

Fig. 4. Color change in lemon verbena leaves at different drying temperatures. Error bars show one standard deviation from the mean and means with different letters are significantly different ($p<0.05$).

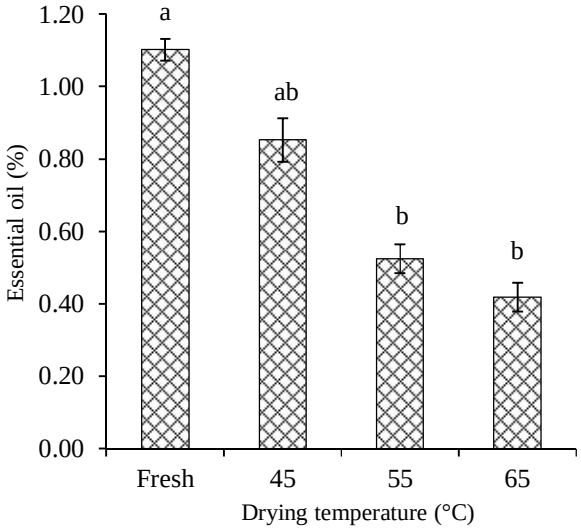

Fig. 5. Essential oil content of lemon verbena leaves at different drying temperatures .Error bars show one standard deviation from the mean and means with different letters are significantly different ($p<0.05$).

Conclusions

This study was focused on investigation of some selected properties of lemon verbena leaves (moisture loss, D_{eff}, color change, essential oil content, and RR) during HAD at

different drying temperatures as well as the empirical modeling of the drying kinetics. A shorter drying time and a higher D_{eff} value were observed ($p<0.05$) with an increase in the drying temperature from 45 to 65°C. The values of D_{eff} ranged from 1.140×10^{-10} to 2.280×10^{-9} m^2/s and the E_a value was found to be 31.04 kJ/mol, all of which were in agreement with the results reported by other investigators in the literature. Our results also showed that the percentage of RR was significantly ($p<0.05$) affected by the air temperature and its maximum (78.24%) and minimum (73.36%) values were attained at 45°C and 65°C, respectively. Essential oil content of the samples dried at different drying temperatures was not significant ($p>0.05$) with respect to each other but was significantly ($p<0.05$) different from the fresh samples. Furthermore, the value of ΔE increased significantly ($p<0.05$) with increasing of hot-air temperature from 45 to 65°C and ranged from 12.24 to 14.92, respectively. The results of modeling ($R^2>0.99$ and low RMSE and SSE values for most of the tested models) indicated a good fit to the experimental data of moisture ratio. Among these, the model proposed in the present study had a better goodness of fit (with an adjusted $R^2 \geq 0.999$ and the lowest RMSE and SSE) and was considered as the best model.

References

Aghbashlo, M., & Samimi-Akhijahani, H., 2008, Influence of drying conditions on the effective moisture diffusivity, energy of activation and energy consumption during the thin-layer drying of berberis fruit (*Berberidaceae*). *Energy Conversion and Management*, 49(10): 2865-2871.

Ahmed, J., Shivhare, U., & Singh, G., 2001, Drying characteristics and product quality of coriander leaves. *Food and Bioproducts Processing*, 79(2): 103-106.

Akbudak, N., & Akbudak, B., 2013, Effect of vacuum, microwave, and convective drying on selected parsley quality. *International Journal of Food Properties*, 16(1): 205-215.

AOAC, 1984. Official Methods of Analysis, Association of the Official Analytical Chemists, Washington, DC.

Aral, S., & Beşe, A. V., 2016, Convective drying of hawthorn fruit (*Crataegus* spp.): Effect of experimental parameters on drying kinetics, color, shrinkage, and rehydration capacity. *Food Chemistry*, 210: 577-584.

Argyropoulos, D., & Müller, J., 2014, Changes of essential oil content and composition during convective drying of lemon balm (*Melissa officinalis* L.). *Industrial Crops and Products*, 52: 118-124.

Chenarbon, H. A., Minaei, S., Bassiri, A. R., Almassi, M., Arabhosseini, A., & Motevali, A., 2012, Effect of drying on the color of St. John's wort (*Hypericum perforatum* L.) leaves. *International Journal of Food Engineering*, 8(4), doi: 10.1515/1556-3758.2545.

Crank, J, 1975. The mathematics of diffusion, 2nd ed., Oxford University Press, London.

Doymaz, İ., 2006, Thin-layer drying behaviour of mint leaves. *Journal of Food Engineering*, 74(3): 370-375.

Doymaz, I., 2009, Thin-layer drying of spinach leaves in a convective dryer. *Journal of Food Process Engineering*, 32(1): 112-125.

Doymaz, I., 2012, Air drying characteristics, effective moisture diffusivity and activation energy of grape leaves. *Journal of Food Processing and Preservation*, 36(2): 161-168.

Doymaz, I., Kipcak, A. S., & Piskin, S., 2015, Characteristics of thin-layer infrared drying of green bean. Czech *Journal of Food Sciences*, 33(1): 83-90.

Erbay, Z., & Icier, F., 2010, Thin-layer drying behaviors of olive leaves (*Olea europaea* L.). *Journal of Food Process Engineering*, 33(2): 287-308.

Ertekin, C., & Heybeli, N., 2014, Thin-layer infrared drying of mint leaves. *Journal of Food Processing and Preservation*, 38(4): 1480-1490.

Funes, L., Fernández-Arroyo, S., Laporta, O., Pons, A., Roche, E., Segura-Carretero, A., Fernández-Gutiérrez, A., & Micol, V., 2009, Correlation between plasma antioxidant capacity and verbascoside levels in rats after oral administration of lemon verbena extract. *Food Chemistry*, 117(4): 589-598.

Jangam, S. V., Joshi, V. S., Mujumdar, A. S., & Thorat, B. N., 2008, Studies on dehydration of sapota (*Achras zapota*). *Drying Technology*, 26(3): 369-377.

Kaya, A., & Aydın, O., 2009, An experimental study on drying kinetics of some herbal leaves. *Energy Conversion and Management*, 50(1): 118-124.

Lemus-Mondaca, R., Vega-Gálvez, A., Moraga, N. O., & Astudillo, S., 2015, Dehydration of Stevia rebaudiana Bertoni leaves: kinetics, modeling and energy features. *Journal of Food Processing and Preservation*, 39(5): 508-520.

Nozad, M., Khojastehpour, M., Tabasizadeh, M., Azizi, M., Ashtiani, S.-H. M., & Salarikia, A., 2016, Characterization of hot-air drying and infrared drying of spearmint (*Mentha spicata* L.) leaves. *Journal of Food Measurement and Characterization*, 10(3): 1-8.

Oberoi, D. P. S., & Sogi, D. S., 2015, Drying kinetics, moisture diffusivity and lycopene retention of watermelon pomace in different dryers. *Journal of food science and technology*, 52(11): 7377-7384.

Pereira, C. G., & Meireles, M. A. A., 2007, Evaluation of global yield, composition, antioxidant activity and cost of manufacturing of extracts from lemon verbena (*Aloysia triphylla* [L'Herit.] Britton) and mango (*Mangifera indica* L.) leaves. *Journal of Food Process Engineering*, 30(2): 150-173.

Rahimmalek, M., & Goli, S. A. H., 2013, Evaluation of six drying treatments with respect to essential oil yield, composition and color characteristics of Thymys daenensis subsp. daenensis. *Celak leaves*. *Industrial Crops and Products*, 42: 613-619.

Roshanak, S., Rahimmalek, M., & Goli, S. A. H., 2016, Evaluation of seven different drying treatments in respect to total flavonoid, phenolic, vitamin C content, chlorophyll, antioxidant activity and color of green tea (*Camellia sinensis* or *C. assamica*) leaves. *Journal of food science and technology*, 53(1): 721-729.

Said, L. B. H., Najjaa, H., Farhat, A., Neffati, M., & Bellagha, S., 2015, Thin layer convective air drying of wild edible plant (*Allium roseum*) leaves: experimental kinetics, modeling and quality. *Journal of food* science and technology, 52(6): 3739-3749.

Salarikia, A., Miraei Ashtiani, S. H., & Golzarian, M. R., 2016, Comparison of drying characteristics and quality of peppermint leaves using different drying methods. *Journal of Food Processing and Preservation*, doi: 10.1111/jfpp.12930 (in press).

Sellami, I. H., Wannes, W. A., Bettaieb, I., Berrima, S., Chahed, T., Marzouk, B., & Limam, F., 2011, Qualitative and quantitative changes in the essential oil of Laurus nobilis L. leaves as affected by different drying methods. *Food Chemistry*, 126(2): 691-697.

Shahhoseini, R., Ghorbani, H., Karimi, S. R., Estaji, A., & Moghaddam, M., 2013, Qualitative and quantitative changes in the essential oil of lemon verbena (*Lippia citriodora*) as affected by drying condition. *Drying Technology*, 31(9): 1020-1028.

Tasirin, S. M., Puspasari, I., Lun, A., Chai, P., & Lee, W., 2014, Drying of kaffir lime leaves in a fluidized bed dryer with inert particles: Kinetics and quality determination. *Industrial Crops and Products*, 61: 193-201.

Therdthai, N., & Zhou, W., 2009, Characterization of microwave vacuum drying and hot air drying of mint leaves (*Mentha cordifolia Opiz ex Fresen*). *Journal of Food Engineering*, 91(3): 482-489.

Vega-Gálvez, A., Ah-Hen, K., Chacana, M., Vergara, J., Martínez-Monzó, J., García-Segovia, P., Lemus-Mondaca, R., & Di Scala, K., 2012, Effect of temperature and air velocity on drying kinetics, antioxidant capacity, total phenolic content, colour, texture and microstructure of apple (var. *Granny Smith*) slices. *Food Chemistry*, 132(1): 51-59.

Zogzas, N., Maroulis, Z., & Marinos-Kouris, D., 1996, Moisture diffusivity data compilation in foodstuffs. *Drying Technology*, 14(10): 2225-2253.

نشریه پژوهشهای علوم و صنایع غذایی ایران
جلد 12، شماره 6، بهمن - اسفند 1395، ص. 729-716

Iranian Food Science and Technology Research Journal
Vol. 12, No. 6, Feb. Mrch. 2017, p. 716-729

خشک‌کردن همرفتی لایه نازک برگ‌های به لیمو

عنایت‌الله نقوی[1*] - صادق ریگی[2]

تاریخ دریافت:1395/09/25
تاریخ پذیرش:1396/02/02

چکیده

برگ به‌لیمو یک افزودنی غذایی طعم‌زا و همچنین منبع خوبی از ترکیبات با ارزش مانند روغن‌های فرّار، فلاوونوئیدها و اسیدهای فنلی است. با این‌حال، همانند بسیاری از گیاهان معطر دیگر، برگ به‌لیمو به دلیل داشتن محتوای رطوبت بالا فسادپذیر است. هدف از این کار پژوهشی مطالعه اثر دمای هوا (45، 55 و 65 درجه سانتی‌گراد) روی ویژگی‌های کیفی برگ به لیمو طی خشک‌کردن هوای داغ (HAD) بود. همچنین، کینتیک خشک‌کردن مدل‌سازی شد. نتایج نشان داد که دمای خشک‌کردن بالاتر منجر به کاهش معنی‌دار ($p<0/05$) نسبت جذب آب مجدد به علت تغییر ویژگی‌های ساختاری برگ‌های خشک شده گردید. محتوای روغن فرار برگ‌های خشک شده نیز به دلیل از دست رفتن مقادیر بالای اجزای فرار به طور معنی‌داری ($p<0/05$) در مقایسه با برگ‌های تازه متفاوت بود و در محدوده 0/42 تا 0/85 قرار داشت. علاوه بر این، با خشک‌کردن نمونه‌ها در 65 درجه سانتی‌گراد در مقایسه با 45 درجه سانتی‌گراد ، افزایش معنی‌دار مقدار ضریب انتشار مؤثر رطوبت (D_{eff}) و تغییر رنگ مشاهده شد. مقدار D_{eff}از $1/140\times10^{-10}$ تا $2/280\times10^{-9}$ m/s متغیر بود و مقدار انرژی فعال‌سازی 31/04 kJ/mol تعیین شد. بیشترین مقدار R^2 (0/999≤) و کمترین مقدار RMSE و SSE برای مدل نقوی و همکاران (پیشنهاد شده در این پژوهش) به دست آمد.

واژه‌های کلیدی: تغییر رنگ، خشک‌کردن همرفتی، ضریب انتشار مؤثر رطوبت، روغن فرّار، مدل‌سازی، برگ به‌لیمو، نسبت جذب آب مجدد

1-باشگاه پژوهشگران جوان و نخبگان، واحد تبریز، دانشگاه آزاد اسلامی، تبریز، ایران
2 - دانش‌آموختهٔ کارشناسی ارشد، گروه علوم و صنایع غذایی، دانشگاه آزاد اسلامی واحد سبزوار، سبزوار، ایران
(*- نویسنده مسئول : Email: E_naghavi@tabrizu.ac.ir)

Iranian Food Science and Technology Research Journal
Vol. 12, No. 6, Feb. Mrch. 2017, p. 730-741

نشریه پژوهشهای علوم و صنایع غذایی ایران
جلد 12، شماره 6، بهمن - اسفند 1395، ص. 741-730

Investigating the relationship between the perceived thickness of the chocolate pudding in sensory and instrumental analysis

N. Samanian[1], S. M. A. Razavi[2*]

Received: 2015.11.08
Accepted: 2016.08.06

Abstract

Sensory evaluation of food materials is an important factor to choose and even produce new formulations. Being time consuming, results in being difficult to interpret and the necessity to educate specialists make these methods kind of impractical. In this study, we have made an effort to introduce physical properties as a substitute for sensory evaluations in a semi solid food such as chocolate pudding. Higher reliability, reproducibility and higher pace are among some of the advantages of instrumental measurements. Thus, if sensory evaluation can be predicted based on physical properties solely, besides increasing the inspection pace, they would be available to be used online. The obtained results can also be used in designing new products for special consumers such as the dysphasia patients. The results showed that parameters such as shear viscosity, plastic viscosity, yield stress, extensional viscosity, apparent modulus and adhesive force can be used to design and produce new materials; they make sense beside each other though. In this way, the products which have been designed for the patients with swallowing difficulties should have suitable texture in mouth and also good swallow ease.

Key words: Dessert, Principal Component Analysis, Rheology, Sensory, Texture, Viscosity.

Introduction

The importance of food texture has been highlighted since 1960; the time where Szczesniak presented a new category for texture attributes (Mathmann, *et al*., 2007). He defined texture as the food structure and a way to physiological sense. The mechanical receptors are sensitive to the strain in the food paste and transmit the signals to brain. But at the moment, the aim of studies in this field is identifying the sensory characteristic independent from the sensory evaluations and just with knowing its physical characteristics (Chen, 2009, Mishellany-Dutour, 2006). To achieve this, the usage of a tongue-palate model system has been well designated. Due to mouth anatomy, including lips, teeth, tongue and palate as the organs responsible for speech, mastication and swallowing, the so-called model is limited thus to the fluid flow between the palate and tongue. Considering these two parallel sheets, the flow can be defined in mouth. (Mathmann, *et al*., 2007).

During chewing, the food material changes shape from its initial form to a bulk which is easy to swallow, this soft bulk which is the result of mastication and being mixed with saliva is called bolus. Chewing is the main oral operation for solids and semi-solids and changes the food pieces to particles which are small enough to be mixed with saliva. Thus the result of chewing is a soft bolus which can be swallowed safely (Chen, 2009; Chen & Lolivert, 2009; Funami, 2011; Loret, *et al*., 2011). Strassburg *et al*., (2005) analyse the intra-oral pressures and stress fields according to the concentration of particles randomly distributed in the food suspensionwith the aim to explain the sensation of grittiness. Even though swallowing is a routine action known well to each health individual, its controlling mechanisms and the determining criteria in triggering a swallowing are still little known. There has been no quantifiable parameter to assess the extent of a food being orally processed and its readiness for swallowing. Hutchings and Lillford (1988)

1 and 2. PhD student and Professor, Department of Food Science and Technology, Faculty of Agriculture, Ferdowsi University of Mashhad, Iran, Respectively.
(Corresponding Author Email:s.razavi@um.ac.ir)
DOI: 10.22067/ifstrj.v12i6.50418

were probably the first to address this issue by proposing three degrees of an eating process: the degree of food structure, the degree of lubrication, and the time. It was proposed that, before a swallowing is triggered, a critical threshold must be reached for all three factors: a long enough oral processing time, small enough food particles, and a proper oral lubrication. Even though there has been no experimental evidence to support this theory then, some complimentary experiments such as Engelen *et al*. placed emphasis on the particles' dimension, shape and quantity (Engelen *et al*., 2005). From this approach, the research on food brittleness and bolus rheology is being rapidly increased nowadays, because it is the key approach to optimize foods for different purposes e.g. dysphasia patients (Funami, 2011). Though this approach has been tested by many researches, it has mostly been focused on the solids and foods with low fluidity and deformability such as vegetables, nuts or different kinds of meat (Jalabert- Malbus *et al*., 2007; Lucas *et al*., 2002; Mishellani-dutour, 2006; Peyron *et al*., 2004). But viscoelastic gels, which can be used as a base for dysphagia food, have rarely been studied (Chen & Lolivert, 2009). The rheology of semi-solid food, such as gels and jams with special focus on the ease of swallowing and food extensionability, as key factors in triggering a swallowing action has recently been noticed (Ishihara *et al*., 2011a). This attitude is different as a result of using shear viscosity as a prominent rheological property. The viscosity is measured at different shear rates so that we can imitate the passage of food through the oral cavity (Kumagai *et al*., 2009).

Mechanical cohesiveness of the food bolus can be the other prominent rheological parameter to describe the swallow act. It has been reported that mechanical properties of the different food bulk are slightly different for different individual (Prinz & Lucas, 1997). This leads us to predict how fast and easy the food turns into its swallowable form, which is a very important feature for designing food for different uses.

Based on Wikipedia definition, chocolate pudding is a kind of milk based dessert which contains starch, sugar and is chocolate flavored. There are two different kinds of this product, a kind which is set after boiling and contains starch, and a kind which is baked by steam and has a cake-like texture.

To achieve the desirable thickness for this dessert we need hydrocolloids. Two frequently used gums in sweet desserts are guar gum and xanthan gum. Guar gum is a kind of galactomannan and its chemical structure is based on a (1, 4)-linked β-D-mannose backbone and (1, 6)-linked-D-galactose side chains. Its mannose to galactose ratio is around 1.8, due to the different substitution of the galactose, this gums have different solubility in water (Alexander, 1999; Anderson, 1988).

Xanthan is a microbial hetero-polysaccharide and is resulted from the aerobic fermentation of the bacteria *Xanthomonas campestris*, which has a main cellulose chain and on each second chain a side chain of two mannose units exist which have been separated from each other by a glucorunic acid chain (Casas, 2000, Dickinson, 2003).

Kokini & Cussler (1987) used a tongue-palate system to predict the thickness perception in mouth for a food suspension. The shear stress caused by the horizontal and vertical movements of the sheets was measured based on the mechanical information and geometrical properties of the system. In that work, a correlation was made between this data and the apparent relative thickness was calculated. Thus the apparent thickness of every food deducted from the shape of its flow diagram. In another work, Kokini, 1987 also observed that the creamy sense can be predicted through three other factors namely thickness, lubricity and fluidity. These three characteristics were able to explain the differences between the creaminess observed in a group of 16 commercial products with different rheological properties.

In the recent works, the rheological properties of the food bolus have been studied using the polysaccharide gels (Ishihara et al., 2011b). The food bolus has being produced through instrumental chewing, with and without artificial saliva. The gels were inserted in an instrument with a flat plunger. The most common gels used, were gellan (a relatively elastic gel) and a mixture of gellan and psyllium (a relatively plastic gel).

The model bolus is tested as a set of micro gels and gels consisting gel parts with different sizes due to the mechanical chewing (Ishihara *et al.*, 2011a). As a conclusion it can be said that finding suitable weak gels with high affinity to saliva is the key step to design foods for dysphasia patient or any other kind of food with desirable texture.

Chen *et al.* (2011) studied the effect of rheological properties, namely shear and extensional flows of the food gels and their relative bolus was measured at body temperature (37°C). It was seen that the shear viscosity has got a positive correlation with difficulty of swallowing, however the extensional behavior of the food products is better correlated to this factor.

To look for possible relationship between the sensory attributes of the chocolate pudding as a suitable and enriched dessert for the patients with swallowing disorders, and the physical properties of this food product, two commercial gums, xanthan and guar gum, were added in different concentrations to the chocolate pudding, so that the sensory evaluation of the individuals can be investigated beside the physical properties such as extensional and shear viscosity and texture parameters. So, the steady shear rheological properties of the samples containing the two gums were measured and the flow behavior was modeled using different time-independent rheological models. Also to find a good relationship between sensory attribute and rheological features extensional viscosity as a less literature highlighted attribute was also measured. To make sure of the so-called correlation, texture studies were also performed and finally the principle component analysis was done to categorize the features and select the most effective ones.

Material and methods

Chocolate pudding preparation

The ingredients including milk, sugar, wheat flour, vanilla and cocoa powder were purchased from the local market. Due to the literature review which was done before, two selected gums i.e. guar and xanthan were used in three concentrations (0.05, 0.075, and 0.1). First of all, the ingredients were added to milk at room temperature and were mixed till they were dissolved adequately. Then, the mixture was heated to fixed temperature of 75°C that is the approximate temperature at which starch is gelatinized. At this temperature, mixing was continued for 10 more minutes. After that, the pudding was transferred into the special plates with randomized colors in order to the sensory evaluations to be performed. Before carrying out the consequent analysis, the samples were kept for 24 hours at refrigerator (4± 1).To prevent the moisture loss, the sample containers were completely sealed.

Sensory evaluations

In order to do the sensory evaluations, 9 judges from both genders and different age range (6 males and 3 females between 18 to 35 years old) were selected. To screen the panelists at the first training session, two identical samples were presented to 15 persons, in two plates with different numbers and colors, and the sensory panel was performed as the main one. Among them, 9 people with best responses were chosen according to the results of statistical analysis.

After receiving the necessary instructions, 50 ml of pudding samples were presented to panelists in colored plates with codes. Every sample was judged twice by the panelist and in each session three samples along with the control sample were tested. The desired

characteristics were appearance, texture, mouth feel, swallow ease and the time needed for swallow, which were marked on a scale of 1 to 5. One is being the least and 5 the most desirable. To obtain the time needed to swallow, the panelists were asked to give a signal by their hands when they have swallowed the sample and the chronometer was started as soon as they put the sample in their mouth (Chen & Lolivert, 2011).

Instrumental texture analysis

The forward extrusion test was performed using a QTS texture analyzer (CNS Farnell Com, U.K). The pudding sample was placed in an aluminum cylinder container (l=0.1m, r=0.05m). The load cell used was 5 kg and the probe (a round aluminum plate 0.01 m thickness and 0.048m thickness) moved downward with a speed of 1mm/s. For each test, some textural parameters including fracture force, apparent modulus, hardness, cohesiveness, adhesiveness and adhesive force were also determined using QTS software from force-deformation data.

Shear viscosity measurement

To determine the flow behavior of the samples, a Bohlin rotational viscometer (Bohlin Model Visco 88, Bohlin Instruments, UK) equipped with a temperature control system (Julabo, Model F12-MC, Julabo Labortechnik, Germany) was used, and the temperature was set as 37°C±0.1. Appropriate measuring spindle (C14) was used during viscosity measurements according to the viscosity of samples. Each sample was subjected to a programmed shear rate logarithmically increasing from 15to 200 s^{-1} and each measurement was repeated 3 times. After the measurements, flow behavior of samples was described by fitting shear stress (τ)-shear rate ($\dot{\gamma}$) data with four models: Power-law, Herschel-Bulkley, Bingham and Sisko (Steffe, 1996). To select the best model describing time-independent rheological properties of pudding samples, two statistical parameters including RMSE (Root Mean Square Error) and R^2 (coefficient of determination) were determined using Excel (2007). Apparent viscosity of all samples at shear rate of 50 s^{-1} was also calculatedto compare the sensory and rheological data. It should be mentioned that viscosity measurements at 50 s^{-1}, as suggested by Wood (1968), were in reasonable agreement with those derived from panel scoresand it has been reported as an effective oral shear rate (Morris, 1993).

Extensional viscosity measurement

Based on Steffe (1996), for a standard material, in which the ratio between shear and extensional viscosities is small, the extensional viscosity is proportional to entrance pressure drop divided by the apparent wall shear rate in the die:

$$\eta_E = C\frac{\delta P_{en}}{\Gamma} \quad (1)$$

Where, C is a dimensionless constant, which is a function of the system geometry, and does not depend on strain rate or rheological properties of the system. This constant can be calculated using a material with known extensional viscosity in the measuring system. In this study, the silicon oil, which is a Newtonian fluid, was used. The apparent wall shear rate is defined as:

$$\Gamma = \frac{4Q}{\pi R^3} \quad (2)$$

Where, Q and R are volumetric flow rate and orifice radius, respectively. This equation can be used for a zero length die where it is assumed that the entire pressure drop is the entrance loss. The system is illustrated in Fig.3. In this system, a plunger is moving down with the constant velocity (u_z) and forces the material out of an orifice with 90° angel. The entrance pressure loss can be calculated using the force on the plunger and its cross sectional area, as given by eqn.3.

$$\delta P_{en} = \frac{F}{\pi R_b^2} \quad (3)$$

Where, R_b is plunger radius. Assuming the material incompressible, the volumetric flow rate through the orifice is

a function of plunger velocity:

$$Q = u_z \pi R_b^2 \quad (4)$$

Using eqn. 1 and the above definitions, eqn.5 can be estimated:

$$\eta_E = \left(\frac{C}{4\pi}\right)\left(\frac{FR^3}{u_z R_b^4}\right) \quad (5)$$

In this work, as shown in Fig.1 we used a cylindrical barrel with 0.05m radius, 0.1m height and a 10 mm orifice. The temperature of system was fixed at 37°C using a water bath. The measuring of maximum force was done using the QTS texture analyzer (CNS Farnell Com, U.K).The plunger velocity was set as 1 mm/s based on the information which exists in literature to imitate swallowing (Ishihara *et al.*, 2011a).

Principle component analysis (PCA)

The PCA analysis was performed to find out the relationship between different variables existing in this study. This analysis was completed using a SPSS package (IBM SPSS statistics 20).

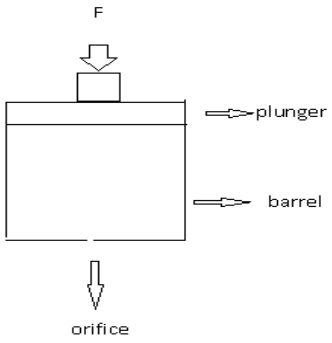

Figure 1.The measuring apparatus of the flow through the orifice is controlled by the plunger

Result and discussion

Sensory attributes

Fig. 2a & b shows the results of the sensory evaluation for samples containing guar and xanthan. It can be seen that the puddings containing guar gum demonstrated a more regular procedure, which is nearly the same for all the parameters. The sample with the highest concentration had the most desirable appearance and texture, and the control sample showed the best mouth feel and highest swallow ease. At 0.075%, a sudden downfall in the desirability of the samples was observed.

The samples containing xanthan showed this trend just for the appearance of the samples and about the other parameters, just opposite of the guar, the sample containing 0.075% xanthan had a relative desirability. This difference may be due to the different thickness caused by these two gums. As xanthan causes a high viscosity at low concentrations, the concentration higher than 0.1, the stiffness of the samples becomes undesirable.

About the mouth feel and swallow ease, due to the data it can be deducted that, the best sample according to the panelists, had an optimum level of thickness. Both the too smooth and too stiff samples were considered undesirable.

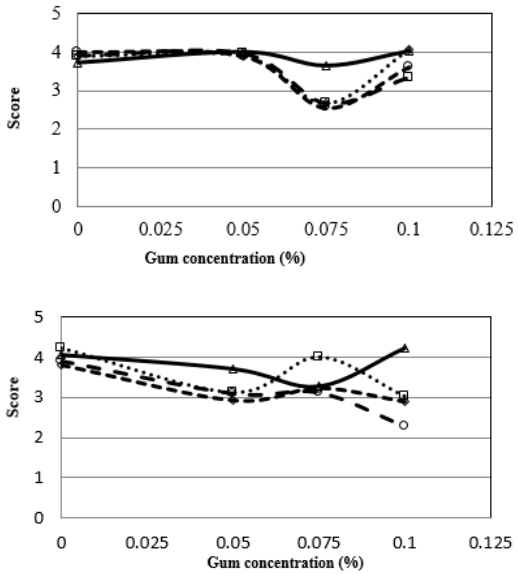

Figure 2.a) Sensory evaluation results obtained for chocolate pudding samples containing guar (Δ, appearance (sdv: 0.81); ◊, texture (sdv: 1.31); ○, mouth feel (sdv: 1.11); □, swallow ease (sdv: 1.08)) b) Figure 3b. Sensory evaluation results obtained for chocolate pudding samples containing xanthan (Δ, appearance (dsv: 0.85); ◊, texture (sdv: 0.91); ○, mouth feel (sdv: 0.80); □, swallow ease (sdv: 0.77))

Textural parameters

The data related to the measured texture parameters for samples containing guar and xanthan are presented in Table 1. As it can be resulted from the data, the control sample, which had the best swallow ease, showed the least adhesive force, least apparent modulus, least hardness and thus

the least stiffness. While the least swallow ease takes place for the sample containing 0.075% guar. Most characteristics of the sample are average and show a significant difference related to its higher and lower concentrations. This behavior is especially significant about apparent modulus, cohesiveness and adhesive force. The so-called data is the same for the sample containing 0.1 % of the xanthan. It can be deducted that about the swallow ease, the sample which has a specific level of thickness, is the most desirable one, i.e. the sample has to be fairly smooth or fairly stiff, and anything between these two is not suitable. This has to be considered while designing food for dysphasia patients (Chen, 2009).

About mouth feel, the sample with the least adhesiveness and the least cohesiveness, i.e. the sample containing 0.05 % guar is the best. Using some additives, it is possible to create a balance between this parameter and swallow ease. About the texture, the

Sample containing 0.1 % guar is evaluated as the best. As it can be seen in Table 1, among the other samples of the same gum, it possesses the highest adhesive force, cohesiveness and apparent modulus. The panelists found the sample which show a resistance to spoon the most suitable, the sample which is fluid-like while spooning is not ideal however.

Shear viscosity

Fig. 3a & b shows how the apparent viscosity of puddings changes with selected gum concentration for guar and xanthan, respectively. As it can be seen, all samples exhibited shear thinning behavior. Thus at the next step, four non-Newtonian rheological models were verified to interpret the steady state flow behavior.

Table 2 shows the values of two statistical parameters (R^2& RSME) determined for validation of the four rheological models used in this study. Based on this, two models i.e. Bingham and Herschel-Bulkley were chosen, due to having the highest R^2 and the least RMSE in all concentrations.

Based on the rheological parameters determined by the Bingham model (Table 3), the sample containing 0.075 % guar, which had the least swallow ease, has the highest plastic viscosity (μ_B).

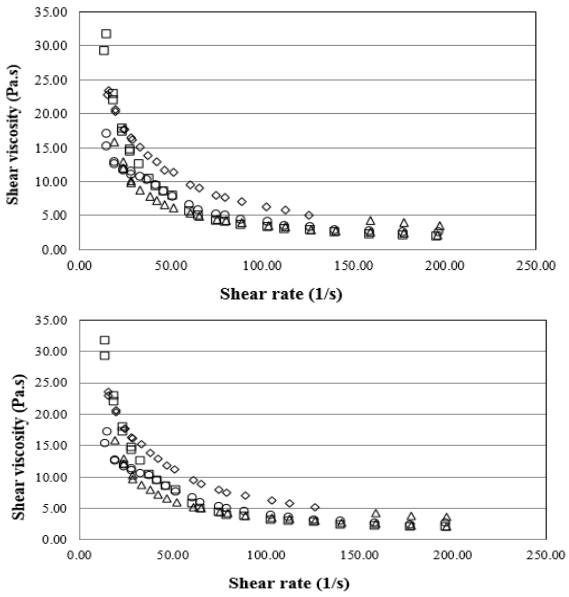

Figure 3. a) Change in apparent shear viscosity of chocolatepuddings containing different concentrations of guar (Δ, 0%; ◊, 0.05%;□, 0.075%; ○, 0.1%) b)Change in apparent shear viscosity of chocolatepuddings containing different concentrations of xanthan (Δ, 0%; ◊, 0.05%;□, 0.075%; ○, 0.1%)

In addition, the control sample, which had the best swallow ease, is the sample with the lowest yield stress (τ_{0B}). The sample with the lowest swallow ease showed an interesting behavior in Herschel-Bulkley model as well and has a higher consistency coefficient (K_{HB}) (Table 4). At the same time, in the Herschel-Bulkley model, it has less yield stress (τ_{0HB}) compared to other samples. It seems that the consumer likes the sample which needs a specific amount of stress to flow and also after being exposed to the stress field of the mouth fluidize faster. The sample containing 0.1% of xanthan has a significant consistency coefficient; however it doesn't have a good mouth feel, suggesting that the yield stress has a more fundamental role in mouth feel perception. This sample also has a high apparent viscosity (η_{app}) which is almost twice as high as the control sample. The

sample containing 0.075% guar which was not desirable enough has a relatively low apparent viscosity in compare to the sample containing xanthan at the same concent- ration. This also suggests that according to the consumers the before-noted optimum apparent viscosity- neither too stiff nor too smooth samples with enough yield stress to be overcame seem to be the best.

Extensional viscosity

The extensional viscosity data is presented in Table 5. The sample containing 0.075 % guar has the least extensional viscosity and is nearly one third of this amount for the control sample. About this also there is a specific amount for being considered suitable. The extensional viscosity cannot be the only criterion to judge from, when assessing the sample for swallowing. The result may be the manifold phenomena involved in swallowing; the effect of the shear stress caused by the sample which is being processed in mouth is one of them. (Kumagai *et al*., 2009).

PCA analysis

Fig 4 shows the result of PCA analysis for the different sensory factors for samples containing xanthan and guar. As it is seen, for guar the sensory attributes have a near relationship, and this relationship is positive, but about xanthan gum, mouth feel and swallow ease, while having a near relationship are not in agreement with texture and appearance. This suggests the need for a change in formulation to improve the appearance and texture of the pudding through other additives or ingredients such as natural colors and milk powder. The PCA analysis about the swallow ease in the samples containing xanthan at different concentrations (Fig. 5) showed that nearly all the shear viscosity parameters of the used models (Herschel-Bulkley and Bingham) and the extensional viscosity have a near relationship, as it can be seen, the plastic viscosity by being exactly on the other side of the diagram's diameter, seems to have a very strong negative effect on swallow ease, and the same thing was deducted based on the sensory analysis results. The other important factor seems to be the yield stress both in Bingham and Herschel-Bulkley models. This again approves the result of the shear viscosity effect on swallow ease. About the mouth feel, the yield stress in both Bingham and Herschel-Bulkley models is more important, which was also reported in shear viscosity data. Fig. 6 shows the PCA analysis for guar gum. As it can be seen, the relationship between the components for samples containing guar gum is more complicated. For this gum, the important effect of plastic viscosity can be seen here; also the extensional viscosity becomes fairly important, which was seen in the extensional viscosity results as well. About mouth feel similar to the shear viscosity results, the yield stress of the Bingham model introduces itself as an effective factor, though this value in Herschel-Bulkley model does not influence mouth feel as strong as it does in xanthan gum. These results also indicate that there is not just a sole factor determining the sensory acceptability, rather it is a result of multiple factors playing their rules together.

Conclusion

In this work, we tried to obtain physical knowledge on chocolate pudding as a nutritious semi-solid dessert, in order to develop correlation between the sensory evaluation and reliable characteristics such as apparent shear viscosity, plastic viscosity, yield stress, extensional viscosit-y and textural parameters of the product.

The results showed that though each of these parameters can be interpreted due to the sensory evaluation results, none can be the only possible answer, because the swallowing action is the result of many physical phenomena cooperating with each other. However, for specific designing goals, they can be looked at individually or as a collection, e.g. the products specialized for dysphasia patient should have suitable swallow ease beside good mouth feel. Thus the sample with average

extensional viscosity, low yield stress and relatively high consistency coefficient can be the right choice that can be achieved using the right additives. At the same time, these parameters can be good evaluation criterion and can eliminate the need for the difficult and time consuming sensory evaluations. Although the PCA analysis showed the more important factors determining the sensory desirability of the chocolate pudding for different purposes, but the effect of the other factors cannot be underestimated. At the moment, the studies in this area are still very naive and more effort is necessary to study the phenomena involved in mastication and chewing and making them closer to real conditions

Table 1. The results of instrumental texture analysis determined for chocolate puddings containing selected gums

Treatment	Concentration (%)	Apparent modulus (N/s)	Fracture force (N)	Hardness (N)	Cohesiveness (Ns)	Adhesiveness (Ns)	Adhesive force (N)
Control	0	14.43±0.23	9.92±0.60	16.20±0.29	114.56±40	-5.14±0.23	-1.61±0.15
Guar	0.05	15.62±0.22	5.88±0.23	16.15±0.20	47.53±0.31	-2.96±0.21	-1.61±0.10
	0.075	32.48±0.30	4.08±o.11	17.63±0.26	56.88±0.28	-5.31±0.17	-1.73±0.25
	0.1	46.34±0.32	10.34±0.40	49.24±0.23	118.99±0.34	-6.07±0.21	-2.67±0.22
Xanthan	0.05	20.26±0.28	20.27±0.26	20.81±0.25	134.00±0.41	-6.43±0.11	-1.53±0.25
	0.075	22.48±0.13	15.31±0.16	19.50±0.33	122.43±0.33	-7.49±0.26	-1.70±0.15
	0.1	37.96±0.33	33.21±0.22	22.07±0.30	144.79±0.36	-6.97±0.20	-1.97±0.13

Table 2. The values of statistical parameters of four non-Newtonian rheological models determined by fitting of flow curves of chocolate puddings containing Guar

Gum (%)	0		0.05		0.075		0.1	
Model	R^2	RMSE	R^2	RMSE	R^2	RMSE	R^2	RMSE
Power law	0.988	0.396	0.991	0.351	0.973	0.690	0.965	0.702
Herschel-Bulkley	0.994	0.572	0.995	0.476	0.972	0.688	0.980	0.933
Sisko	0.994	0.994	0.996	0.216	0.978	0.432	0.993	0.581
Bingham	0.994	0.266	0.995	0.253	0.972	0.652	0.988	0.365

R^2, coefficient of determination; RSME, Root Mean Square Error

Table 3. The values of statistical parameters of four non-Newtonian rheological models determined by fitting of flow curves of chocolate puddings containing Xantan

Gum (%)	0		0.05		0.075		0.1	
Model	R^2	RMSE	R^2	RMSE	R^2	RMSE	R^2	RMSE
Power law	0.988	0.396	0.966	0.209	0.97	0.69	0.96	0.70
Herschel-Bulkley	0.994	0.572	0.972	0.210	0.995	0.212	0.995	0.212
Sisko	0.994	0.994	0.979	0.211	0.998	0.213	0.996	0.210
Bingham	0.994	0.266	0.934	0.206	0.967	0.209	0.994	0.212

R^2, coefficient of determination; RSME, Root Mean Square Error

Table 4. The parameters of Bingham model (μ_B, Bingham plastic viscosity; τ_{0B}, Bingham yield stress; η_{app}, apparent viscosity at 50 s^{-1}) obtained for chocolate puddings containing selected gums

Treatment	Concentration (%)	μ_B (Pa.s)	τ_{0B} (Pa)	η_{app} (Pa.s)
Control	**0**	**0.844**	**184.41**	**4.532**
Xanthan	0.05	0.730	209.35	4.917
	0.075	0.374	276.06	5.895
	0.1	2.478	445.15	11.381
Guar	0.05	2.218	224.15	6.701
	0.075	3.449	332.49	10.098
	0.1	1.319	455.70	10.433

Table 5. The parameters of Herschel-Bulkley model (K_{HB}, consistency coefficient; τ_{0HB}, yield stress; n_{HB}, flow behaviour index; η_{app}, apparent viscosity at 50 s^{-1}) obtained for chocolate puddings containing selected gums

Gum	Concentration (%)	K_{HB} (Pa.s^n)	τ_{0HB} (Pa)	n_{HB}	η_{app} (Pa.s)
Control	**0**	**44.431**	**205.66**	**0.14**	**5.64**
Xanthan	0.05	40.919	301.01	0.260	8.28
	0.075	14.691	386.66	0.200	8.37
	0.1	51.334	507.89	0.376	14.52
Guar	0.05	19.526	625.41	0.114	13.11
	0.075	63.4	191.41	0.184	6.43
	0.1	45.1	415.42	0.316	11.40

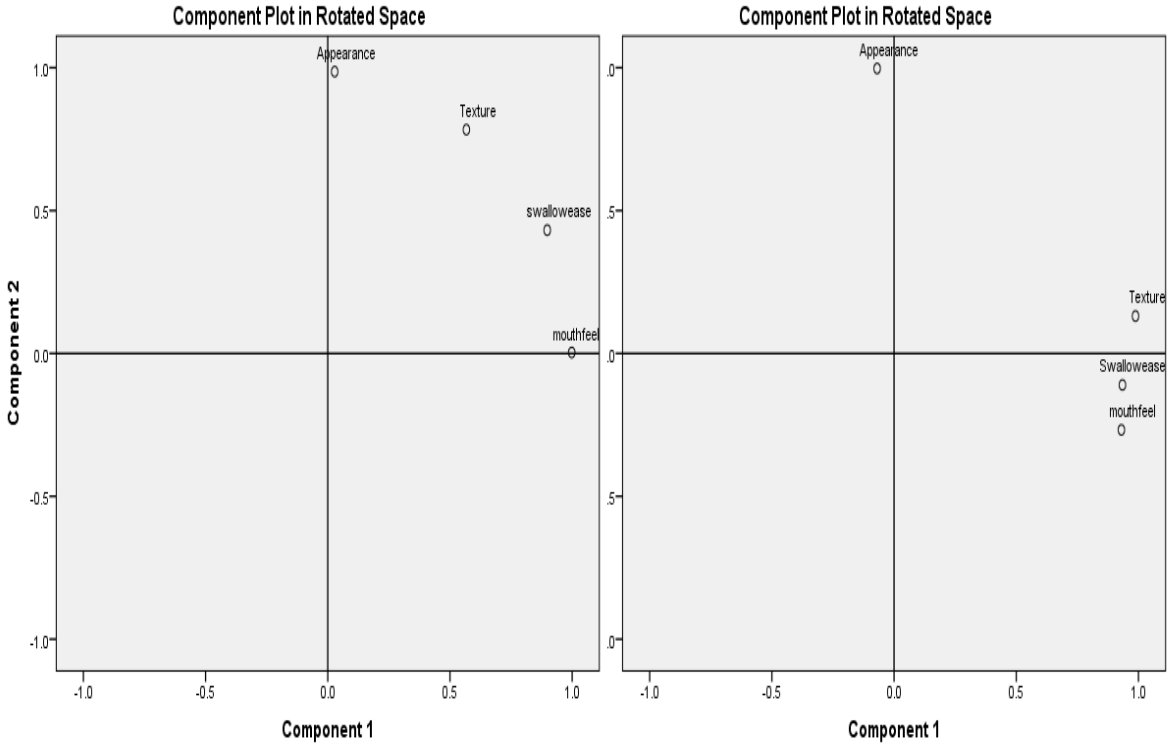

Figure 4. The PCA analysis for the sensory factors of chocolate puddings containing guar (left) and xanthan (right)

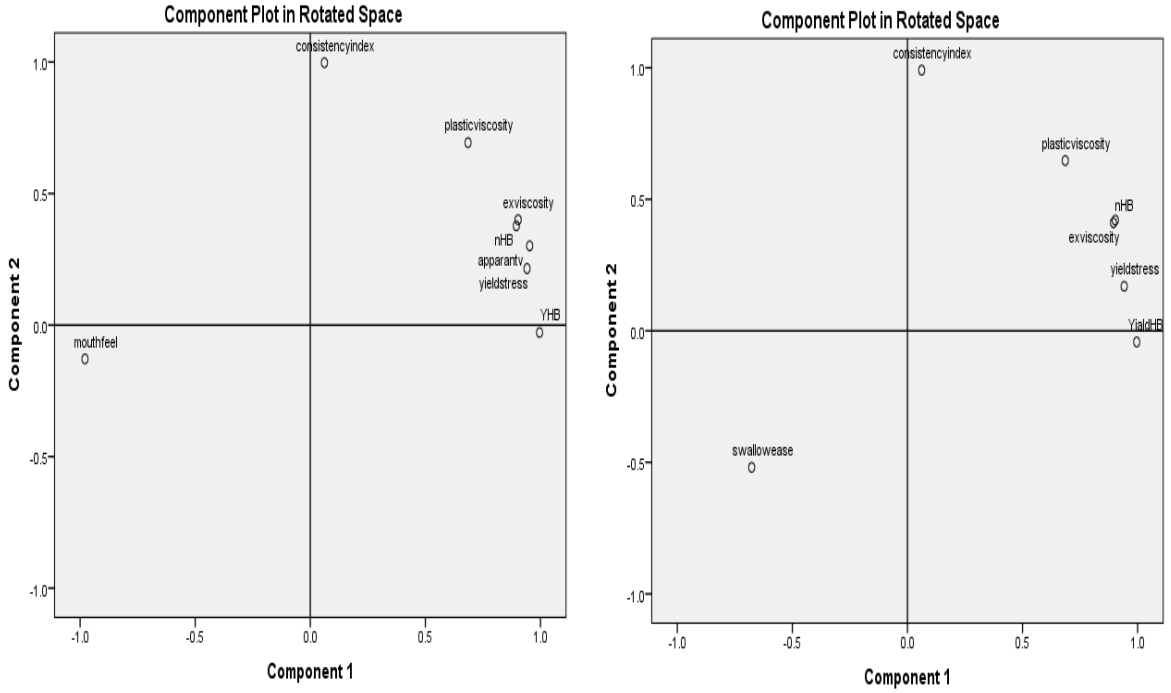

Figure 5. The PCA analysis diagram for xanthan gum on mouth feel (left) and swallow ease (right) with shear viscosity parameters and extensional viscosity

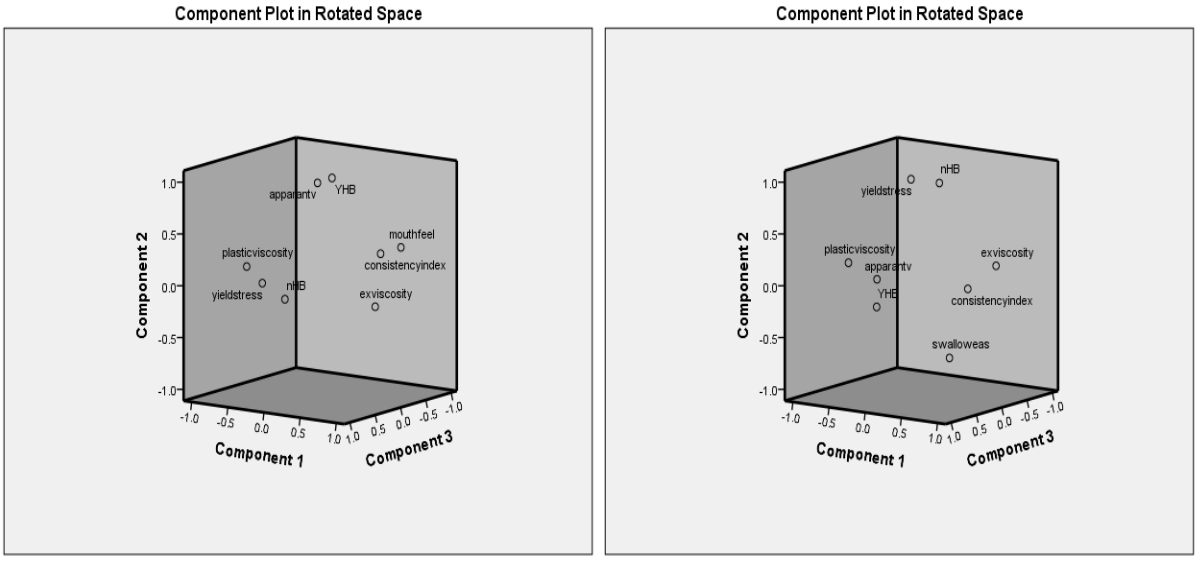

Figure 6. The PCA analysis diagram for guar gum on mouth feel (left) and swallow ease (right) with shear viscosity parameters and extensional viscosity

Table 6. Extensional viscosity of chocolate puddings as a function of gum type and concentration

Treatment	Concentration (%)	Extensional viscosity (Pa.s)
Control	**0**	**922.268±6.0**
Xanthan	0.05	1884.512±2.2
	0.075	1423.379±1.3
	0.1	3087.551±4.0
Guar	0.05	544.807±2.6
	0.075	379.320±1.6
	0.1	961.315±2.2

References

Alexander, R. J. (1999). Hydrocolloid gums. Part I: Natural products. *Cereal Foods World*, 44: 684–687.

Alexander, R. M. (1998). News of chews: the optimization of mastication. Nature: 391, 329.

Anderson, D. M. W., &Andon, S. A. (1988). Water-soluble food gums andtheir role in product development. *Cereal Foods* World, 33: 844.

Arcia ,P.L., Costell, V., Tárrega, V. (2010). Thickness suitability of prebiotic dairy desserts: Relationship with rheological properties. *Food Research International* 43: 2409–2416.

Casas, J. A., Santosa, V. E., & Garcı´a-Ochoa, A. (2000). Xanthan gumproduction under several operational conditions: Molecular structure and rheological properties. *Enzyme and Microbial Technology*, 26: 282–291.

Chen, J. (2009). Food oral processes a review. Food Hydrocolloids, 23:1-25.

Chen, J., & Lolivret, L. (2011). The determining role of bolus rheology in triggering a swallowing. *Food Hydrocolloids*, 25: 325-332.

Dickinson, E. (2003). Hydrocolloids at interfaces and the influence on the properties of dispersed systems. *Food Hydrocolloids*, 17: 25–39.

Engelen, L., van der Bilt, A., Schipper, M. & Bosman, F. (2005). Oral size perception of particles: effect of size, type, viscosity and method. *Journal of Texture Studies*, 36, 373–386.

Hutchings, J. B., & Lillford, P. J. (1988). The perception of food textured the philosophy of the breakdown path. *Journal of Texture Studies*, 19, 103-115.

Ishihara, S., Nakauma, M., Funami, T., Odake, S., & Nishinari, K. (2011a).Swallowing profiles of food polysaccharide gels in relation to bolus rheology. *Food Hydrocolloids*, 25: 1016-1024.

Ishihara, S., Nakauma, M., Funami, T., Odake, S., & Nishinari, K. (2011b).Viscoelastic and fragmentation characters of model bolus from polysaccharide gels after instrumental mastication. *Food Hydrocolloids*, 25: 1210-1218.

Jalabert-Malbos, M. L., Mishellany-Dutour, A., Woda, A., &Peyron, M. A. (2007). Particle size distribution in the food bolus after mastication of natural foods. *Food Quality and Preference*, 18:803-812.

Kohyama, K., Sasaki, T., & Hayakawa, F. (2008).Characterization of food physical properties by the mastication parameters measured by electromyography of the jaw-closing muscles and mandibular kinematics in young adults. *Bioscience, Biotechnology, and Biochemistry*, 72: 1690-1695.

Kokini,J.L., (1987).The physical basis of liquid food texture and texture-taste interactions. *Journal of Food Engineering* 6: 5l-81.

Kokini, J.L. & Cussler, E.L. (1987).The psychophysics of fluid food texture. In: Food Texture – Instrumental and Sensory Measurement (edited by H.R. Moskowitz). Pp. 97–127. New York, NY: Marcel Dekker.

Kumagai, H., Tashiro, A., Hasegawa, A., Kohyama, K., & Kumagai, H. (2009). Relationship between flow properties of thickener solutions and their velocity through the pharynx measured by the ultrasonic pulse Doppler method. *Food Science and Technology Research*, 15: 203-210.

Lucas, P. W., Prinz, J. F., Agrawal, K. R., & Bruce, I. C. (2002). Food physics and oral physiology. *Food Quality and Preference*: 13, 203-213.

Mathmann, K., Kowalczyk, W., Petermeier, H., Baars, A., Eberhardl, M. & Delgado, A. (2007).A numerical approach revealing the impact of rheological properties on mouthfeel caused by food. International *Journal of Food Science and Technology*.42: 739–745

Mioche, L., Bourdiol, P., Monier, S., Martin, J. F., & Cormier, D. (2004). Changes in jaw muscles activity with age: effects on food bolus properties. *Physiology & Behavior*: 621-627.

Mishellany-Dutour, A., Woda, A., Labas, R., & Peyron, M. A. (2006). The challenge of mastication: preparing a bolus suitable for deglutition. *Dysphasia*: 21: 87-94.

Peyron, M. A., Mishellany-Dutour, A., &Woda, A. (2004).Particle size distribution of food boluses after mastication of six natural foods. *Journal of Dental Research*, 83: 578-582.

Steffe, J.F., (1996). Rheological methods in food process Engineering. Second Edition. Freeman Press, USA.

Strassburg, J., Engmann, J., Burbidge, A.S., Hartmann, C. & Delgado, A. (2005). Sandigkeitsempfindung von Lebensmitteln im Mund– Ein fluidmechanisches Modell im Mikromassstab. Kurzfassung der Referate – Interne Arbeitssitzung des VDI-GVC-Fachausschusses 'Lebensmittelverfahrenstechnik', 7–9 March, Berlin.

Wood, F.W. (1968). Rheology and Texture of Foodstuffs, SCI Monograph, London

نشریه پژوهشهای علوم و صنایع غذایی ایران
جلد 12، شماره 6، بهمن - اسفند 1395، ص. 741-730

Iranian Food Science and Technology Research Journal
Vol. 12, No. 6, Feb. Mrch. 2017, p. 730-741

بررسی ارتباط بین قوام پودینگ شکلات در ارزیابی های حسی و دستگاهی

نرگس سامانیان[1]- سید محمد علی رضوی[2*]

تاریخ دریافت:1394/09/07
تاریخ پذیرش:1395/05/16

چکیده

ارزیابی حسی مواد غذایی فاکتور مهمی در انتخاب و تولید فرمولاسیون‌های جدید است. وقت‌گیر بودن، سختی تحلیل نتایج و لزوم تربیت متخصص این روش را تقریبا غیرکاربردی می‌کند. در این پژوهش ما تلاش کردیم ویژگی‌های فیزیکی را به‌عنوان جایگرین روش‌های حسی در ارزیابی محصولات نیمه جامد مانند پودینگ شکلاتی معرفی نماییم. اعتبار بالاتر، تکرار پذیری و سرعت بالاتر از جمله مزایای اندازه‌گیری‌های دستگاهی است. بنابر این اگر بتوان ویژگی‌های حسی را تنها بر اساس ویژگی‌های فیزیکی پیش‌بینی نماییم، علاوه بر افزایش سرعت بازرسی می‌توان از آنها به‌صورت برخط نیز بهره جست. همچنین می‌توان از نتایج به‌دست آمده برای طراحی محصولات جدید برای مشتری‌های خاص مانند افراد مبتلا به سختی بلع استفاده کرد. نتایج نشان داد پارامترهایی مانند ویسکوزیته برشی، ویسکوزیته پلاستیک، تنش تسلیم، ویسکوزیته کششی مدول ظاهری و نیروی چسبندگی می‌توانند در طراحی و تولید محصولات جدید مورد استفاده قرار گیرند، هر چند این پارامترها در کنار یکدیگر است که معنی‌دار می‌شوند. در این صورت محصولات تولید شده برای بیماران مبتلا به سختی بلع در کنار سهولت خورده شدن بافت مناسب هم خواهند داشت.

واژه‌های کلیدی: دسر، آنالیز اجزا اصلی، رئولوژی، حسی، بافت، ویسکوزیته

1 و 2- به‌ترتیب دانشجوی دکتری و استاد، گروه علوم و صنایع غذایی، دانشکده کشاورزی، دانشگاه فردوسی مشهد
(*- نویسنده مسئول : Email: s.razavi@um.ac.ir)

Iranian Food Science and Technology Research Journal
Vol. 12, No. 6, Feb. Mrch. 2017, p. 742-749

نشریه پژوهشهای علوم و صنایع غذایی ایران
جلد 12، شماره 6، بهمن - اسفند 1395، ص. 749-742

Isolation and identification of antioxidants components From Cumin seed (*Cuminum cyminum)*

S. Einafshar [1]*, H. Poorazarang[2], R. Farhoosh[2], J. Asili [3]

Received: 2016.01.25
Accepted: 2016.08.16

Abstract

Natural materials are complicated compositions; therefore, a rapid screening of the active antioxidants is being challenged in the literature. Different polarity solvents were applied to isolate four fractions (F1, F2, F3 and F4) of methanolic extract of *Cuminum cyminum*. Their anti-oxidative properties were tested using radical scavenging and FRAP assays. F3 (with IC_{50}=0.006mg/mL and FRAP= 521.95 mmolFe^{2+}/L) was significantly the most active fraction. Guided isolation through bio-autography on TLC using 1, 1- diphenyl- 2 – picryl-hydrazyl radical (DPPH) as a detection reagent led to the isolation of two antioxidant compounds from F3. F3 was injected to a preparative HPLC with the proper mobile phase (acetonitril: methanol/ water) and isolated two main compounds. These compounds were identified as Luteolin 7 glugoside and Apigenin 7 glucoside by means of ^{1}HNMR and ^{13}CNMR and compare them with references.

Key words: Antioxidant, Apigenin, *Cuminum cyminum*, Luteolin.

Introduction

A growing amount of evidence has shown that free radicals such as superoxide radical ($O^{\bullet -}_2$), hydroxyl radical (OH•), peroxyl radical (ROO•), and nitric oxide radical (NO•), attack biological molecules, such as lipids, proteins, enzymes, DNA and RNA. They play an important role in several pathological processes, such as cancer, atherosclerosis, and negative cellular changes associated with aging (Fisch *et al*., 2003; Nakman *et al*., 2003; shon, *et al*., 2003; Valentao, *et al*., 2002). Antioxidants are effective in protecting the body against these degenerative events. Synthetic antioxidants, such as butylated hydroxyanisol (BHA) and butylated hydroxytoluene (BHT) that are commonly used in lipid-containing food have safety and toxicity problems (Amarowicz *et al*., 2000; Howell, 1968). There is an increasing interest to seek for antioxidants naturally present in vegetables, fruits and functional herbs. Natural materials are complicated compositions therefore a rapidly screening of the active antioxidants is being challenged. A crude natural product extract is generally an extremely complicated mixture of several compounds possessing varying chemical and physical properties. The fundamental strategy for separating these compounds is based on their physical and chemical properties that can be effectively separated them into various chemical groups (Amarowicz *et al*., 2000).

Plant natural products are usually extracted with solvents of increasing polarity, for instance, at first extracted with petroleum ether, dichloromethane followed by more polar solvents, i.e., ethyl acetate. Methanolic extracts of plant materials contain a wide range of polar and moderately polar compounds (otsuka, 2006). By virtue of the co solubility, many compounds, which are insoluble individually in pure state in methanol can be extracted quiet easily with these solvents. Herein we use an activity guided

1. Department of Agricultural Engineering Institute, Khorasan Razavi Agricultural and Natural Resources Research and Education Center, AREEO, Mashhad, IRAN.
2. Ferdowsi University of Mashhad, Faculty of Agriculture, Department of Food Science and Technology, Mashhad, Iran.
3. Medical science of Mashhad, Faculty of medicine, Department of pharmacognosy.
Corresponding Author Email:Soodabeheyn@yahoo.com
DOI: 10.22067/ifstrj.v1395i0.53312

purification of natural antioxidants from methanolic extract of cumin seed (*Cuminum cyminum*) by partitioning between insolvable solvents (Satti *et al*., 2009).

Cumin seed L. is widely used as a spice. Crushed cumin seeds are used as a condiment in a variety of dishes. The proximate composition of the seeds indicates that it contains fixed oil (10%), protein, cellulose, sugar and other mineral elements (Winton, 1939). Cumin seed contains essential oil (2%–5%) that imparts the characteristic aroma to the seeds and the physicochemical properties of it have been reported (Guenther, 1950).

Phenolic compounds present in spices with natural antioxidant properties have been studied for substitution of synthetic antioxidants. Compare to many traditional medicinal plants, little is known about the active antioxidant matter of Cumin seed. Active principles of cuminaldehyde (cumin) are reported to inhibit lipid peroxidation (Shobana and Akhilender, 2000) and it has been reported that the ether extract of cumin seed inhibits biosynthesis of eicosanoids (Satti *et al*., 2009) which are a pain mediators. Modulating effects of cumin seed was explored and its active compound, immuno-modulatory properties were evaluated in normal and immune- suppressed animals (Chauhan, et al., 2009). A preliminary study of cumin seed chemical composition was made on its essential oil had shown the presence of flavonoid compounds (Gachkar et al., 2007; Li *et al*., 2009; Behera, *et al*., 2004) which act as antioxidants in edible oils (Vekiari *et al*., 1993). Einafshar (2012) showed that Cuminum cyyminum has antioxidative effects in both bulk amd emulsion systems.

In the present study an activity guided purification was conducted to isolate the free radical scavenging compounds from Cumin seed, the bioactive constituents from the seeds of *Cuminum cyminum* was isolated and quantificated and their chemical compositions identified.

Materials and Methods

Materials

Cumin seeds were obtained from international company of Pegah Saffron and Zire Green Gold (Mashhad, Iran). Refined, bleached, and deodorized sunflower oil (SFO) with no added antioxidant was supplied by Shadgol (Nishbour, Iran). All chemicals and solvents used in this study were of analytical reagent grade and supplied by Merck and Sigma Chemical Companies.

Plant material

The sample seeds were dried in an cabin drier at 55ºC for 2 days, ground into a fine powder in a mill (Mulinex Depose-Brevete S.G.C.G., France). The powders were extracted with methanol (1:20 w/v) by agitation in a dark place at ambient temperature for 48 h. The solvent was evaporated in vacuum at 40ºC. The desolventized extract (DEx) stored at -18ºC until use.

Extraction and isolation of antioxidant compounds

60 mg the methanolic extract of *Cumin seed* was dissolved in 100 ml methanol and extracted thrice using 100 ml petroleum ether under stir for 10 minutes. The upper phase of petroleum ether, contains nonpolar compounds such as lipids, chlorophyls and so on. This process is sometimes referred to as defatting. Although methanol and petroleum ether are not completely miscible, they are miscible to some extent. A small amount of water is added to methanol to obtain a 95% aqueous methanolic solution to get two distinct layers with similar volumes. Petroleum ether in the upper phase was removed by evaporation at 50°C under vacuum to give a residue named F1. The lower phase is partitioned in Dichloromethan and upper phase in ethylacetate successively and named F2 and F3 respectively. Less polar compounds are present in the dichloromethane soluble fraction and polar compounds, probably up to mono-glycosides, in the ethylacetate. The methanol fraction contains polar compounds mainly glycosides named F4.

The conventional spectrophotometric DPPH• scavenging capacity assay

The radical-scavenging activity was evaluated according to Chung *et al*. Two ml of the methanol solution of F1, F2, F3 and F4 were mixed with 1 ml of 0.5 mM DPPH• methanol solution and 2 ml of 0.1 M sodium acetate buffer (pH 5.5). After shaking, the mixture was incubated at room temperature in the dark for 30 min, and then the absorbance was measured at 517 nm using a Shimadzu UV-160A spectrometer, Kyoto (Japan). The IC_{50} value was determined as the concentration of each sample required to give 50% DPPH• radical scavenging activity.

FRAP test

Acetate buffer (0.3 M, pH 3.6) was prepared by dissolving 3.1 g $C_2H_3O_2Na.3H_2O$ and 16 ml of acetic acid in 1 l of distilled water. TPTZ (2, 4, 6 -tripyridyl-S-triazine) solution was prepared by dissolving 23.4 mg of TPTZ in 7.5 ml of 40 mM HCl solution. Ferric solution (20 mM) was prepared using $FeCl_3.6H_2O$. The final working FRAP reagent was prepared freshly by mixing acetate buffer, TPTZ and ferric solutions at a ratio of 10:1:1.

In brief, 900 µl FRAP (ferric reducing-antioxidant power) working reagent was mixed with 90 µl distilled water and was warmed to 37 ºC in a water bath. The reagent control reading was recorded at 595 nm, followed by adding 30 µl of sample solutions (100 mg in 10 ml of n-hexane). The absorbance was taken at 595 nm, against the control solution. A standard curve was prepared using different concentrations of $FeSO_4.7H_2O$ (200–2000 µmol/l). All solutions were freshly prepared. The results were expressed in mmol Fe^{2+}/l (Capannesi, et al., 2000).

HPLC preparative analysis

F3 methanol solution (1.0 mg/mL) was filtered through cellulose acetate membrane filter (0.45 mm, Anpu Co.,Shanghai, China) prior to HPLC analysis. 1 ml aliquot of the filtrate of concentration 3mg ml^{-1} in methanol was injected into a Wellchrom KNAUER HPLC, with reverse column (C18, 250 ×4.6 mm i.d., 5 mm), HPLC pump: KNAUER k-1001, UV detector: KNAUER k-2600, and eluted with a mobile phase containing solvent A (methanol) solvent B (acetonytril) and solvent C (water) (90:5:5) iso-cratically pumped at a flow rate of 1.0 mL/min. In the chromatogram the peaks of interest were observed at t_R 22.5 min and 27 min, detection was at 250nm. Compounds were collected in a clean, weighed flask from 21.5 to 25 min at room temperature under a room temperature. Multiple preparative HPLC separation was done and fractions for two peaks combined.

Processing of the collected fractions

The solvent was removed from the samples at 20°C with N_2 gas and the residual aqueous phases were shell-frozen on dry ice prior to freeze-drying. The freeze-dried samples were stored at -20°C until NMR analyses were performed. Complete removal of solvent was done by freeze drier and resulted yellow and yellow fade compounds powder.

NMR identification of compounds

NMR spectroscopy experiments on the compounds were performed on a Bruker Avance 500 at 500 MHz for ^1H NMR and ^{13}C NMR with CD_3OD and DMSO as solvent in 25 centigrade.

TLC bioautography analysis

An aliquot of AMS methanol solution (1 mg/mL, 3 mL) or individual pure isolate methanol solutions (1.0 mg/mL, 2 mL) was directly deposited (as spots or bands) onto the TLC plates. TLC plates were developed in a presaturated solvent chamber with ethyl acetate- acetonytril- formic acid- water- ethyl formiate (7:1:1:1.1:12) as developing reagents until the solvent front reached 1 cm from the top of plates. The developed TLC plates were then removed from Fig. 1. TLC plates stained with 2.54 mM DPPH_ solution in methanol, and visualized (A) under visible light, (B) under UV 254 nm, and (C) under UV 366 nm. Three microlitres Silica gel 60 F254 TLC plates (Merck, Germany) were used for TLC

bioautography analysis.

Result and discussion

DPPH• scavenging activity and FRAP tests of isolates

The conventional spectrophotometric DPPH• scavenging capacity assay was first used to screen the potential antioxidant of F1, F2, F3 and F4.The DPPH• scavenging activities of all the fractions were estimated using the conventional spectrophotometric DPPH• scavenging capacity assay. table.1 shows the quantities related to the DPPH radical-scavenging activities of the F1, F2, F3 and F4 compare to that of BHT (butylated hydroxy toluen) as an synthetic antioxidant. All fracions except F3 showed DPPH radical-scavenging activities extremely lower than that of BHT (F3=0.006, BHT=0.007, F1=1.47, F2=0.119 and F4=0.24 mg mL^{-1}). F3 showed significant DPPH• scavenging activities which were similar to that of BHT.

Table 1. The DPPH radical-scavenging activity (IC_{50}) and ferric reducing-antioxidant power (FRAP) of the total extract and four fractions of *Cumin seed*. Diethylether fraction (F1), dichloromethane fraction (F2), Ethyl acetate fraction (F3) and methanolic fraction (F4).τ

Antioxidant matter (100 ppm)	IC_{50} (mg/mL)	FRAP (mmol Fe^{2+}/L)
Total extract	0.74 ± 0.10 b	459.46 ± 0.81e
F1	1.47 ± 0.03 a	229.63 ± 0.28 f
F2	0.119 ± 0.003 d	495.52 ± 0.37 d
F3	0.006 ± 0.001 f	521.95 ± 0.91 b
F4	0.24 ± 0.002 e	500.82 ± 0.69 c
BHT	0.007±0.002 f	1955.72±0.98 a

τ Means ± SD (standard deviation) within a column with the same lowercase letters are not significantly different at $P < 0.05$

The antioxidant activity decreased as follows: F3> F2> F4 > F1

Many similarities were found to exist between the results of the FRAP test and those of the DPPH radical-scavenging activity assay. Table 1 demonstrates that the reducing power of F3 (521.95 mmol/L) was significantly lower than that of BHT and higher than those of total extract (459.46 mmol/L) and other fractions. The chelating abilities of F3 on ferrous ion were good as shown by their low IC_{50} value (0.006 mg/mL). This indicates that the chelating activity of F3 in metal ion may play an important role in their antioxidant activity.

In the present study the F3 was selected for further purification, since less is known about the antioxidants components in the seeds of Cumin seed.

Isolation of antioxidant compounds

F3 fraction was then monitored by a TLC bio-autography method to guide the separation procedure because this method gives quick access for detection and localization of the active compounds in a complicated plant extract (Tasdemir, *et al*., 2004). In this method, the DPPH• scavenging activity was observed visually as white yellow spots on a purple background. Fig. 1-A shows the profile of the antioxidant components in the F3 fraction of the methanolic extract of Cumin seed under visible light. At least two spots (such as a and b) in the chromatograms were observed to have DPPH• scavenging activities. In addition, the same stained TLC plate was also inspected under UV 254 and 366 nm.

Note that the antioxidant spots shown in Fig. 2A were also observed in those of Fig. 2B and C. However, it needs to be pointed out that the different detection sensitivities observed among Fig. 2 A–C were due to the diverse nature of the anti-oxidative compounds. For example, spot (a) was easily better visualized under 254 and 366 nm than that under visible light.

The F3 fraction was directly subjected to a preparative HPLC C18 column and eluted isocratically with methanol, acetonytril and water (90:5:5). Finally, two compounds were separated and identified, the structures of which are Apigenin-7-*O* glucoside and Luteolin- 7- *O* glucoside presented in Fig 2

and 3.

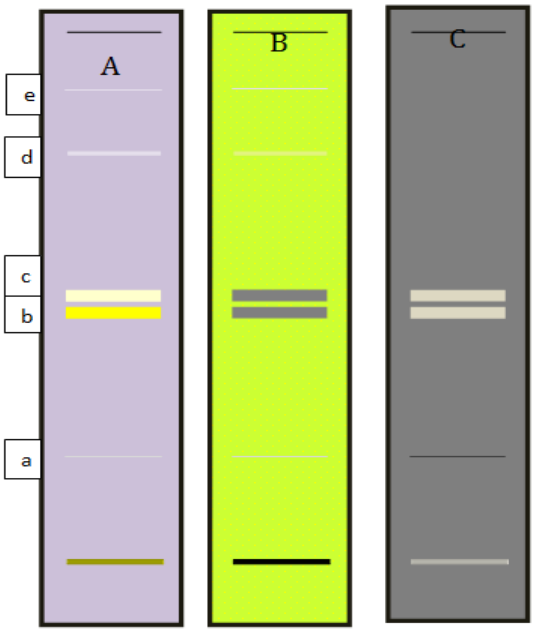

Fig. 1. TLC plates stained with 2.54 mM DPPH_ solution in methanol, and visualized (A) under visible light, (B) under UV 254 nm, and (C) under UV 366 nm. Three microlitres of the 80% methanol extract (AMS, 1 mg/mL) of *Cuminum cyminum* was applied as dots on TLC layer. The spots marked with b and c indicate compounds with DPPH_ scavenging activities.

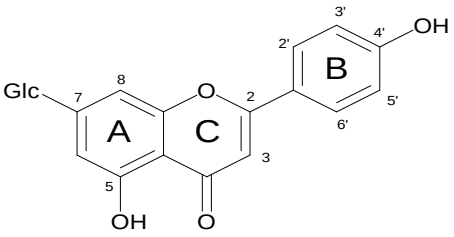

Fig 2. Apigenin-7-*O* glucoside

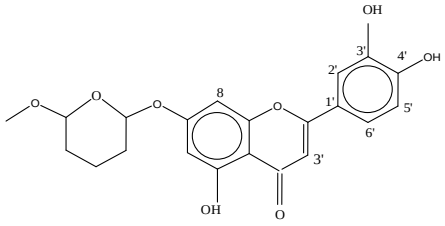

Fig 3. Luteolin- 7- *O* glucoside

Structure determinations of isolated compounds

The purity and identity of the compounds were established by use of spectroscopic techniques (^{1}H and ^{13}C NMR) and by comparison with the literature data. Compound 1 was also obtained as a yellow powder, and gave a positive reaction with natural products plus poly ethylen glycole reagent, probably indicating a flavonoid nature. Its UV spectrum was consistent with that of a flavonoid with maxima at 252, 265, and 347 nm (Gonza´ lez and Molina, 2006) A direct comparison of ^{1}H, ^{13}C NMR data (Table 2) with the reported data (Shen et al., 2004; Li *et al.*, 2007) led to identification of 2 as Luteolin-7-Glucosyde. This is the first report on the isolation of luteolin-7 –*O* glucoside from Cumin seed.

Compound 2 was obtained as a pale yellow powder, and showed characteristic flavonoid reaction with natural products plus poly ethylen glycole reagent. Its detailed UV (MeOH, λmax 265, 335 nm), 1H and 13C NMR data (Table 3), negative ESI MS data (m/z 269 [M_ H]_), agreed well with the previous reported data (Shen et al., 2004; Li *et al.*, 2007). Therefore, this compound was

identified as Apigenin-7-*O* Glucoside, and isolated from Cumin seed for the first time.

Table 2. NMR data of compound 1

Position	^{1}H-NMR data		^{13}C-NMR data	
	Compound 1	Ref [23,24]	Compound 1	Ref [23,24]
2	-	-	165.8	165.8
3	6.63,s	6.63,s	103.7	103.7
4	-	-	183.1	183.1
5	-	-	161.8	161.8
6	6.44, d,1.8H2	6.44, d,1.8H2	100.5	100.5
7	-	-	163.9	163.9
8	6.83,d,J=1.8H2	6.83,d,J=1.8H2	95.8	95.8
9	-	-	158	158
10	-	-	106.3	106.3
Glucose	-	-	122.6	122.6
1'	7.43,bs	7.43,bs	113.8	113.8
2'	-	-	146.3	146.3
3'	-	-	150.4	150.4
4'	6.95,d,J=8H_2	6.95,d,J=8H_2	116.5	116.5
5'	7.41,d,J=8H_2	7.41,d,J=8H_2	120.4	120.4
6'	-	-		
1"	5.1,d,J=7.8	5.1,d,J=7.8	100.7	100.7
2"	3.49,t,J=9H_2	3.49,t,J=9H_2	73.8	73.8
3"	3.56,t,J=9H_2	3.56,t,J=9H_2	76.8	76.8
4"	3.42,t,J=9H_2	3.42,t,J=9H_2	70.3	70.3
5"	360,m,	360,m,	77.4	77.4
6"	3.68,dd,J=12.2,5.6 H_a 3.85,dd,J=12.2, 1.8H_b	3.68,dd,J=12.2,5.6 H_a 3.85,dd,J=12.2, 1.8H_b	61.3	61.3

Table 3. NMR data of compound 2

Position	^{1}H-NMR data		^{13}C-NMR data	
	Compound 2	Ref[23,24]	Compound 2	Ref[23,24]
Aglycon	-			
2	-	-	166.77	164.7
3	6.8, S	6.8,S	104.14	103.4
4	-	-	184.08	182.4
5	-	-	162.93	161.9
6	6.5, S	6.5, d, J=2 Hz	96.07	95
7	-	-	164.81	163.1
8	6.6, S	6.6, d, J=2 Hz	101.19	104.7
9	-	-	158.96	157.3
10	-	-	107.1	105.7
1'	-	-	123.08	121.2
2'	7.9, d, J=8.0 Hz	7.9, d, J=8.8 Hz	129.64	128.9
3'	6.9, d, J=8.5 Hz	6.9, d, J=8.8 Hz	117.05	116.4
4'	-	-	162.93	161.4
5'	6.9, d, J=8.5 Hz	6.9, d, J=8.8 Hz	117.05	116.4
6'	7.9, d, J=8.0 Hz	7.9, d, J=8.8 Hz	129.64	128.9
Glucose	-			
1"	5.2, d, J=7H_2	5.2, d, J=7 Hz	101.64	99.9
2"	3.4 -4	3.4 -4	73.9	73.9
3"			75.2	75.2
4"			71	71
5"			76.1	76.1
6"			66.7	66.7

References

Amarowicz, R., Naczk, M., Shahidi, F. 2000. Antioxidant activity of various fractions of non-tannin phenolics of Canola hulls, *Journal of Agricultural and Food Chemistry*,48: 2755–2759.

Behera, S., Nagarajan, S., Jagan, S., M Rao, L. J. 2004. Microwave heating and conventional roasting of cumin seeds (*Cuminum cyminum* L.) and effect on chemical composition of volatiles, *Journal of Food Chemistry*, 87: 25–29.

Capannesi, C., Palchetti, I., Mascini, M., Parenti, A. 2000. Electrochemical sensor and biosensor for polyphenols detection in olive oils, *Food Chemistry*, 71: 553–562.

Chauhan, P. S., Satti, N. K., Suri, K. A., Amina, M., Bani, S. 2009. Stimulatory effect of *Cuminum cyminum* and flavonoid glycoside on Cyclosporine- A and restraint stress induced immune- Supperession in Swiss albino mice, *Chemico- Biological Interactions* 2009; 185: 66-72.

Gachkar, L., Yadegari, D., Rezaei, M. B., Taghizadeh, M. 2011. Chemical and biological characteristics of *Cuminum cyminum* and *Rosmarinus officinalis* essential oils, *Food Chemistry*, 102: 898–904.

Chung, Y., Chien, C., Teng, K., Chou, S. 2006. Antioxidative and mutagenic properties of Zanthoxylum ailanthoides Sieb & zucc, *Food Chemistry*, 97: 418–425.

Einafshar, S., Purazarang, H., Farhoosh, R., Seyedi, S. M. 2012. Antioxidant activity of the essential oil and methanolic extract of cumin seed (*Cuminum cyminum*), *European Journal of Food Lipid Sciences and Technology*, 114: 168-174.

Fisch KM, Bo¨hm V, Wright AD, Ko¨ nig GM. 2003.Antioxidative meroterpenoids from the brown alga Cystoseira crinita, *Journal of Natural Products*, 66: 968–975.

Gonza´ lez-Lavaut, J. A., Molina-Torres, J. 2006. Flavonoid glycosides from Cuban Erythroxylum species, *Biochemical Systematics and Ecology*, 34: 539–542.

Guenther, E. 1950. The essential oils. Vol. 4, D. Von Nostrand Company Inc. New York, 615–619.

Howell, J. C. 1986. Food antioxidants: international perspectives welcome and introductory remarks, *Food and Chemical Toxicology*, 24: 997-1003.

Ito, N., Hirose, M., Fukushima, S., Tsuda, H. 1986. Studies on antioxidants: their carcinogenic and modifying effects on chemical carcinogenesis, *Food and Chemical Toxicology*, 24: 1071–1082.

Li, H. J., Luo, Y. G., He, Z.H., Zhang, G. L. 2007. Chemical constituents from Lonicera saccata, Chinese *Journal of Applied and Environmental Biology*, 13:188–191.

Li, X. M., Tian, S. L., Pang, Z. C., Shi, J. Y. 2009. Extraction of *Cuminum cyminum* essential oil by combination technology of organic solvent with low boiling point and steam distillation, *Food Chemistry*; 115: 1114–1119.

Nakamura Y, Watanabe S, Miyake N, Kohno H, Osawa T. 2003. Dihydrochalcones: evaluation as novel radical scavenging antioxidants, *Journal of Agricultural and Food Chemistry*, 51: 3309–3312.

Otsuka, H. 2006. Crystallization in Final stages of purification, In: Methods in Biothechnology 20" Natural products isolation" second Ed. Satyait D. Sarker Zahid Latif, Alexander I.Gray (eds.). Human press, New Jersi, 114-126.

Satti, N. K., Amina, M., Dutti, P., Sharma, B. 2009. A simple and reliable preparative high performance liquid chromatographic technique for isolation of a bioactive flavones diglycoside from and extract of *Cuminum cyminum* seeds, *Acta chromatographica*, 21, 499-512.

Shen, J., Liang, J., Peng, S. L., Ding, L. S. 2004. Chemical constituents from Saussurea stella, *Natural Product Research and Development*. 16**:** 391–394.

Shobana, S., Akhilender, K. N. 2000. Antioxidant activity of selected Indian spices, *Prostaglandins Leukotrienes and Essential Fatty Acids, 62: 107–110.*

Shon, M. Y., Kim, T. H., Sung, N. J. 2003. Antioxidants and free radical scavenging activity of Phellinus baumii (*Phellinus of Hymenochaetaceae*) extracts *Food Chemistry*, 82: 593–597.

Tasdemir, D., Donmez, A. A., Calis, I., Ruedi, P. 2004. Evaluation of biological activity of Turkish plants. Rapid screening for the antimicrobial, antioxidant, and acetylcholinesterase inhibiting potential by TLC bioautographic method, *Pharmaceutical Biology*, 42: 374–383.

Valentao, P., Fernandes, E., Carvalho, F., Andrade, P. B. 2002. Antioxidative properties of Cardoon (*Cynara cardunculus* L.) infusion against superoxide radical, hydroxyl radical, and hypochlorous acid, *Journal of Agricultural and Food Chemistry*,50: 4989–4993.

Vekiari, S. A., Oreopoulou, V., Tzia, C., 1993. Thomopoulos CD. Oregano Flavonoids as lipid Antioxidants, *Journal American Oil Chemistry Society*, 70: 483–489.

Winton, A. L., Winton, K. B. 1939. The structure and composition of foods. Vol. 4, Wiley, New York, 420–423.

نشریه پژوهشهای علوم و صنایع غذایی ایران
جلد 12، شماره 6، بهمن - اسفند 1395، ص. 749-742

Iranian Food Science and Technology Research Journal
Vol. 12, No. 6, Feb. Mrch. 2017, p. 742-749

جداسازی و شناسایی ترکیبات دارای خواص آنتی اکسیدانی زیره سبز(*Cuminum cyminum*)

سودابه عین‌افشار[1*]- هاشم پورآذرنگ[2]، رضا فرهوش[2]، جواد اصیلی[3]

تاریخ دریافت: 1394/11/05
تاریخ پذیرش: 1395/05/26

چکیده

مواد طبیعی ترکیبات پیچیده‌ای هستند که استخراج سریع مواد فعال آنتی‌اکسیدانی از اهمیت خاصی برخوردار است. برای جداسازی چهار جزء (F1، F2، F3 و F4) موجود در عصاره متانولی زیره سبز از حلال‌هایی با قطبیت متفاوت استفاده شد. خواص آنتی‌اکسیدانی اجزاء فوق، با استفاده از آزمون تعیین قدرت‌گیرندگی رادیکال و آزمون FRAP تعیین شد. جزء F3 با (میلی-گرم بر میلی لیتر) IC500/006= و (میلی مول آهن 2+ در لیتر) 95 /521 FRAP= فعال‌ترین جزء بود. با استفاده ازکروماتوگرافی لایه نازک (TLC) و ارزیابی قدرت‌گیرندگی رادیکال آزاد (DPPH) دو ترکیب دارای خاصیت آنتی‌اکسیدانی از جزءF3 استخراج شد. به‌منظور تعیین ترکیب شیمیایی این دو جزء با استفاده از کروماتوگرافی تهیه‌ای (HPLC preparative) به همراه فاز متحرک مناسب (استونیتریل: متانول/ آب) مقدار لازم از این دو ترکیب استخراج شد و با استفاده از HNMR و CNMR و مقایسه با منابع موجود، دو ترکیب لوتئولین 7 گلوکوزید و آپیژنین 7 گلوکوزید شناسایی گردیدند.

واژه‌های کلیدی: آنتی‌اکسیدان، آپیژنین، زیره سبز، لوتئولین.

1 – استادیار، بخش تحقیقات فنی و مهندسی کشاورزی، مرکز تحقیقات و آموزش کشاورزی و منابع طبیعی خراسان رضوی، سازمان تحقیقات، آموزش و ترویج کشاورزی، مشهد، ایران.
2- استاد، گروه علوم و صنایع غذایی، دانشکده کشاورزی، دانشگاه فردوسی مشهد.
3- عضو هیئت علمی گروه فارماکوگنوزی ، دانشکده داروسازی دانشگاه علوم پزشکی مشهد.
(*- نویسنده مسئول : Email: Soodabeheyn@yahoo.com)

Iranian Food Science and Technology Research Journal
Vol. 12, No. 6, Feb. Mrch. 2017, p. 750-757

نشریه پژوهشهای علوم و صنایع غذایی ایران
جلد 12، شماره 6، بهمن - اسفند 1395، ص. 757-750

Drying kinetics and optimization of microwave- assisted drying of quince pomace

A. Anvar[1], B. Nasehi[2*], M. Noshad[3], H. Barzegar[3]

Received: 2016.10.25
Accepted: 2017.01.05

Abstract

In this study, microwave drying conditions of quince pomace optimized with respect to quality attributes (moisture content, color change and consumer acceptance). Response surface methodology (RSM) technique was used to develop models to respond to the microwave power (100, 2000, 300 W), and microwave time (5, 10, 15 min). The models obtained from the responses were adequate and acceptable because the coefficient of determination R^2 of the models was relatively high. Microwave power of 200W and microwave time of 8 minutes were concluded as the optimum conditions prior to air-drying at 50°C. To describe the drying process, the experimental data for moisture loss was converted to moisture ratios. The effective moisture diffusivity increased with increase in microwave power and its values varied from 1.83-4.87×10^{-9} m^2/s. Using an exponential expression based on Arrhenius equation the activation energy and was found to be 16.41 W/mm.

Key words: Quince pomace; Microwave drying; optimization; Effective moisture diffusivity; Activation energy

Introduction

By-products of fruits and vegetables are given importance for human health because they contain high levels of dietary fiber and bioactive components (Hernandez-Ortega *et al.*, 2013). In the quince juice processing, quince pomace is a by-product that contains plenty of poly phenol, vitamin C, mineral and dietary fiber. Quince pomace has high moisture content (78 ± 1.37 % (w.b.)), making it susceptible to microbial decomposition. Most commonly preservation method is drying, mainly because of water removal and consequently a reduction in enzymatic deterioration. Hot air drying is the most common technique for fruits dehydration. Nevertheless, this thermal process is a very energy-consuming operation and results in too much degradation of product quality. Therefore, to reduce long drying times and improve the poor product quality of conventional hot air-drying, it is often recommended to combine this method with an advanced method of drying (Amiri Chayjan *et al.*, 2015; Noshad *et al.*, 2011a).

Microwave offers advantages that have been employed prior to or with conventional drying in food processing technologies. Several researchers have provided strong evidence that microwave-assisted drying is ideal for fruits and vegetables, which speed up drying process, increase mass transfer, and produce good quality products (Abano and Amoah, 2015; Tian *et al.*, 2015).

For the efficient operation of processing systems and unit processes yielding a highly acceptable product in food engineering, the optimization has been used. RSM has been reported to be used to determine the independent variables have a combined effect on the desired response. RSM is a collection of statistical and mathematical system that has been successfully used for developing, improving and optimizing such processes. This experimental strategy has been widely used in the development of food processes (Noshad et al., 2011b).

Therefore, the aims of this study were: 1) Optimization of the microwave- assisted drying of quince pomace, 2) Mathematical modeling for drying of quince pomace, and 3)

1, 2 and 3. Former MSc Student, Associate Professor and Assistant Professor, Department of Food Science and technology, Ramin Agriculture and Natural Resources University of Khuzestan, Respectively.
Corresponding Author Email:nasehibehzad@gmail.com
DOI: 10.22067/ifstrj.v12i6.59815

Computing effective moisture diffusivity and activation energy of the quinces pomace.

Material and method

Fresh quinces were supplied from a local market in Ahvaz, Iran. The quince pomace consisted of the peel, pulp and remaining after juicing. It was kept in air tight plastic bottles and stored at a temperature of 4°C until the drying process. The moisture content was determined by heating in a drying oven (HERAEUS, Germany) at 105 ºC for 24h (Noshad et al., 2011b).

Microwave drying, experimental design

Response Surface Methodology (RSM) was used to find the best microwave drying conditions. The independent factors were power (100, 200, and 300 Watts), and time (5, 10, and 15 min). The responses were moisture content (Y_1), color change (ΔE) (Y_2) and acceptance (Y_3) of quince pomace. Actual and coded values of variation levels are shown in Table 1. The moisture losses of samples were recorded at 30s intervals during the drying process by a digital balance (AND DG 200) and an accuracy of ± 0.001 g. Drying process was carried out to reach moisture content of 40% on a wet basis.

After the microwave pretreatment, the slices were removed, weighed, and immediately subjected to a hot air cabinet dryer (Binder, Germany) set at the temperature of 50°C .The drying procedure was continued till the moisture content of the sample was reduced to about 5% (wet basis, wb), when the moisture content would not change any more(Wang *et al.*, 2007b). Each run was performed in triplicate.

Table1. Independent variables in this process

Factor	Name	Unit	Min	Max
X_1	Microwave power	Watt	100	300
X_2	Microwave time	min	5	15

Moisture content

The moisture content was determined by heating in a drying oven at 105 ºC for 24h (Noshad *et al.*, 2011b).

Color analysis

Since the computer vision system perceived color as RGB signals, which is device-dependent (Fernandez et al., 2005), the images taken were converted into L*a*b* units to ensure color reproducibility. Conversion from RGB to L*a*b* Transformation RGB into L*a*b space was performed using Color Space Converter plug-in of ImageJ software Ver.1.4g. Magic wand tool which is based on the Laplacian-of-Gaussian filter, used for selection of the true image of quince from the background in converted images. Statistical parameters of L*, a* and b* values were extracted from converted image. Color changes (ΔE) during drying process evaluated using equation (1):

$$\Delta E = \left[(L^*_2 - L^*_1)^2 + (a^*_2 - a^*_1)^2 + (b^*_2 - b^*_1)^2\right]^{\frac{1}{2}} \quad (1)$$

Sensory evaluation of quince pomace powder (acceptance)

A panel consisting of 10 trained panelists evaluated the quince pomace powder for different sensory attributes such as color, texture, taste and overall quality.

Determination of ascorbic acid (vitamin c)

The 2, 6-dichloroindophenol titrimetric method (AOAC Int. 967.21, 45.1.14, 1995) was used to determine the vitamin C content of quince pomace and powder. This method is based on the extraction of ascorbic acid, oxalic acid or met phosphoric acid, along with acetic acid titration with 2, 6-dichloroindophenol mentioned compounds to be bright pink color.5 mL of the clear sample obtained was diluted to 50 mL with met phosphoric acid–acetic acid solution and 7 mL was titrated against standard indophenols solution. Extractions and titrations were performed in triplicate (Gabriel et al., 2015).

Crude fiber content

The crude fiber content of quince pomace powder was measured using the AOAC (962.09, 1971) method. The sample was digested with 1.25% H_2SO_4 and 1.25% NaOH

solutions under specific conditions. The residue was dried and then ignited. Crude fiber was measured by calculation of the loss on ignition of the residue (Mohanty et al., 2015). Crude fiber content test was performed in triplicate.

Calculation of effective diffusivities

The Fick's diffusion equation used to describe the drying characteristics of biological products in falling rate period. Crank (1979) developed this equation to use for various regularly shaped bodies such as rectangular, spherical and cylindrical products (Crank, 1979). By assuming uniform initial moisture distribution in products can be used the Eq. (2) for particles with slab geometry (Shen et al., 2011; Wang *et al*., 2007a):

$$MR=\frac{8}{\pi^2}\sum_{n=0}^{\infty}\frac{1}{(2n+1)^2}\exp\left(-\frac{(2n+1)^2\pi^2 D_{eff}\, t}{4L_0^2}\right) \quad (2)$$

Where D_{eff} is the effective diffusivity (m^2/s); L_0 is the half thickness of slab (m). For the long drying period, Eq. (2) can be further simplified to only the first term of series (Ozbek and Dadali, 2007). Thus, Eq. (3) is written in a logarithmic form as follows:

$$\text{Ln MR}=\ln\frac{8}{\pi^2}-\frac{\pi^2 D_{eff}\, t}{4L_0^2} \quad (3)$$

Diffusivities are typically determined by plotting experimental drying data in terms of ln MR versus drying time t in Eq. (4), because the plot gives a straight line with a slope as follows:

$$\text{Slope}=\frac{\pi^2 D_{eff}}{4L_0^2} \quad (4)$$

Calculation of activation energy

According to Abano (2016), for the standard microwave oven drying procedure, the internal temperature of the sample was not an assessable variable (Abano, 2016). Therefore, the use of Arrhenius-type equation was considered for illustrating the relationship between the diffusivity coefficient and the ratio of the microwave power output to sample thickness instead of temperature for the calculation of the activation energy. The activation energy is found as modified from the revised Arrhenius (Zarein et al., 2015):

$$D_{eff}=D_0\exp\left(-\frac{E_a q}{P}\right) \quad (5)$$

Where D_0 is the pre-exponential factor of the Arrhenius equation (m^2/s), Ea is the activation energy (w/mm), P is the microwave power (W), and q is the sample thickness (mm).

Statistical analysis:

Statistical significance of the terms in the regression equations was examined. The significant terms in the model were found by analysis of variance (ANOVA) for each response. The adequacy of the model was evaluated based on the R^2 and adjusted-R^2. Numerical and graphical optimization technique of the Design- Expert software was used for simultaneous optimization of the multiple responses. The desired goals for each variable and response were chosen. All the independent's variables were kept within range while the responses were either maximized or minimized (Eren and Kaymak-Ertekin, 2007; Noshad et al., 2011b).

Result and discussion

The effects of three microwave powers on the drying curve of quince pomace are shown in figure (1). It is obvious from Figs. 1 that increasing the microwave power cause an increase in drying rate so that, the time required to dry quince pomace samples from an initial moisture content of 78 ± 1.37 % (w.b) to the moisture content of 40 + 1.1% (w.b) was approximately 38, 18 and 11 min at 100, 200 and 300 W, respectively. Several researchers reported that considerable increase in microwave power causes an important increase in the drying rate in drying of various vegetables such as green bean slice (Doymaz *et al*., 2015), apple slice (Zarein *et al*., 2015) and kiwifruit (Tian *et al*., 2015). This could be due to the fact that at higher microwave power levels more heat is generated within the sample which thus results in creating a large vapor pressure difference between the center and the surface of the product (Wang *et al*., 2007a).

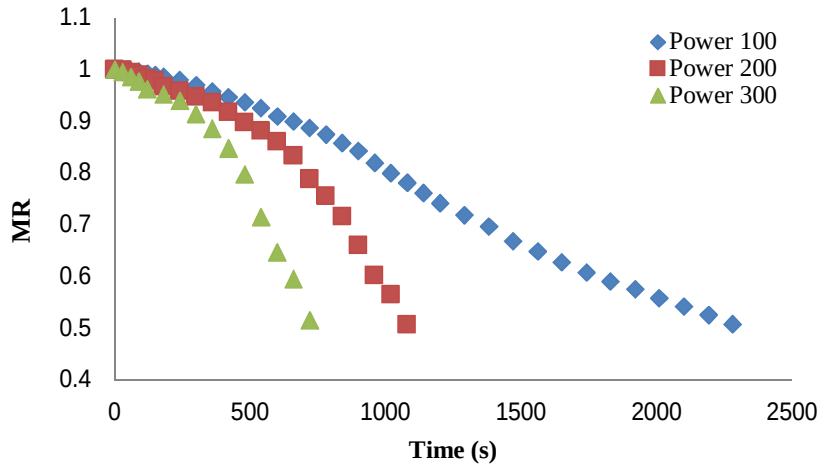

Fig1. Drying curves of quince pomace at different microwave power

Moisture content

The magnitude of P values in table (2) indicates the linear effects of all variables show a negative effect on moisture content. As expected, Fig. 2 shows that increase in microwave power and microwave time decrease the moisture content. Similar results have been reported by different researchers (Evin, 2011; Ozbek and Dadali, 2007). While, the quadratic terms of microwave power and time have a positive effect on moisture content, the interactions of 'microwave power and time' has not any significant effect on moisture content. A quadratic model (R^2= 96) described the effect of tested factors (microwave power and microwave time) on moisture content. The model and their coefficients showed in Eq. (6):

Moisture content= 57.62 -0.193 ×Power - 4.212 ×Time+3.24E- 04 ×Power^2 +0.156 × Time^2 (6)

Color change (ΔE)

The color change in the dried quince pomace was characterized in terms of ΔE, which varied from 11.45 to 37.72. The magnitude of p values in table (2) only indicates t the linear effects positive contribution of microwave power and time on color change. As shown in Fig.3 with the increase in microwave power and time, the color change value of quince pomace decreases. Compared to other treatment combination, microwave drying at lowest power in combination with time at lowest temperature is reduced color change. This trend may be due to the fundamental decrease in Millard reaction occurred at high air microwave power level and time (Omolola *et al.*, 2015). The linear model (R^2=0.89) describe the effect of factors on color change value (Eq.7). The ANOVA results for color change value are shown in table 2.

Delta E = -1.19 + 0.09×Power+0.73× Time (7)

Sensory evaluation and consumer acceptance

Sensory evaluation and consumer acceptance is one of the most important quality factors. As shown in table 2, the linear and quadric effects of microwave power and linear effect of microwave time were statistically significant ($p \leq 0.05$) effect on acceptance. As shown in Fig 4 with the increase in microwave power and microwave time, the acceptance of quince pomace powder decreases as a result of the formation of undesirable compounds from the Maillard non-enzymatic reaction which reduces the acceptance of the product in terms of color, taste and odor (Hashemi Shahraki et al., 2012). The quadric model (R^2 = 93.8) describe the effect of factors on the acceptance (Eq. 8).

The ANOVA results for the acceptance are

shown in table 2. $-0.0916\times Time-3.976E\text{-}005\times Power^2$ (8)

Consumer acceptance=5.17+3.9E-003× Power

Fig 2.Response surface plot for the effects of microwave power and drying time on moisture content

Table 2. ANOVAs evaluation of linear, quadratic and interaction terms for each response variable and coefficient of prediction models:

Source	Moisture content			Color change			consumer acceptance		
	DF	Sum of squares	p-value	DF	Sum of squares	p-value	DF	Sum of squares	p-value
Model	4	535,58	0.001	2	564.4	0.001	3	10.41	0.001
X_1	1	243.21	0.001	1	483.75	0.001	1	8.64	0.001
X_2	1	178	0.001	1	80.64	0.0052	1	1.26	0.001
$X_1 X_2$									
X^2_1	1	29.06	0.0075				1	0.51	0.029
X^2_2	1	42.08	0.0027						
Lack of fit	4	14.38	0.1251	6	26.17	0.47	5	0.31	0.665
R^2	0.966			0.898			0.938		
Adj-R^2	0.95			0.87			0.917		

p-value < 0.05 is significant at ≤ 0.05. ,Lack of fit is not significant at p-value > 0.05.

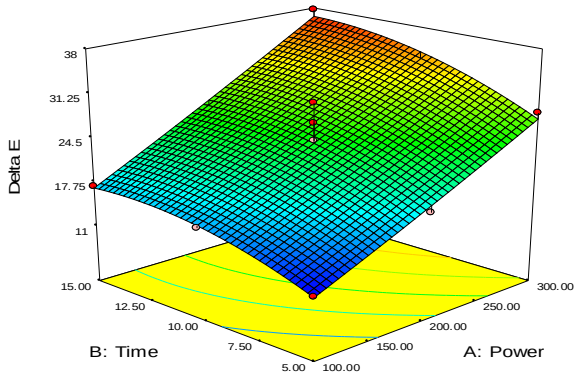

Fig3. Response surface plot for the effects of microwave power and drying time on color change

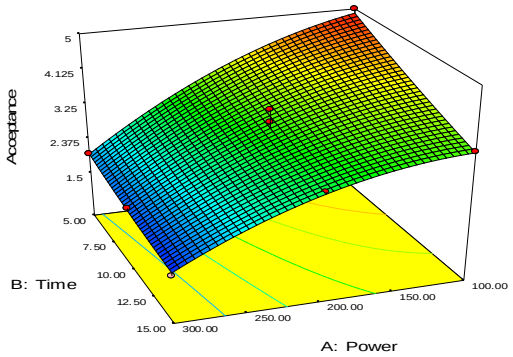

Fig4. Response surface plot for the effects of microwave power and drying time on consumer acceptance

Optimization

The optimum condition for microwave

drying of quince pomace was determined to obtain maximum acceptance and minimum moisture content and color change. Second order polynomial models obtained in this study were utilized for each response in order to determine the specified optimum conditions. These regression models are valid only in the selected experimental domain. So, optimization criteria were selected based on different parameters including economic and product quality related attributes (Eren and Kaymak-Ertekin, 2007; Noshad *et al.*, 2015).

By applying desirability function method, a solution was obtained for the optimum covering the criteria as 8 min for microwave time and 200 W for microwave power.

Analysis of quince pomace powder was carried out at optimal conditions to measure the amount of vitamin C and crud fiber. The vitamin C and crude fiber content of quince pomace powder were 4.27±0.14 and 12.27 ±0.21, respectively while vitamin C content of fresh quince pomace was 19.95±1.03.

Effective diffusivities and activation energy

The calculated values of D_{eff} for different microwave power are presented in Table 3. The effective diffusivity values of dried samples at 100-300 W were altered in the range of 1.83-4.87×10^{-9} m^2/s. It is obvious from table 3 that increasing the microwave power caused an increase in D_{eff}. Increased heat energy as a result of an increase in microwave power is reported to enhance the activity of the water molecules leading to higher moisture diffusivity these values are within the general range 10^{-8}-10^{-12} m^2/s for drying of food materials (Darvishi *et al*., 2013; Sadi and Meziane, 2015).

Table 3.Values of effective diffusivities obtained for quince pomace at different condition drying

Microwave Power	Effective diffusivity (m^2/mm)
100	1.83×10^{-9}
200	3.25×10^{-9}
300	4.87×10^{-9}

The energy needed to initiate internal moisture diffusion is the active energy. It is an indication of the temperature sensitivity of $D_{eff.}$ The activation energy obtained for drying process was 16.41 W/mm. The activation energy values obtained in this study were lower than the 46.91W/mm reported for microwave-vacuum-drying of tomato slices (Abano *et al.*, 2012) but generally higher than the 5.54W/mm for okra (Dadali *et al*., 2007).

Conclusion

Regression models were developed to effectively predict the quality parameters at any given microwave power and drying time using RSM. The moisture content of quince pomace powder was observed to decrease significantly as a result of both processes. Color change values increased significantly due to browning and Millard reactions which take place during drying of samples. Acceptance of samples decreased as a result of the formation of undesirable compounds from the Maillard non-enzymatic reaction which reduces the acceptance of the product in terms of color, taste and odor. The drying conditions of 200 W microwave power and 8 min drying time were found optimum for product quality**.** The effective moisture diffusivity values varied from 1.83-4.87×10^{-9} m^2/s and increased with increase in microwave power. The activation energy was calculated using an exponential expression based on Arrhenius equation and was found to be 16.41 W/mm.

Reference

Abano E., Ma H., Qu W. (2012) Influence Of Combined Microwave-Vacuum Drying On Drying Kinetics And Quality Of Dried Tomato Slices. J*ournal of Food Quality* 35:159-168.

Abano E.E. (2016) Kinetics and Quality of Microwave-Assisted Drying of Mango (*Mangifera indica*). I*nternational Journal of Food Science* doi:10.1155/2016/2037029.

Abano E.E., Amoah R.S. (2015) Microwave and blanch-assisted drying of white yam (*Dioscorea rotundata*). *Food science & nutrition* 3:586-596.

Amiri Chayjan R., Kaveh M., Khayati S. (2015) Modeling Drying Characteristics of Hawthorn Fruit under Microwave- Convective Conditions. Journal of Food Processing and Preservation 39:239-253.

Crank J. (1979) The mathematics of diffusion Oxford University Press, USA.

Dadali G., Kilic Apar D., Ozbek B. (2007) Microwave drying kinetics of okra. *Drying Technology* 25:917-924.

Darvishi H., Asl A.R., Asghari A., Najafi G., Gazori H.A. (2013) Mathematical modeling, moisture diffusion, energy consumption and efficiency of thin layer drying of potato slices. *Journal of Food Processing & Technology* doi:10.4172/2157-7110.1000215.

Doymaz I., Kipcak A.S., Piskin S. (2015) Microwave Drying of Green Bean Slices: Drying Kinetics and Physical Quality. *Czech Journal of Food Sciences* 33:367-376.

Eren I., Kaymak-Ertekin F. (2007) Optimization of osmotic dehydration of potato using response surface methodology. *Journal of food engineering* 79:344-352.

Evin D. (2011) Microwave drying and moisture diffusivity of white mulberry: experimental and mathematical modeling. *Journal of mechanical science and technology* 25:2711-2718.

Fernandez L., Castillero C., Aguilera J. (2005) An application of image analysis to dehydration of apple discs. *Journal of food engineering* 67:185-193.

Gabriel A.A., Cayabyab J.E.C., Tan A.K.L., Corook M.L.F., Ables E.J.O., Tiangson-Bayaga C.L.P. (2015) Development and validation of a predictive model for the influences of selected product and process variables on ascorbic acid degradation in simulated fruit juice. *Food chemistry* 177:295-303.

Hashemi Shahraki M., Ziaiifar A., Kashaninejad S., Ghorbani M. (2012) Optimization of Pre-Fry Microwave Drying of French Fries Using Response Surface Methodology and Genetic Algorithms. *Journal of Food Processing and Preservation* 38:535-550.

Hernandez-Ortega M., Kissangou G., Necoechea-Mondragon H., Sanchez-Pardo M.E., Ortiz-Moreno A. (2013) Microwave dried carrot pomace as a source of fiber and carotenoids. *Food and Nutrition Sciences*:Doi:10.4236/fns.2013.410135.

Mohanty C.S., Pradhan R.C., Singh V., Singh N., Pattanayak R., Prakash O., Chanotiya C.S., Rout P.K. (2015) Physicochemical analysis of *Psophocarpus tetragonolobus* (L.) DC seeds with fatty acids and total lipids compositions. *Journal of food science and technology* 52:3660-3670.

Noshad M., Mohebbi M., Shahidi F., Mortazavi S.A. (2011a) Kinetic Modeling Of Rehydration In Air-Dried Quinces Pretreated With Osmotic Dehydration And Ultrasonic. J*ournal of Food Processing and Preservation* 36:383-392.

Noshad M., Mohebbi M., Shahidi F., Mortazavi S.A. (2011b) Multi-objective optimization of osmotic-ultrasonic pretreatments and hot-air drying of quince using response surface methodology. *Food and Bioprocess Technology* 5:2098-2110.

Noshad M., Mohebbi M., Koocheki A., Shahidi F. (2015) Microencapsulation of vanillin by spray drying using soy protein isolate-maltodextrin as wall material. *Flavour and Fragrance Journal* 30:387-391.

Omolola A.O., Jideani A.I.O., Kapila P.F., Jideani V.A. (2015) Optimization of microwave drying conditions of two banana varieties using response surface methodology. *Food Science and Technology* (*Campinas*) doi : 10.1590/1678-457X.6700

Ozbek B., Dadali G. (2007) Thin-layer drying characteristics and modelling of mint leaves undergoing microwave treatment. J*ournal of Food Engineering* 83:541-549.

Sadi T., Meziane S. (2015) Mathematical modelling, moisture diffusion and specific energy consumption of thin layer microwave drying of olive pomace. *International Food Research Journal* 22:494-501.

Shen F., Peng L., Zhang Y., Wu J., Zhang X., Yang G., Peng H., Qi H., Deng S. (2011) Thin-layer drying kinetics and quality changes of sweet sorghum stalk for ethanol production as affected by drying temperature. *Industrial Crops and Products* 34:1588-1594.

Tian Y., Wu S., Zhao Y., Zhang Q., Huang J., Zheng B. (2015) Drying Characteristics and Processing Parameters for Microwave-Vacuum Drying of Kiwifruit (*Actinidia deliciosa*) Slices. *Journal of Food Processing and Preservation* 39:2620-2629.

Wang Z., Sun J., Chen F., Liao X., Hu X. (2007a) Mathematical modelling on thin layer microwave drying of apple pomace with and without hot air pre-drying. *Journal of Food Engineering* 80:536-544.

Wang Z., Sun J., Liao X., Chen F., Zhao G., Wu J., Hu X. (2007b) Mathematical modeling on hot air drying of thin layer apple pomace. *Food Research International* 40:39-46.

Zarein M., Samadi S.H., Ghobadian B. (2015) Investigation of microwave dryer effect on energy efficiency during drying of apple slices. *Journal of the Saudi Society of Agricultural Sciences* 14:41-47.

نشریه پژوهشهای علوم و صنایع غذایی ایران
جلد 12، شماره 6، بهمن - اسفند 1395، ص. 757-750

Iranian Food Science and Technology Research Journal
Vol. 12, No. 6, Feb. Mrch. 2017, p. 750-757

ارزیابی کینتیک خشک شدن و بهینه یابی شرایط خشک کردن مایکروویو- هوای داغ پسماند میوه به

عادیه انور[1]- بهزاد ناصحی[2*]- محمد نوشاد[3]- حسن برزگر[3]

تاریخ دریافت:1395/08/04
تاریخ پذیرش:1395/10/16

چکیده

در این پژوهش روش سطح پاسخ برای بهینه یابی شرایط خشک کردن پسماند میوه به توسط امواج مایکروویو مورد استفاده قرار گرفت. اثر توان مایکروویو (300-100 وات) و زمان خشک کردن (15-5 دقیقه) به عنوان متغییرهای مستقل بر میزان رطوبت، تغییرات رنگ و پذیرش کلی پودر پسماند میوه به، به عنوان متغییر وابسته (پاسخ) مورد ارزیابی قرار گرفت. مدل های رگرسیونی به دست آمده برای تمام پاسخ ها در سطح 95% اطمینان معنی دار بود. شرایط بهینه به دست آمده برای کمینه میزان رطوبت و تغییرات رنگ و بیشینه پذیرش کلی عبارت بود از: توان 200 وات و زمان 8 دقیقه. ضریب نفوذ موثر پودر پسماند به در خشک کن مایکروویو بین ($\frac{m^2}{s}$) $1/83 - 4/87 \times 10^{-9}$ ، به دست آمد مقدار انرژی فعال سازی با استفاده از معادله آرنیوس برمبنای رابطه بین توان مایکروویو و ضریب نفوذ موثر محاسبه شد که $\frac{W}{mm}$ 16/41، بود.

واژه های کلیدی: پسماند به، مایکروویو، بهینه یابی، نفوذپذیری موثر رطوبت، انرژی فعال سازی

1، 2 و 3- به ترتیب دانش‌آموخته کارشناسی ارشد، دانشیار و استادیار، گروه علوم و صنایع غذایی، رامین، دانشگاه کشاورزی و منابع طبیعی رامین خوزستان، خوزستان، ایران.
(*- نویسنده مسئول : Email: nasehibehzad@gmail.com)

Iranian Food Science and Technology Research Journal
Vol. 12, No. 6, Feb. Mrch. 2017, p. 758-766

نشریه پژوهشهای علوم و صنایع غذایی ایران
جلد 12، شماره 6، بهمن - اسفند 1395، ص. 766-758

Experimental and modeling investigation of mass transfer during infrared drying of Quince

M. A. Mehrnia [1*], A. Bashti[2], F. Salehi[3]

Received: 2017.01.10
Accepted: 2017.05.08

Abstract

In this research, an experimental and modeling study on mass transfer analysis during infrared drying of quince was undertaken. In the experimental part, the effects of various drying conditions in terms of infrared radiation power (150-375 W) and distance (5-15 cm) on drying characteristics of quince were investigated. Both the infrared power and distance influenced the drying time of quince slices. Moisture ratios were fitted to 8 different mathematical models using nonlinear regression analysis. The regression results showed that the logarithmic model satisfactorily described the drying behavior of quince slices with highest R value and lowest SE values. The effective moisture diffusivity increases as power increases and range between 1.15 and 3.72 $\times 10^{-8}$ m^2/s. The rise in infrared power has a negative effect on the ΔE and with increasing in infrared radiation power it was increased. Chroma and hue values were in ranges between 43.28 and 46.99, 80.82° and 86.14°, respectively.

Keywords: Effective moisture diffusivity, Image processing; Infrared dryer; Quince.

Introduction

Fruits have very short shelf-life due to high moisture content (above 82% by weight), and it is necessary to use various preservation methods to increase its shelf life (Cassano *et al.*, 2006). Drying appears to be a potential food preservation option to extend their storage/shelf-life. Maskan (2001) studied to comparison of the microwave, hot air and hot air-microwave drying methods for the processing of kiwifruits in respect to drying, shrinkage and rehydration characteristics obtained by the three drying techniques. Chen *et al*. (2001) established the drying kinetics parameters through the experiments performed on pulped kiwifruit flesh spread onto a shallow metal tray (forming a layer) to simulate the process of making fruit leather.

Quince, (*Cydonia oblonga*) from Rosaceae family, is a tree cultivated as a medicinal and nutritional plant in the Middle East, South Africa, and central Europe (Hemmati *et al*., 2012). They are used to make jam, marmalade, jelly and quince pudding (de Escalada Pla *et al*., 2010). Drying is one of the important preservation methods employed for storage of quince. Drying kinetics of quince slices was investigated by Kaya *et al*. (2007) and the effect of drying method on bulk density, substance density, porosity, and shrinkage of quinces at various moisture contents was studied by Koç *et al*. (2008).

One of the ways to shorten the drying time is to supply heat by infrared radiation. Its efficiency is between 80% and 90%, the emitted radiation is in narrow wavelength range and they are miniaturized (Sakai and Hanzawa, 1994; Sandu, 1986). Advantages of infrared radiation over convective heating include high heat transfer coefficients, short process times and low energy costs (Ratti and Mujumdar, 1995). Comparison of infrared drying with convective drying of apple showed that time of the process can be shortened by up to 50% when heating is done with infrared energy (Nowak and Lewicki, 2004). The combination of infrared with hot air provides

1. Assistant professor, Department of Food Science & Technology, Shoushtsar Branch, Islamic azad university, shoushtar ,Iran
2. Assistant professor , Department of Chemistry, Shoushtar Branch, Islamic Azad university, Shoushtar, Iran.
3. Assistant professor , Department of Food Science and Technology, Bu-Ali Sina University, Hamedan, Iran.
Corresponding Author Email: mamehrnia@yahoo.com
DOI: 10.22067/ifstrj.v12i6.61732

the synergistic effect, resulting in an efficient drying process. Energy and quality aspects were studied during combined far infrared and convective drying of barley (Afzal *et al*., 1999).

Infrared drying was applied before or after freeze-drying of shiitake mushroom to shorten the drying time, enhance the rehydration, and for better preservation of the aroma compounds and color (Wang *et al*. (2015). The reported results showed that the combination of freeze-drying (for 4h) followed by infrared drying saves 48% time compared to freeze-drying while keeping the product quality at an acceptable level. The application of infrared drying also helps produce a more porous microstructure in dried shiitake mushrooms.

Pan *et al*. (2008) used sequential infrared and freeze-drying (SIRFD) to produce high-quality dried fruits at reduced cost. The products dried using SIRFD had better color, higher crispness, higher shrinkage but poor rehydration propensity compared to those produced by using regular freeze-drying (Pan *et al*., 2008).

Infrared drying method, when properly applied, can be used for achieving a high-quality product. There for, the aim of the present work was to investigate infrared drying characteristics of quince slices in respect to drying kinetics, moisture diffusivity and color changes of the dried products.

Materials and methods

Infrared drying

Quinces used in this study were purchased from a local market and they had no external defects. The initial moisture content of quinces was found to be 84% ± 1.05 (wet basis). Prior to drying, samples were taken out of storage, peeled with a sharp vegetable peeler, and cut into 5 mm thick slices with a steel cutter.

The quince slices were dried in an infrared dryer (Infrared radiation lamp (NIR), Noor, Iran). The effect of infrared radiation power (at three levels 150, 250 and 375 W) and distance (at three levels 5, 10 and 15 cm) on the drying kinetics and characteristics of quince slice were investigated. Then the dried samples stored in an air-tight packet till the experiments.

Weight loss of samples was recorded by using a digital balance (Digital balance, Lutron GM-300p, Taiwan), with a sensitivity of ±0.01 g. The initial moisture content of the samples was obtained according to the AOAC method no. 934.06 (AOAC 1990). Experiments were carried out in triplicate and an arithmetic average was taken for data processing.

Drying kinetics

The experimental moisture content data were nondimensionlized using the equation 1:

$$MR = \frac{M_t - M_e}{M_0 - M_e} \quad (1)$$

Where MR is the dimensionless moisture ratio, M_t, M_0 and M_e are moisture content at any time, initial moisture content and equilibrium moisture content (kg water/kg dry matter), respectively. $(M_t–M_e)/(M_0–M_e)$ was simplified to M_t/M_0 as the relative humidity of drying air continuously fluctuated during drying experiments (Ceylan *et al*., 2007; Doymaz, 2011).

Selected thin-layer drying models (Approximation of diffusion, Page, Newton, Midilli, Logarithmic, Verma, Two term, Quadratic) were fitted to the drying curves (MR versus time) (Akpinar and Bicer, 2005; Doymaz, 2011). A nonlinear estimation package (Curve Expert, Version 1.34) was used to estimate the coefficients of the given models. The two criteria of statistic analysis have been used to evaluate the adjustment of the experimental data to the different models, r (correlation coefficient) and SE (standard error). A good fitting between the experimental data and the correlations is obtained when there is a combination of the high r value and the values of SE, which should be as low as possible (Doymaz, 2011).

Calculation of Moisture Diffusivity

In most of drying studies, diffusion is generally accepted to be the main mechanism during the transport of moisture to the surface to be evaporated (Doymaz, 2011). Fick's second law of diffusion has been widely used

to describe the drying process during the falling rate period for most food materials (Sacilik, 2007). The solution of diffusion model, considering negligible external resistance, in terms of average moisture content, negligible shrinkage, constant diffusion coefficients and temperature, is presented for slab geometry as follows (Doymaz, 2011):

$$MR = \frac{8}{\pi^2}\sum_{n=0}^{\infty}\frac{1}{(2n+1)^2}\exp(-(2n+1)^2\frac{\pi^2 D_{eff}t}{4L^2}) \quad (2)$$

Where MR is the moisture ratio (dimensionless); t is the drying time (s), D_{eff} is the effective diffusivity (m^2/s); and L is the half slab thickness of the slices (m). For long drying periods, equation 2 can be further simplified to only the first term of the series. Equation 2 thus simplifies to:

$$MR = \frac{8}{\pi^2}\exp\left[\frac{-\pi^2 D_{eff}t}{4L^2}\right] \quad (3)$$

The effective diffusivity was calculated through equation 3 by using the method of slopes. The effective diffusivities are typically determined by plotting experimental drying data in terms of lnMR versus time (as given in equation 3). From equation 3, a plot of lnMR versus time gives a straight line with a slope (K) of:

$$K = \frac{\pi^2 D_{eff}}{4L^2} \quad (4)$$

Color measurement

In order to investigate the effect of drying condition on the color changes of dried quince, a computer vision system was applied. Sample illumination was achieved with HP Scanner (Hp-G3110). Since the computer vision system perceived color as RGB signals, which is device-dependent, the taken images were converted into $L^*a^*b^*$ units to ensure color reproducibility. In the L*a*b* space, the color perception is uniform, and therefore, the difference between two colors corresponds approximately to the color difference perceived by the human eye. L^* (lightness/darkness that ranges from 0 to 100), a^*(redness/greenness that ranges from -120 to 120) and b^* (yellowness/blueness that ranges from -120 to 120) were measured. In this study, the image analysis of dried quince was performed using Image J software version 1.42e, USA.

The hue angle (°), hue = arctg (b^*/a^*), expresses the colour nuance and values are defined as follows: red-purple: 0°, yellow: 90°, bluish-green: 180°, and blue: 270°. Hue angle (H) of the films was calculated as follows (Bhat *et al.*, 2013):

$H = \tan^{-1}(b^*/a^*)$ when $a^* > 0$ and $b^* > 0$

$H = 180° + \tan^{-1}(b^*/a^*)$ when $a^* < 0$

$H = 360° + \tan^{-1}(b^*/a^*)$ when $a^* > 0$ and $b^* < 0$

The calculation of color changes (ΔE) for total color difference and C^* (Chroma) for saturation were made with the following equations (Liu *et al*., 2010):

$$\Delta E = \sqrt{(\Delta L^*)^2 + (\Delta a^*)^2 + (\Delta b^*)^2} \quad (5)$$

$$C^* = \sqrt{(a^*)^2 + (b^*)^2} \quad (6)$$

Results and discussion

Drying time

During drying, radiation properties of the material are changing due to decreasing water content. As a consequence, its reflectivity increases and the absorptivity decrease. Generally, solid materials absorb infrared radiation in a thin surface layer (Lampinen *et al*., 1991).

The effects of infrared power and distance on the moisture content of quince slices are shown in figures 1 and 2. As expected, the moisture content was decreased by increasing the power because of the increased temperature and heat transfer gradient between the air and samples. The drying times of quince samples were 18, 29 and 44 min at 150, 250 and 375 W, respectively (10 cm). In conclusion, experimental results showed that the infrared power has a significant effect on the evolution of moisture content.

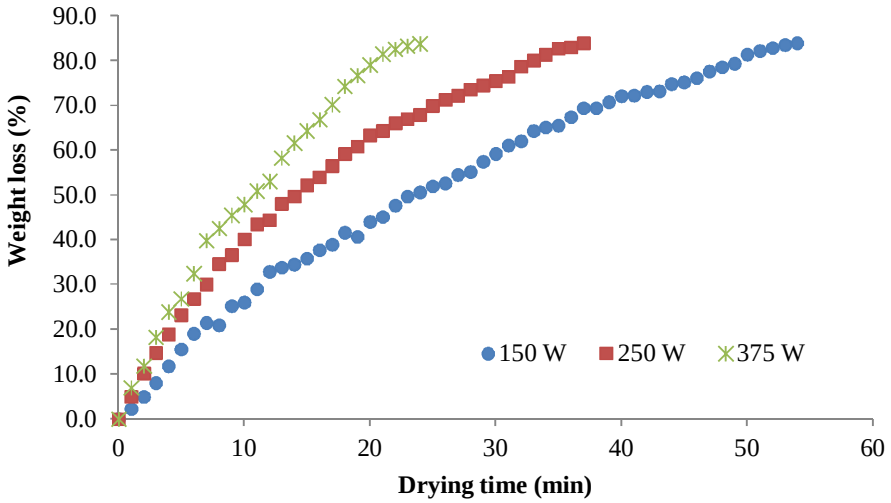

Figure 1. Variations of moisture content with drying time of quince slices at different infrared power.

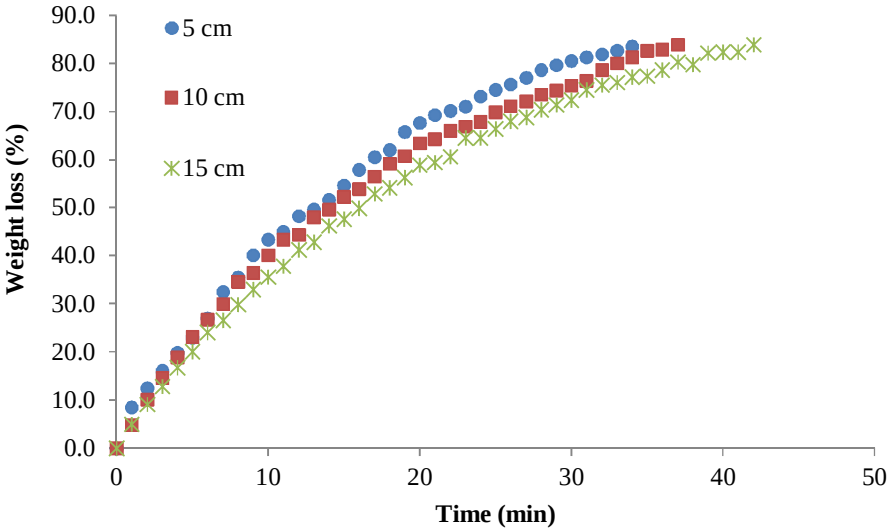

Figure 2. Variations of moisture content with drying time of quince slices at different distance.

Hence, drying of thin layers seems to be more efficient at far-infrared radiation (FIR, 25–100 μm), while drying of thicker bodies should give better results at near-infrared radiation (NIR, 0.75–3.00 μm) (Nowak and Lewicki, 2004). The drying time reduced from 31 to 25 min when the distance was increased from 15 to 5 cm (250 W).

Fitting of the Drying Curves

Different mathematical models were fitted to the drying data and among them; the Logarithmic model showed the highest r and the lowest SE values. Estimated parameters and statistical data obtained for this model are shown in Table 1. In all the cases, the r values for the models were greater than 0.997, indicating a good fit. It can be seen that there was a very good agreement between the experimental and predicted moisture ratio values, which are closely banding around at a 45° straight line.

Table 1. Curve-fitting coefficients of the Logarithmic model.

Power (W)	Distance (cm)	a	k	c	r	SE
150	5	1.309	0.026	-0.355	0.999	0.014
250	10	1.335	0.024	-0.353	0.999	0.015
375	15	1.345	0.020	-0.376	0.999	0.013
150	5	1.189	0.053	-0.205	0.999	0.011
250	10	1.145	0.051	-0.158	0.999	0.009
375	15	1.172	0.044	-0.181	0.999	0.006
150	5	3.631	0.020	-2.604	0.997	0.025
250	10	1.469	0.049	-0.481	0.999	0.015
375	15	1.322	0.053	-0.304	0.999	0.010

Moisture Diffusivity

The effective diffusivities are determined by plotting experimental drying data in terms of lnMR versus time. The effects of infrared radiation power and distance on the lnMR are shown in Figures 3 and 4. The D_{eff} values lie within in general range of 10^{-11} to 10^{-9} m^2/s for food materials (Rizvi, 1986). The values of D_{eff} at different condition drying of quince slice obtained by using Eq. (4) and estimated values are shown in Table 2. The effective diffusivity values of quince slices were ranged from 1.00 and 3.72 $\times 10^{-8}$ m^2/s. Effective diffusivity values increased with increasing infrared radiation power because of the rapid movement of water at high temperatures (Doymaz, 2011).

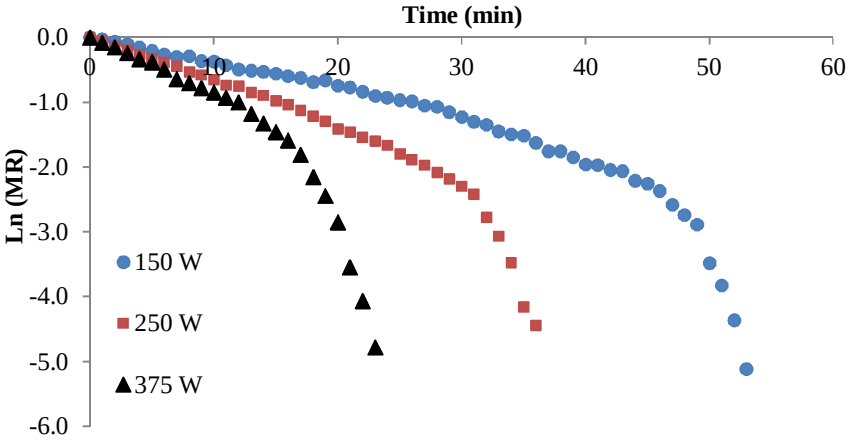

Figure 3. Effect of infrared power on the Ln(MR) during drying of quince slices.

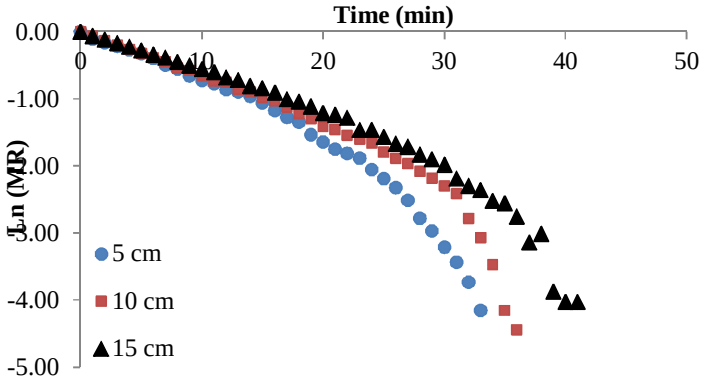

Figure 4. Effect of infrared source distance on the Ln(MR) during drying of quince slices.

Table 2. Values of effective moisture diffusivity of quince slice obtained from drying experiments.

Power (W)	Distance (cm)	Effective diffusivity (m^2/s)	r
150	5	1.15×10^{-8}	0.928
250	10	1.08×10^{-8}	0.918
375	15	1.00×10^{-8}	0.902
150	5	1.83×10^{-8}	0.969
250	10	1.62×10^{-8}	0.945
375	15	1.43×10^{-8}	0.963
150	5	3.72×10^{-8}	0.886
250	10	2.82×10^{-8}	0.920
375	15	2.30×10^{-8}	0.933

The values of D_{eff} are comparable with the reported values of 0.85 to 1.75 $\times10^{-10}$ m^2/s for hull-less seed pumpkin at 40–60°C (Sacilik, 2007), 0.46–3.45 $\times10^{-10}$ m^2/s mentioned for drying carrot in the temperature range of 60–90°C (Zielinska and Markowski, 2007), 3.0 to 17.12 $\times10^{-10}$ m^2/s for kiwifruit at 30–90°C (Simal *et al*., 2005), 3.2 to 11.2 $\times$ 10^{-9} m^2/s for red bell pepper at 50–80°C (Vega *et al*., 2007), 2.52 to 13.0×10^{-10} m^2/s for curd at 45–50°C (Shiby and Mishra, 2007), and 4.27 to 13.0×10^{-10} m^2/s okra at 50–70°C (Doymaz, 2005). These values are consistent with the present estimated D_{eff} values for quince slices

Color measurement

The fresh quince exhibited a light yellow color, with L*, a* and b* equal to 89.13, -2.763 and 54.962, respectively. The results of color measurement of dried quince slices at different conditions are presented in Table 3. The infrared radiation power was found to have a significant effect on the colour of quince slices. The rise in power has a negative effect on the ΔE and with increasing in infrared radiation power from 250 to 375 W, it was increased from 15.34 to 24.84, respectively. Therdthai and Zhou (2009) reported that high temperature during drying of mint leaves could lead to increase ΔE values (Therdthai and Zhou, 2009).

As shown in table 3, the L^* values varied from 65.74 to 79.61 at different drying condition. Chroma and hue values were in ranges between 43.28 and 46.99, 80.82° and 86.14°, respectively. The chroma value indicates the degree of saturation of colour and is proportional to the strength of the colour. The changes in Hue angle values were not significant compared to drying processes.

Table 3. Comparison the effect of different drying methods on color change of quince slices.

Power (W)	Distance (cm)	a^*	b^*	L^*	ΔE	C*	Hue value (°)
150	5	3.23±1.37	29.40±14.26	45.54±3.03	15.18	45.65	85.94
250	10	3.05±1.30	35.85±12.84	45.21±2.89	16.40	45.32	86.14
375	15	3.06±1.34	34.69±13.81	45.5±2.76	18.05	45.16	86.11
150	5	4.43±2.33	32.73±13.98	46.78±5.49	14.46	46.99	84.59
250	10	4.16±1.57	30.05±12.57	46.56±2.79	15.05	46.75	84.89
375	15	4.05±1.59	31.93±13.33	46.38±2.85	16.51	46.56	85.02
150	5	5.41±2.02	28.45±11.68	44.36±4.89	20.23	44.69	83.04
250	10	6.94±1.95	31.55±14.02	42.93±3.22	26.20	43.48	80.82
375	15	6.87±2.22	33.52±14.21	42.73±4.39	28.10	43.28	80.87

Conclusions

An infrared system was used for drying of quince. A drying system was fitted with near-infrared (NIR) heaters for radiative heating. The drying times of quince samples were 18, 29 and 44 min at 150, 250 and 375 W, respectively. The drying times was reduced when the distance of sample from infrared source was decreased. The drying characteristics were satisfactorily described by Logarithmic model with the latter providing the best representation of the experimental data. Values for the effective moisture diffusivity of quince samples were obtained in the range of 1.00 and 3.72 $\times10^{-8}$ m^2/s. The present study also verified that the color of

quince was influenced by the drying process. The rise in power has a negative effect on the ΔE and with increasing in infrared radiation power from 250 to 375 W, it was increased from 15.34 to 24.84, respectively. The changes in Hue angle values were not significant compared to drying processes.

References

Afzal, T., Abe, T., Hikida, Y., 1999. Energy and quality aspects during combined FIR-convection drying of barley. *Journal of Food Engineering*, 42(4), 177-182.

Akpinar, E.K., Bicer, Y., 2005. Modelling of the drying of eggplants in thin-layers. I*nternational Journal of Food Science & Technology*, 40(3), 273-281.

Bhat, R., Abdullah, N., Din, R.H., Tay, G.-S., 2013. Producing novel sago starch based food packaging films by incorporating lignin isolated from oil palm black liquor waste. *Journal of Food Engineering*, 119(4), 707-713.

Cassano, A., Figoli, A., Tagarelli, A., Sindona, G., Drioli, E., 2006. Integrated membrane process for the production of highly nutritional kiwifruit juice. *Desalination*, 189(1), 21-30.

Ceylan, I., Aktaş, M., Doğan, H., 2007. Mathematical modeling of drying characteristics of tropical fruits. *Applied Thermal Engineering*, 27(11), 1931-1936.

Chen, X., Pirini, W., Ozilgen, M., 2001. The reaction engineering approach to modelling drying of thin layer of pulped Kiwifruit flesh under conditions of small Biot numbers. *Chemical Engineering and Processing: Process Intensificat*ion, 40(4), 311-320.

de Escalada Pla, M.F., Uribe, M., Fissore, E.N., Gerschenson, L.N., Rojas, A.M., 2010. Influence of the isolation procedure on the characteristics of fiber-rich products obtained from quince wastes. *Journal of Food Engineering*, 96(2), 239-248.

Doymaz, I., 2011. Drying of eggplant slices in thin layers at different air temperatures. *Journal of Food* P*rocessing and Preservation*, 35(2), 280-289.

Doymaz, İ., 2005. Drying characteristics and kinetics of okra. Journal of Food Engineering, 69(3), 275-279.

Hemmati, A.A., Kalantari, H., Jalali, A., Rezai, S., Zadeh, H.H., 2012. Healing effect of quince seed mucilage on T-2 toxin-induced dermal toxicity in rabbit. *Experimental and Toxicologic Pathology*, 64(3), 181-186.

Kaya, A., Aydin, O., Demirtas, C., Akgün, M., 2007. An experimental study on the drying kinetics of quince. *Desalination*, 212(1–3), 328-343.

Koç, B., Eren, İ., Kaymak Ertekin, F., 2008. Modelling bulk density, porosity and shrinkage of quince during drying: The effect of drying method. Journal of Food Engineering, 85(3), 340-349.

Lampinen, M.J., Ojala, K.T., Koski, E., 1991. Modeling and measurements of infrared dryers for coated paper. *Drying Technology*, 9(4), 973-1017.

Liu, F., Cao, X., Wang, H., Liao, X., 2010. Changes of tomato powder qualities during storage. *Powder Technology*, 204(1), 159-166.

Maskan, M., 2001. Drying, shrinkage and rehydration characteristics of kiwifruits during hot air and microwave drying. J*ournal of Food Engineering*, 48(2), 177-182.

Nowak, D., Lewicki, P.P., 2004. Infrared drying of apple slices. *Innovative Food Science & Emerging Technologies*, 5(3), 353-360.

Pan, Z., Shih, C., McHugh, T.H., Hirschberg, E., 2008. Study of banana dehydration using sequential infrared radiation heating and freeze-drying. *LWT-Food Science and Technology*, 41(10), 1944-1951.

Ratti, C., Mujumdar, A., 1995. Infrared drying. Handbook of Industrial Drying, Ed. Mujumdar, A. S., Second edition, New York, NY, *Marcel Dekker* Inc., 1, 567-588.

Rizvi, S.S., 1986. Thermodynamic properties of foods in dehydration, Engineering properties of foods. CRC Press, pp. 239-251.

Sacilik, K., 2007. Effect of drying methods on thin-layer drying characteristics of hull-less seed pumpkin (*Cucurbita pepo* L.). *Journal of Food Engineering*, 79(1), 23-30.

Sakai, N., Hanzawa, T., 1994. Applications and advances in far-infrared heating in Japan. Trends in Food Science & Technology, (11), 357-362.

Sandu, C., 1986. Infrared radiative drying in food engineering: a process analysis. *Biotechnology Progress*,

2(3), 109-119.
Shiby, V., Mishra, H., 2007. Thin layer modelling of recirculatory convective air drying of curd (*Indian yoghurt*). *Food and Bioproducts Processing*, 85(3), 193-201.
Simal, S., Femenia, A., Garau, M., Rosselló, C., 2005. Use of exponential, Page's and diffusional models to simulate the drying kinetics of kiwi fruit. *Journal of Food Engineering*, 66(3), 323-328.
Therdthai, N., Zhou, W., 2009. Characterization of microwave vacuum drying and hot air drying of mint leaves (Mentha cordifolia Opiz ex Fresen). *Journal of Food Engineering*, 91(3), 482-489.
Vega, A., Fito, P., Andrés, A., Lemus, R., 2007. Mathematical modeling of hot-air drying kinetics of red bell pepper (var. *Lamuyo*). *Journal of Food Engineering*, 79(4), 1460-1466.
Wang, H.-c., Zhang, M., Adhikari, B., 2015. Drying of shiitake mushroom by combining freeze-drying and mid-infrared radiation. Food and Bioproducts Processing, 94, 507-517.
Zielinska, M., Markowski, M., 2007. Drying behavior of carrots dried in a spout–fluidized bed dryer. *Drying Technology*, 25(1), 261-270.

نشریه پژوهشهای علوم و صنایع غذایی ایران
جلد 12، شماره 6، بهمن - اسفند 1395، ص. 766-758

Iranian Food Science and Technology Research Journal
Vol. 12, No. 6, Feb. Mrch. 2017, p. 758-766

ارزیابی تجربی و مدل سازی انتقال جرم طی خشک کردن مادون قرمز به

محمدامین مهرنیا[1]- آیگین باشتی[2]- فخرالدین صالحی[3]

تاریخ دریافت: 1395/10/21
تاریخ پذیرش: 1396/02/18

چکیده

در این تحقیق بررسی تجربی و مدل سازی انتقال جرم در طی خشک کردن مادون قرمز به مورد مطالعه قرار گرفت. در بخش تجربی، اثرات شرایط مختلف خشک کردن مانند توان پرتودهی مادن قرمز (W 375-150) و فاصله منبع مادون قرمز (cm 15-5) بر روی ویژگی های خشک کردن به مورد ارزیابی قرار گرفت. هر دوی توان پرتودهی و فاصله بر روی زمان خشک کردن قطعات به تاثیر گذار بودند. نسبت های رطوبت بر روی 8 مدل ریاضی مختلف با استفاده از آنالیز رگرسیون غیر خطی برازانده شد. نتایج رگرسیون نشان داد که مدل رگرسیونی به شکل رضایت بخشی رفتار خشک کردن را توصیف می کند. ضریب انتشار رطوبت موثر با افزایش توان در دامنه 1/15 تا $3/72\times 10^{-8}$ m^2/s افزایش یافت. افزایش توان مادن قرمز اثر منفی بر روی ΔE اثر منفی داشته و با افزایش توان پرتو دهی مقدار آن کاهش یافت. مقادیر کروما و هیو به ترتیب در دامنه های 43/8 تا 46/99 و °80/82 تا °86/14 قرار داشت.

واژه های کلیدی: ضریب انتشار موثر، پردازش تصویر، خشک کن مادن قرمز، به

1-استادیار، گروه علوم و صنایع غذایی، واحد شوشتر، دانشگاه آزاد اسلامی، شوشتر، ایران
2- استادیار، گروه شیمی، واحد شوشتر، دانشگاه آزاد اسلامی، شوشتر، ایران
3- استادیار، گروه علوم و صنایع غذایی، دانشگاه بوعلی سینا، همدان، ایران
(*- نویسنده مسئول : Email: mamehrnia@yahoo.com)

Iranian Food Science and Technology Research Journal
Vol. 12, No. 6, Feb. Mrch. 2017, p. 767-779

نشریه پژوهشهای علوم و صنایع غذایی ایران
جلد 12، شماره 6، بهمن - اسفند 1395، ص. 779-767

Estimation of papaw (*Carica papaw* L.) moisture content using adaptive neuro-fuzzy inference system (ANFIS) and genetic algorithm-artificial neural network (GA-ANN)

A. R. Yousefi*

Received: 2017.02.10
Accepted: 2017.05.20

Abstract

Adaptive neuro-fuzzy inference system (ANFIS) and genetic algorithm-artificial neural network (GA-ANN) were used for modeling of the hot-air drying kinetics of papaw slices. The ANFIS and GA-ANN were fed with 3 inputs of drying time (0-320 min), drying temperature (40, 50 and 60 °C) and slice thickness (3, 5 and 7 mm) for prediction of moisture ratio (MR). The triangular membership functions (MFs) were applied and 27 rules were provided for the ANFIS designing. The developed ANFIS predictions were relatively similar to the experimental data (R^2 = 0.9967 and *RMSE* = 0.0161). The optimized GA-ANN, which included 7 hidden neurons, predicted the MR with a good precision (R^2 = 0.9936 and *RMSE* = 0.0220). The effective diffusivity for papaw slices was within the range of 6.93×10^{-10} to 1.50×10^{-9} m^2/s over the temperature range. The activation energy was found to be 32.5 kJ/mol indicating the effect of temperature on diffusivity.

Keywords: ANFIS; GA-ANN; Modeling; Papaw

Introduction

Papaw (*Carica papaw* L.), known as an important fruit crop is grown widely in tropical and subtropical regions. This fruit is nutrient and rich in vitamins A and C, and has good organoleptic characteristics as well (Fernandes *et al.*, 2006). According to the report of FAO, papaw has been ranked third with 11.2 million tons or 15.36 percent of the total tropical fruit production in 2010.

Water, as one of the major food components, has a decisive directly influence on the quality and durability of food materials via its impact on many physico-chemical and biological changes (Lenart, 1996). Drying due to the water removal or making water hard to access for microbe development is one of effective operations to reduce the spoilage of agricultural products (Izadifar and Mowla, 2003).

In characterizing the drying parameters, the thin-layer drying procedure was found to be the most feasible tool (Aghdam *et al.*, 2015; Yousefi *et al.*, 2013a). Several models have been used by several authors to estimate the moisture content/drying rate of materials which eventually led to different expression for the prediction of moisture content/drying rate (Yousefi *et al.*, 2013a; Yousefi *et al.*, 2013b). Most of these models are mathematical models which classified to theoretical, semi-theoretical and empirical ones (Demirtas *et al.*, 1998; Midilli *et al.*, 2002). Nowadays, researchers have asserted on the potential of artificial neural networks (ANNs) and adaptive neuro-fuzzy inference system (ANFIS). These techniques can be used as good substitutions for conventional modeling ones such as multiple regression analysis and response surface methodology. Artificial intelligent method has been developed and is extensively used for simulation of drying of agricultural and food materials (Tripathy and Kumar, 2009). Erenturk *et al.* (2004) studied the thin-layer drying of *Echinacea Angustifolia* root. According to their report, the comparison between the obtained R^2 and *RMSE* values for neural network and regression models revealed that neural network was better than the all mathematical models for predicting the moisture content of the samples. Bala *et al.*

Assistant Professor, Department of Chemical Engineering, University of Bonab, Bonab, Iran
(*- Corresponding Author Email: a_yousefi@bonabu.ac.ir)
DOI: 10.22067/ifstrj.v12i6.62521

(2005) modelled drying kinetic of jackfruit in a solar dryer using neural network model. It was reported that a suitable trained model could predict the drying process of jackfruit. Comparison of two modeling methods of mathematical and ANNs to estimate moisture content of papaya fruit slices during hot air drying has been studied (Yousefi *et al*., 2013a). The results showed that estimation of moisture content of papaya fruit could be better modeled by a neural network (R^2 = 0.9994 and *RMSE* = 0.0070) than by the mathematical models (R^2 = 0.9974 and *RMSE* = 0.0123). Prakash and Kumar (2014) generated an ANFIS model to predict the jaggery temperature, the greenhouse air temperature and the moisture evaporation for drying of jaggery inside the greenhouse for natural convection mode. Their results demonstrated that the analytical and experimental results for jaggery drying are in good agreement (R^2 = 0.999-1.00). Tao *et al.* (2016) utilize an ANFIS model to estimate the physicochemical and microbiological parameters of partially dried cherry tomatoes during storage. For all the ANFIS models used, the R^2 values were higher than 0.86 and showed better performance for prediction.

Based on the literature review, no research study has been done on modeling of hot-air drying of papaw using ANFIS and genetic algorithm-artificial neural network (GA-ANN). Therefore, the purpose of this work was to investigate the thin-layer drying process of papaw slices during hot-air drying and modeling of the experimental data using ANFIS and GA-ANN to estimate the moisture content of papaw fruit.

Material and methods

Experimental Study

Papaw fruits were purchased from a local market in the Bahookalat region (Sistan & Baluchestan province, Iran) and stored in a refrigerator at 4 ± 1 °C before they were subjected to the drying process. The fruits were washed, peeled and cut into 3, 5 and 7 mm thick slices. A cabinet dryer (Model JE10 TECH, F-02G, South Korea) with controllable airflow, temperature and air humidity monitoring systems was used for the hot air drying process. The absolute humidity and the hot-air flow ratio for all drying temperatures were 0.6 ± 0.02 g kg^{-1} dry air and 1± 0.1 ms^{-1}, respectively. The initial moisture content was measured using a laboratory oven dryer (Galenkamp, UK) operated at 105 °C. Initial moisture content of the slices was 84.48% ± 0.05% (w. b.). The weight of the samples was recorded by programmable balance software at 5-min intervals until the moisture of the samples reached 5 ± 0.02% (w. b.) in the final product. Drying was carried out at three temperature levels (40, 50 and 60 °C). Moisture ratio (MR) variations with time were plotted for various conditions. MR is defined by the equation (1):

$$MR = \frac{M - M_e}{M_0 - M_e} \qquad (1)$$

Where M is the moisture content of the samples at any drying time and M_0 is the initial moisture content. The moisture ratio equation was simplified to M/M_0 as value of M_e (equilibrium moisture content) is relatively small compared with that of M or M_0 (Akgun and Doymaz, 2005).

ANFIS model

Fuzzy inference systems (FISs) and ANNs can be combined into an integrated system named ANFIS; the integrated system has the advantages of both ANNs (e.g., learning abilities, optimization abilities, and connectionist structure) and FISs (e.g., human like if–then rules, and ease of incorporating expert knowledge available in linguistic terms) (Yolmeh *et al.*, 2014).

In ANFIS technique, the neural network learning functions are used for refining each part of the fuzzy knowledge separately. One method for the derivation of a fuzzy rule base is to use the self learning features of artificial neural networks, to define the membership function (MF) based on input– output data. In this study, a hybrid training method (the combination of least-squares and back propagation algorithms) was applied as the training method of the ANFIS.

ANFIS modeling was launched by providing a data set of input-output data points. The data order was the first randomized and then all data were divided into three partitions: 60, 10 and 30% of total data were used for training, validating and testing the network, respectively. Each input-output pair contained three inputs (drying time, drying temperature and thickness) and one output (moisture ratio). It should be noted that the number of MFs applied for each input variable was chosen by trial and errors. The results were obtained using ANFIS toolbox of MATLAB 8.1 (reference the software provider).

GA-ANN model

In brief, the artificial neural network (ANN) is a renowned tool for solving complex, non-linear biological systems and it can give logical results even in complicated cases or in the event of technological faults (Yousefi *et al*., 2013a). The most popular ANN is the back-propagation feed forward type, whose architecture is based on an input layer comprising all the input variables that feed the network, an output layer which comprises the response of ANN to the desired problem, and hidden layers which are placed between the two layers. The number of input neurons corresponds to the number of input variables into the neural network, and the number of output neurons is the same as the number of target output variables. The number of neurons in the hidden layer depends on the application of the network (Liu and Baughman, 1995). The optimum number of neurons in hidden layer is usually performed by trial and error method. The number of neurons which are respectively placed in the input, hidden and output layers, named topology. The performance of an ANN network is strongly affected by the topology used.

Genetic algorithm (GA) is an optimization technique which can be used for training ANN to overcome inherent limitations of back-propagation (BP). Genetic algorithm can be used in two different ways for training neural networks: (a) Weights optimization and (b) structure and topology optimization (Irani and Nasimi, 2011). The methodology utilized in this work was a hybrid genetic algorithm–neural network strategy. In learning process, weights and biases of neural network were optimized.

The hyperbolic tangent activation functions f (x) (Eq. (2)) were used as the transfer function in the hidden and output layers, because lower normalized mean square error values were obtained for that comparing to sigmoid activation and linear functions.

$$f(x)=\frac{e^{x}-e^{-x}}{e^{x}+e^{-x}} \qquad (2)$$

The output neurons of the hidden and last layers are calculated by Eqs. (3) and (4) as follows:

$$X_j = f(\sum_{i=1}^{n} x_i w_{ji} + w_{j0}) \qquad (3)$$

$$\hat{\psi}_{nl} = f(\sum_{j=1}^{n} X_j w_{kj} + w_{k0}) \qquad (4)$$

where x_i is a variable input, w_{ji} is connection weight between hidden and input neurons, w_{kj} is connection weight between output and hidden neurons, w_{j0} and w_{k0} are biases for the j^{th} and k^{th} neuron, respectively, i is the number of neurons for input and j is the number of neurons for the hidden layer, and k is the number of output neurons. Output of the network, $\hat{\psi}_{nl}$, was compared with the desired output, ψ_{nl}, in the training phase (training by GA), and the error in the form of mean square error (MSE) was calculated for all data. The MSE was obtained from the following equation:

$$MSE=\frac{1}{h}\sum_{p=1}^{h}[(\psi_{nl})_p-(\hat{\psi}_{nl})_p]^{0.5} \qquad (5)$$

Where h is the number of data in the training phase. The goal was to reduce the amount of errors.

In this work, the collected data from the experiments were randomly divided into three partitions consisting training (60%), validation

(10%) and test (30%). To estimate the performance of the trained network, the testing data were compared with the data obtained by the network. The probabilities of the crossover and mutation operators were adjusted at 0.9 and 0.01, respectively.

Besides, a sensitivity analysis was carried out to provide a measure of the relative importance among the inputs of the neural network model and to indicate how the model output varied in response to variation of an input (Bahramparvar *et al.*, 2014). In this research, the NeuroSolution software (version 5.0, NeuroDimension, Inc., USA) was used to design the GA-ANN model.

Results and discussion

The amounts of MR of papaw slices obtained at different drying times for the three thicknesses and three temperatures experimented are depicted in Fig. 1 and Fig. 2, respectively.

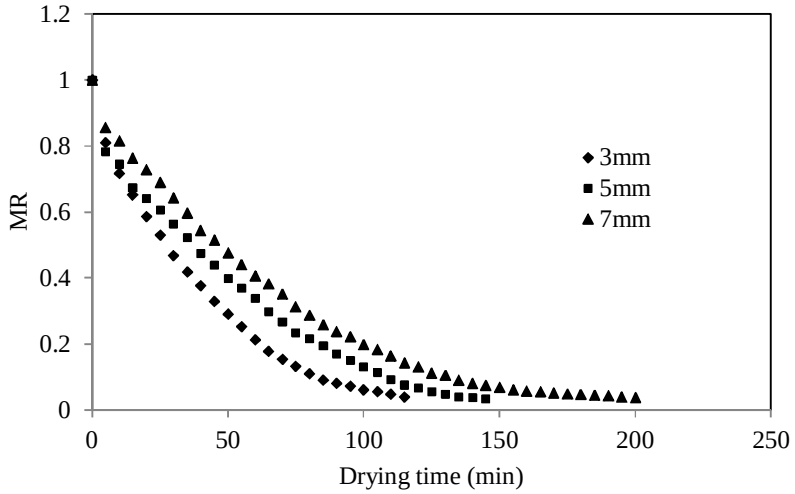

Fig. 1. The influence of papaw slices thickness on moisture ratio (MR) at 60 ˚C.

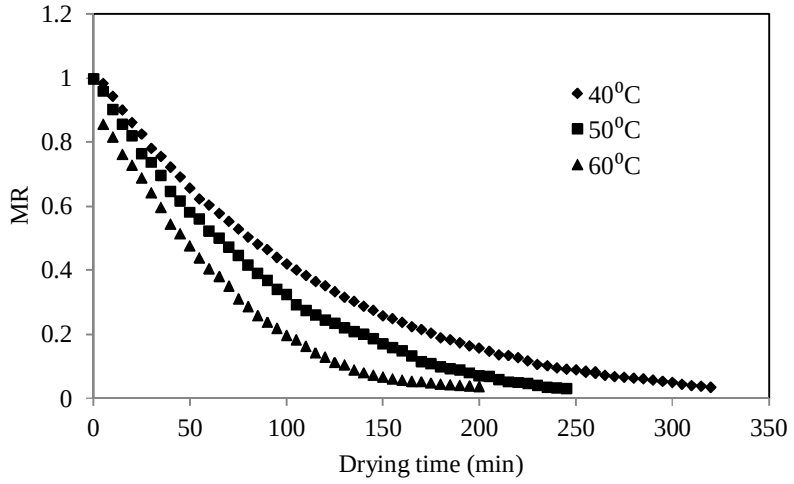

Fig. 2. The influence of drying temperatures on moisture ratio (MR) for the slices with thickness of 7 mm.

As it can be seen, the drying duration at drying temperature of 60 ℃ was increased (from 115 to 200 min) with increasing thickness from 3 to 7 mm. Similar results have been reported for sweet potato (Diamante and Munro, 1991) and tomato slices (Sadin *et al.*,

2014).The air temperature also had a direct effect on drying rate. As the air temperature increased from 40 to 60 °C for the slices with 7 mm, the drying duration was reduced (from 320 to 200 min). The results of statistical analysis by factorial test proved that drying time (5, 50, 100 and 150 min), temperature (40, 50 and 60 °C) and slices thickness (3, 5 and 7mm) selected in this study had significant effects on moisture content ($p < 0.05$). At higher temperatures, due to the quick removal of moisture, the drying process occurred in a shorter period. The decrease in drying time with increase in drying temperature may be due to increase in water vapor pressure within the papaw slices, which enhances the migration of moisture. Similar observation was reported for apple purees (Vergara *et al*., 1997). The moisture ratio of papaw reduced exponentially as the drying time increased. Continuous decrease in moisture ratio indicates that diffusion governed the internal mass transfer (Haghi and Amanifard, 2008).

ANFIS

The ANFIS network parameters such as the type and number of MF and epochs, have been changed to obtain the best results in terms of model validation. Fig. 3 shows the ANFIS architecture used in the study. The final ANFIS architecture for estimating the MR, with three triangular type MFs for each input (3 inputs) and linear MF for output, and constructed 27 rules resulted high accurate estimation.

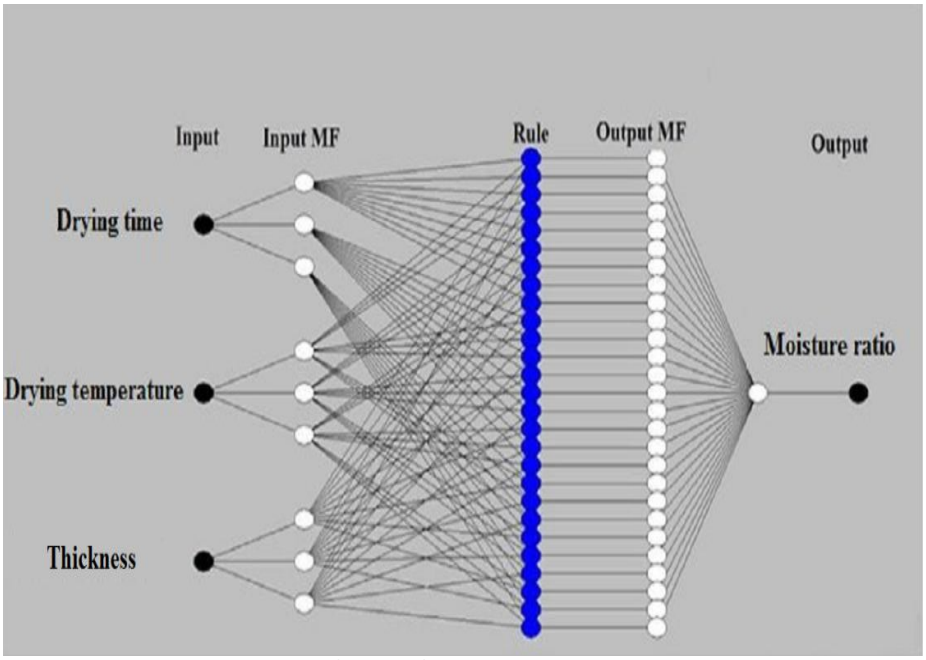

Fig. 3. The general structure of ANFIS for moisture ratio (MR) model with 3 inputs.

As it can be seen in Fig. 4(a), the network is trained well, because the output data are completely near to the train ones and also the training error is low (0.0053) (Fig. 4(b)). Moreover, it was observed that the number of epochs had not a significant influence on the error calculated. Fig. 5 shows the experimental MR values against ANFIS predictions for test data (unseen data) points. As it can be seen, the system was completely efficient to estimate the values of MR obtained in all conditions experimented (R^2 = 0.9967 and *RMSE* = 0.0161).

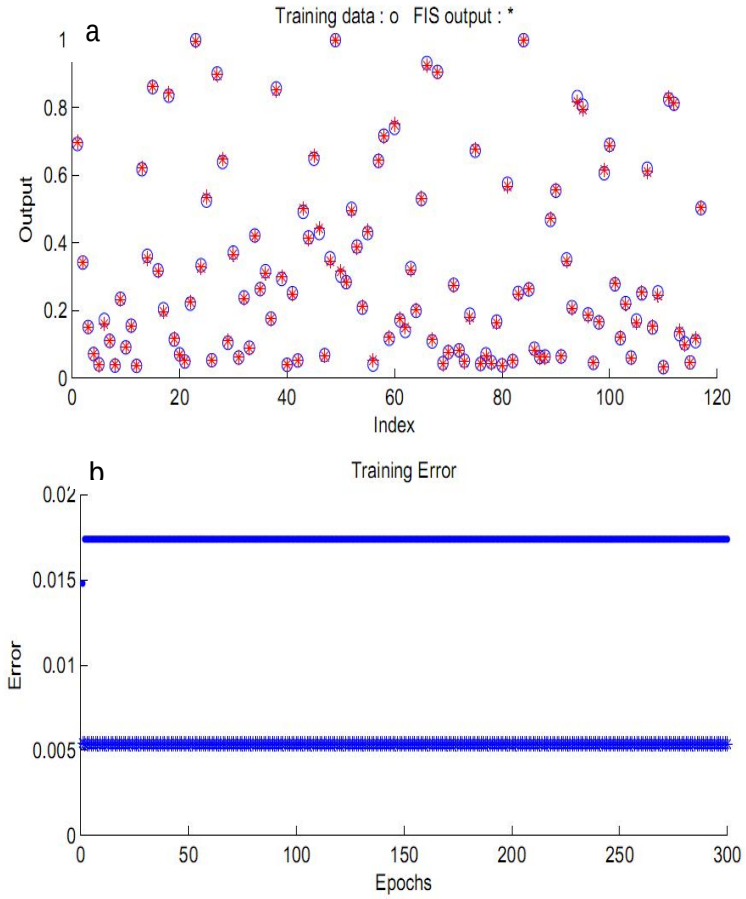

Fig. 4. (a) Comparison of training data with the output of developed FIS, (b) effect of the number of epochs on error obtained for trained network

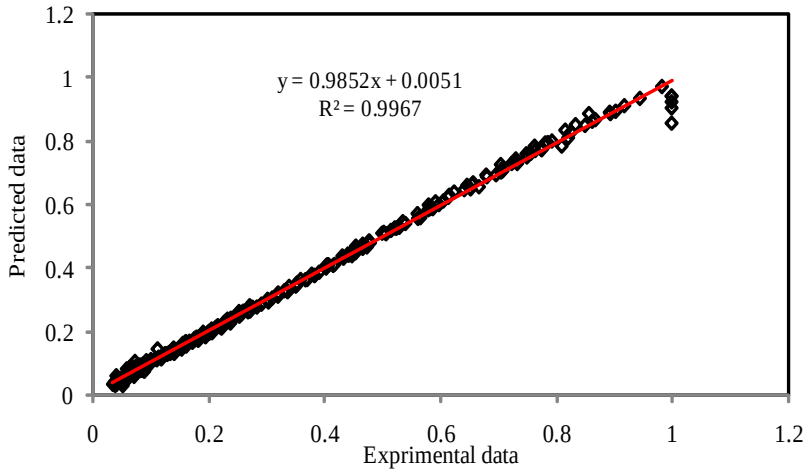

Fig. 5. Experimental against predicted values of MR by ANFIS model for the test data set (R^2 = 0.9967 and *RMSE* = 0.0161).

Figure 6 indicates two three-dimensional surfaces obtained after running the ANFIS model developed. As a result, the data show that decrease in slice thickness and increase in drying temperature both diminish the moisture content with increasing drying time. Ziaforoughi *et al.* (2016) reported similar results in the case of the effect of drying time and temperature using ANFIS model for infrared drying of quince slices. Yuzgec et al. (2009) developed an ANFIS model for fluidized bed drying to model Baker's yeast production to predict the yield of dry product and product temperature. It was found that the overall performance of ANFIS model was better than the three other conventional modeling tools (R^2 = 0.815-0.985). Al-Mahasneh *et al.* (2016) applied ANFIS in comparison with conventional thin-layer drying models to estimate moisture ratio in open sun drying of roasted green wheat. ANFIS represented higher performance in comparison with two-term exponential mode with RMSE = 1.2×10^{-6} and R^2 = 0.999 and *RMSE* = 0.038 and R^2= 0.988, respectively.

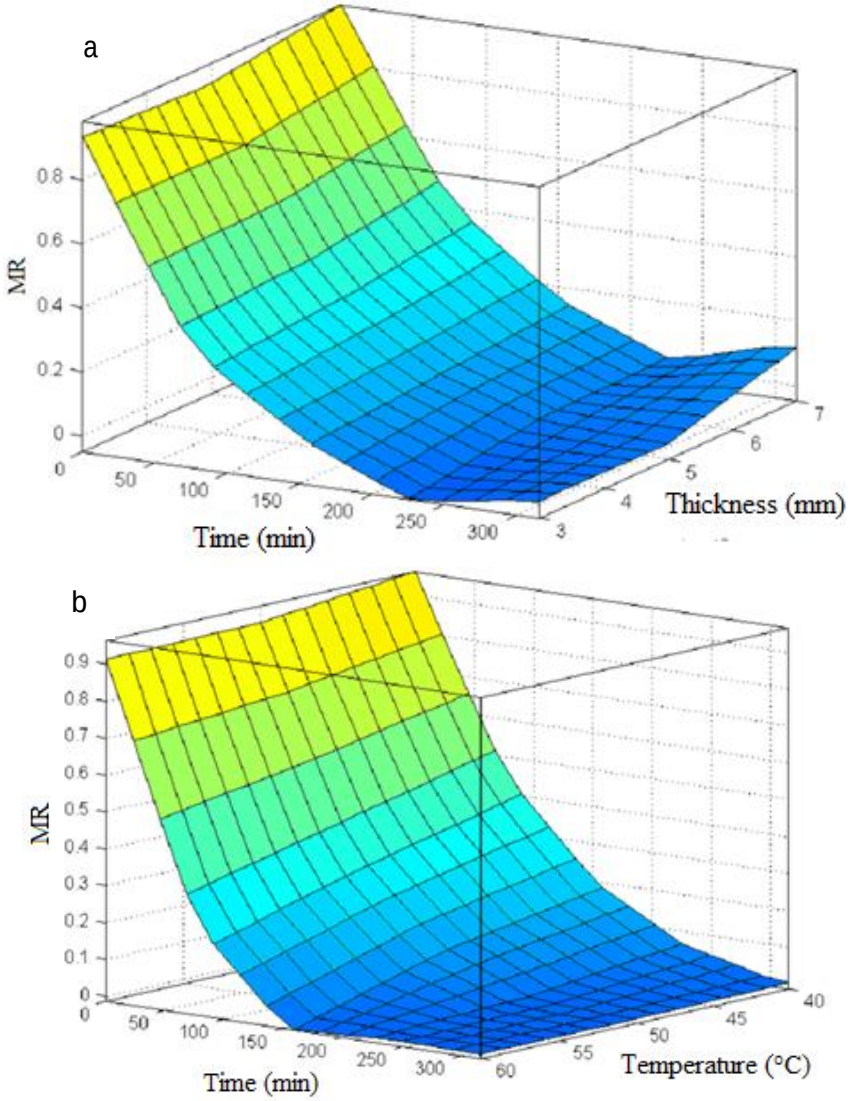

Fig. 6. Three-dimensional surface for the ANFIS model using two input variables of (a) time and thickness, (b) time and temperature.

GA-ANN model

GA-ANN model was developed for estimation of the moisture content obtained during hot-air drying of papaw slices in the cabinet dryer. To find the optimal network configuration, the number of neurons in hidden layer of ANN structure was changed by GA. The results revealed that GA-ANN model with 7 neurons in one hidden layer (topology of 3-7-1) could precisely estimate the amount of moisture content for the drying process of thin-layer papaw slices (R^2 = 0.9936 and *RMSE* = 0.0220). The experimental data *vs.* predicted data by the best GA-ANN models are shown in Fig. 7.

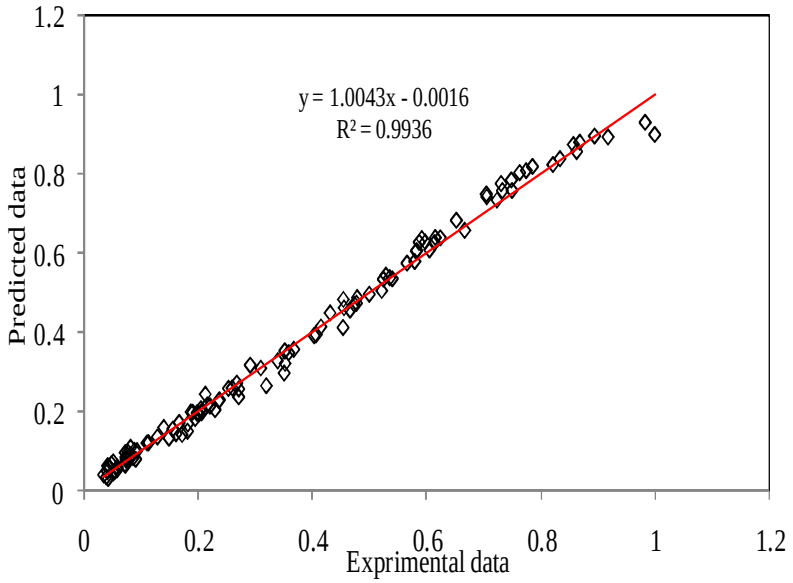

Fig. 7. Experimental against predicted values of MR by GA-ANN model for the test data set (R^2 = 0.9936 and *RMSE* = 0.0220).

It can be seen from Fig. 7 that the predicted data are highly similar to the experimental ones, indicating high efficiency of GA-ANN models used in prediction. Table 1 shows the weights and bias extents of the best GA-ANN models used, which could be applied in a computer program for prediction of the amount of moisture content during the drying process.

It can be observed that among the selected inputs, thickness was the most sensitive factor for estimation of the MR of papaw slices, followed by drying temperature and time. It means that the amount of moisture content for the papaw slices during hot-air drying were remarkably affected by thickness than the other studied favtors. Based on the literature review, the GA-ANNs had been a precise and appropriate instrument for modeling of drying process of banana (Mohebbi *et al.*, 2011), kiwifruit (Fathi *et al.*, 2011) and button mushroom (Salehi *et al.*, 2017) slices. Yolmeh *et al.* (2014) developed ANFIS and GA-ANN models to model the influence of annatto dye on *Salmonella enteritidis* population in mayonnaise using three inputs (annatto dye concentration at 0, 0.1, 0.2 and 0.4 %, storage time of 1–20 days and storage temperatures at 4 and 25 °C). Their results showed that both ANFIS and GA-AN N were able to predict *S.enteritidis* population with high accuracy of 0.998 and 0.999, respectively. The high performance of GA-ANN based model even reported in the case of prediction of amount of glucose release during *in vitro* gastrointestinal digestion of native and chemically modified starches (r = 0.984-0.993 and *RMSE* = 0.338-0.588) (Yousefi and Razavi, 2017)

Table 1. The bias and weights values for the optimized GA-ANN models obtained

Hidden neurons	Bias	Input neurons			Output neurons
		Time	Temperature	Thickness	Moisture ratio (MR)
1	0.942	0.680	-0.177	0.110	-0.266
2	0.358	0.011	0.135	1.158	0.597
3	-0.801	0.082	-2.647	0.069	0.429
4	-2.464	-1.511	0.064	-0.011	0.876
5	-0.140	-0.716	-0.002	0.448	0.002
6	1.145	0.341	-0.062	0.274	-0.442
7	-0.211	-1.068	0.239	-0.106	-0.177
Bias					0.437

In addition, in this study to find the sensitiveness of GA-ANN models used toward the selected inputs, sensitivity analysis was performed (Fig. 8). The sensitivity analysis demonstrates that which of the inputs has the greatest influence on the output and has more control on the amount of output.

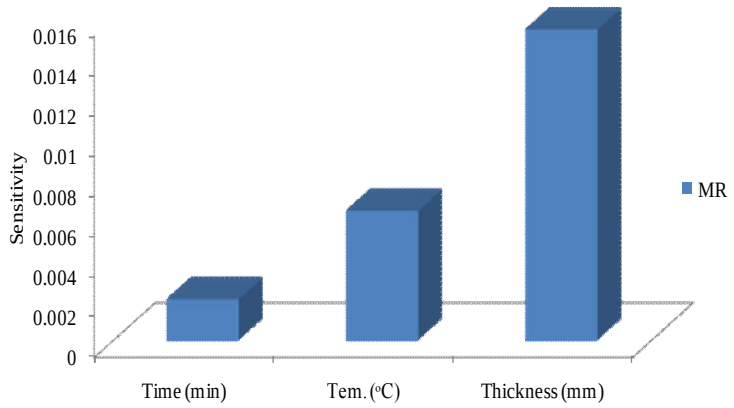

Fig. 8. The sensitivity of moisture ratio (MR) to the input variables.

Estimation of effective diffusivity coefficient

It is reported that the drying characteristics of biological products in falling rate period can be described by using Fick's second law of diffusion (Falade and Solademi, 2010). Crank (1975) solved this equation and introduced the Eq. (6), which can be used for slab geometry with uniform initial moisture diffusion, constant diffusivity and insignificant shrinkage:

$$MR = \frac{8}{\pi^2}\sum_{n=0}^{\infty}\frac{1}{(2n+1)^2}\exp\left(-\frac{(2n+1)^2\pi^2 D_{eff}t}{4L^2}\right) \quad (6)$$

In this equation, D_{eff} is the effective diffusivity (m^2/s); n is positive integer, t is drying time, and L is the half thickness of the slab in samples (m). In practice, only the first term in Eq. (6) is used yielding:

$$MR = \frac{8}{\pi^2}\exp\left(-\frac{\pi^2 D_{eff}t}{4L^2}\right) \quad (7)$$

Therefore, D_{eff} can be calculated from the slope of Eq. (7) using natural logarithm plot of MR versus drying time.

The calculated D_{eff} values for different drying temperatures are shown in Fig. 9. D_{eff} value for papaw slices increased with air temperature. This value for papaw slices was within the range of 6.93×10^{-10} to 1.50×10^{-9} m^2/s over the temperature range. It has been reported that the D_{eff} value for food materials is within the range of 10^{-11} to 10^{-9} (Sadin et al., 2014). The results obtained were in agreement with the results of other studies (Doymaz, 2007; Kaleemullah and Kailappan, 2005; Sacilik *et al.*, 2006).

The effective moisture diffusivity represents overall mass transport of moisture

in the material, including liquid diffusion, vapor diffusion, or any other possible mass transfer mechanism (Afzal and Abe, 1998).

Estimation of activation energy

The dependence of D_{eff} to temperature can be explained using the Arrhenius-type relationship (Simal et al., 1996). This matter is shown in the following equation:

$$D_{eff} = D_0 \exp\left(-\frac{E_a}{R(T+273.15)}\right) \quad (8)$$

In this equation, D_0 is the pre-exponential factor of Arrhenius equation (m^2s^{-1}), E_a is the activation energy (kJ/mol), T is the drying temperature (°C) and R is the gas constant (kJ/(mol.K)).

The E_a can be calculated from the slope of the plot on ln (*Deff*) vs. 1/ (T+273.15) (Fig. 10). This value was 32.5 (kJ/mol) for papaw slices. This value was lower than the E_a of green peppers drying (51.4 kJ/ mol) (Kaymak-Ertekin, 2002), mint drying (82.93 kJ/mol) (Park et al., 2002), but was higher than that of red chillies drying (24.47 kJ/ mol) (Kaleemullah and Kailappan, 2005).

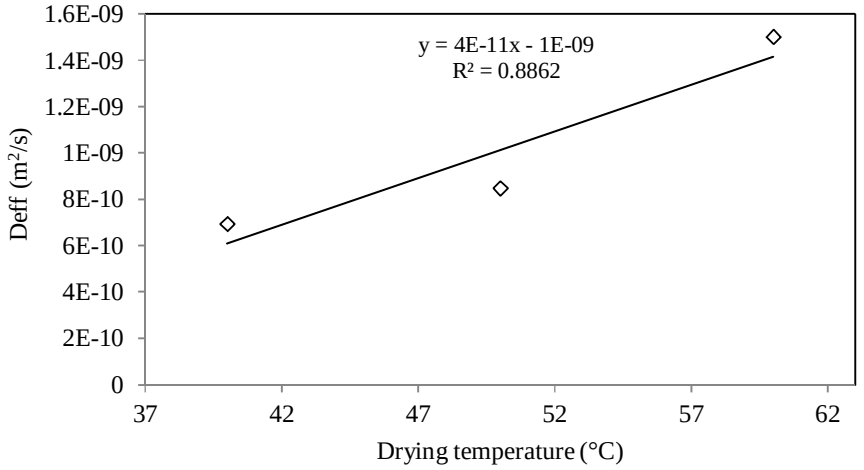

Fig. 9. Effect of drying temperature on the effective moisture diffusivity in papaw slices.

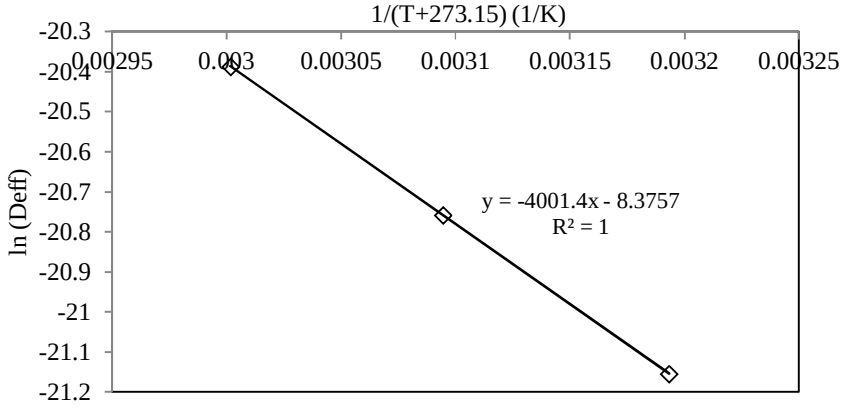

Fig. 10. Effect of drying temperature on the effective moisture diffusivity for calculation of activation energy.

Conclusions

The proficiency of ANFIS and GA-ANN modeling techniques for estimation of moisture content of papaw slices (3, 5 and 7 mm) during hot-air drying (40, 50 and 60 °C) was investigated. Accordingly, the results demonstrated that ANFIS model with three triangular type MFs (trimf) for all input variables (drying time, drying temperature, slice thickness) and linear for output (moisture ratio) gives the best fitting with the experimental data, which made it possible to predict the MR with high precision (R^2 = 0.9967 and *RMSE* = 0.0161). In addition, it was found that GA-ANN technique with 1 hidden layer including 7 neurons (topology of 3-7-1), predicts the nearest data to the experimental data (R^2 = 0.9936 and *RMSE* = 0.0220). More sensitivity of MR to slice thickness observed in this study demonstrates that this factor plays more significant role in hot-air drying process of papaw.

References

Afzal, T., Abe, T. 1998. Diffusion in potato during far infrared radiation drying. *Journal of food engineering*. 37, 353-365.

Aghdam, S., Yousefi, A., Mohebbi, M., Razavi, S., Orooji, A., Akbarzadeh-Totonchi, M. 2015. Modeling for drying kinetics of papaya fruit using fuzzy logic table look-up scheme. *International Food Research Journal*. 22.

Akgun, N.A., Doymaz, I. 2005. Modelling of olive cake thin-layer drying process. *Journal of Food Engineering*. 68, 455-461.

Al-Mahasneh, M., Aljarrah, M., Rababah, T., Alu'datt, M. 2016. Application of Hybrid Neural Fuzzy System (ANFIS) in Food Processing and Technology. *Food Engineering Reviews*. 8, 351-366.

Bahramparvar, M., Salehi, F., Razavi, S. 2014. Predicting total acceptance of ice cream using artificial neural network. *Journal of Food Processing and Preservation*. 38, 1080-1088.

Bala, B., Ashraf, M., Uddin, M., Janjai, S. 2005. Experimental and neural network prediction of the performance of a solar tunnel drier for drying jackfruit bulbs and leather. *Journal of Food Process Engineering*. 28, 552-566.

Crank, J. 1975. The Mathematics of Diffusion: 2d Ed. Clarendon Press.

Demirtas, C., Ayhan, T., Kaygusuz, K. 1998. Drying behaviour of hazelnuts. *Jo*urnal of the Science of Food *and Agriculture*. 76, 559-564.

Diamante, L., Munro, P. 1991. Mathematical modelling of hot air drying of sweet potato slices. *International journal of food science & technology*. 26, 99-109.

Doymaz, I. 2007. The kinetics of forced convective air-drying of pumpkin slices. *Journal of food engineering*. 79, 243-248.

Erenturk, K., Erenturk, S., Tabil, L.G. 2004. A comparative study for the estimation of dynamical drying behavior of Echinacea angustifolia: regression analysis and neural network. *Computers and Electronics in Agriculture*. 45, 71-90.

Falade, K.O., Solademi, O.J. 2010. Modelling of air drying of fresh and blanched sweet potato slices. *International journal of food science & technology*. 45, 278-288.

Fathi, M., Mohebbi, M., Razavi, S.M. 2011. Effect of osmotic dehydration and air drying on physicochemical properties of dried kiwifruit and modeling of dehydration process using neural network and genetic algorithm. *Food and bioprocess technology*. 4, 1519-1526.

Fernandes, F.A., Rodrigues, S., Gaspareto, O.C., Oliveira, E.L. 2006. Optimization of osmotic dehydration of papaya followed by air-drying. *Food Research International*. 39, 492-498.

Haghi, A., Amanifard, N. 2008. Analysis of heat and mass transfer during microwave drying of food products. *Brazilian Journal of Chemical Engineering*. 25, 491-501.

Irani, R., Nasimi, R. 2011. Evolving neural network using real coded genetic algorithm for permeability estimation of the reservoir. *Expert Systems with Applications*. 38, 9862-9866.

Izadifar, M., Mowla, D. 2003. Simulation of a cross-flow continuous fluidized bed dryer for paddy rice. *Journal of Food Engineering*. 58, 325-329.

Kaleemullah, S., Kailappan, R. 2005. Drying kinetics of red chillies in a rotary dryer. *Biosystems*

Engineering. 92, 15-23.
Kaymak-Ertekin, F. 2002. Drying and rehydrating kinetics of green and red peppers. *Journal of Food Science*. 67, 168-175.
Lenart, A. 1996. Osmo-convective drying of fruits and vegetables: technology and application. *Drying technology*. 14, 391-413.
Liu, Y.A., Baughman, D.R. 1995. Neural Networks in Bioprocessing and Chemical Engineering. *Academic Press*, Inc., San Diego.
Midilli, A., Kucuk, H., Yapar, Z. 2002. A new model for single-layer drying. *Drying technology*. 20, 1503-1513.
Mohebbi, M., Shahidi, F., Fathi, M., Ehtiati, A., Noshad, M. 2011. Prediction of moisture content in pre-osmosed and ultrasounded dried banana using genetic algorithm and neural network. *Food and Bioproducts Processing*. 89, 362-366.
Park, K.J., Vohnikova, Z., Brod, F.P.R. 2002. Evaluation of drying parameters and desorption isotherms of garden mint leaves (*Mentha crispa* L.). *Journal of Food Engineering*. 51, 193-199.
Prakash, O., Kumar, A. 2014. ANFIS modelling of a natural convection greenhouse drying system for jaggery: an experimental validation. *International Journal of Sustainable Energy*. 33, 316-335.
Sacilik, K., Keskin, R., Elicin, A.K. 2006. Mathematical modelling of solar tunnel drying of thin layer organic tomato. *Journal of food Engineering*. 73, 231-238.
Sadin, R., Chegini, G.-R., Sadin, H. 2014. The effect of temperature and slice thickness on drying kinetics tomato in the infrared dryer. *Heat and Mass Transfer*. 50, 501-507.
Salehi, F., Kashaninejad, M., Mahoonak, A., Ziaiifar, A. 2017. Drying of Button Mushroom by Infrared-Hot Air System. I*ranian Jounal of Food Science and Technology*. 13, 151-159.
Simal, S., Mulet, A., Tarrazo, J., Rosselló, C. 1996. Drying models for green peas. *Food Chemistry*. 55, 121-128.
Tao, Y., Li, Y., Zhou, R., Chu, D.-T., Su, L., Han, Y., Zhou, J. 2016. Neuro-fuzzy modeling to predict physicochemical and microbiological parameters of partially dried cherry tomato during storage: effects on water activity, temperature and storage time. *Journal of food science and technology*. 53, 3685-3694.
Tripathy, P., Kumar, S. 2009. Neural network approach for food temperature prediction during solar drying. I*nternational Journal of Thermal Sciences*. 48, 1452-1459.
Vergara, F., Amezaga, E., Barcenas, M., Welti, J. 1997. Analysis of the drying processes of osmotically dehydrated apple using the characteristic curve model. *Drying Technology*. 15, 949-963.
Yolmeh, M., Najafi, M.B.H., Salehi, F. 2014. Genetic algorithm-artificial neural network and adaptive neuro-fuzzy inference system modeling of antibacterial activity of annatto dye on Salmonella enteritidis. *Microbial pathogenesis*. 67, 36-40.
Yousefi, A., Asadi, V., Nassiri, S.M., Niakousari, M., Aghdam, S.K. 2013a. Comparison of mathematical and neural network models in the estimation of papaya fruit moisture content. T*he Philippine Agricultural Scientist*. 95.
Yousefi, A., Niakousari, M., Moradi, M. 2013b. Microwave assisted hot air drying of papaya (*Carica papaya* L.) pretreated in osmotic solution. *African Journal of Agricultural Research*. 8, 3229-3235.
Yousefi, A., Razavi, S.M. 2017. Modeling of glucose release from native and modified wheat starch gels during in vitro gastrointestinal digestion using artificial intelligence methods. *International Journal of Biological Macromolecules*. 97, 752-760.
Yuzgec, U., Becerikli, Y., Turker, M. 2009. Comparison of different modeling concepts for drying process of baker's yeast. IEEE T*ransactions on Neural Networks*. 19, 1231-1242.
Ziaforoughi, A., Yousefi, A.R., Razavi, S. 2016. A Comparative Modeling Study of Quince Infrared Drying and Evaluation of Quality Parameters. *International Journal of Food Engineering*. 12, 901-910.

نشریه پژوهشهای علوم و صنایع غذایی ایران
جلد 12، شماره 6، بهمن - اسفند 1395، ص. 779-767

Iranian Food Science and Technology Research Journal
Vol. 12, No. 6, Feb. Mrch. 2017, p. 767-779

تخمین میزان محتوای رطوبتی میوه پاپایا با استفاده از سیستم تلفیقی عصبی-فازی و الگوریتم ژنتیک-شبکه عصبی

علیرضا یوسفی*

تاریخ دریافت: 1395/11/22
تاریخ پذیرش: 1396/02/30

چکیده

در این تحقیق از سیستم تلفیقی عصبی-فازی (ANFIS) و الگوریتم ژنتیک-شبکه عصبی (GA-ANN) برای مدلسازی سینتیک خشک شدن ورقه‌های پاپایا به وسیله هوای داغ استفاده گردید. ورودی های سیستم مدلسازی شامل سه ورودی زمان خشک شدن (320-0 دقیقه)، دمای خشک شدن (40، 50 و 60 درجه سانتیگراد) و ضخامت ورقه‌ها (3، 5 و 7 میلی متر) و خروجی سیستم شامل نسبت رطوبتی (MR) بود. در طراحی سیستم مدلسازی ANFIS از توابع عضویت مثلثی و 27 قانون استفاده گردید. نتایج نشان داد که داده های پیش بینی شده توسط سیستم ANFIS دارای تطبیق بالایی با نتایج آزمایشگاهی بود (R^2= 0.9967, RMSE= 0.0161). همچنین سیستم مدلسازی GA-ANN بهینه شده، شامل 7 نرون در لایه مخفی، با دقت بالایی میزان رطوبت را پیش‌بینی نمود (R^2= 0.9936, RMSE= 0.0220). ضریب انتشار موثر ورقه‌های پاپایا در بازه دمایی مورد آزمایش بین $10^{-10}\times$ 6.93 و $10^{-09}\times$ 1.50 مترمربع بر ثانیه تعیین شد. همچنین مقدار بدست آمده برای انرژی فعالسازی (32.5 کیلوژول بر مول) به خوبی تاثیر دمای خشک کردن بر روی ضریب انتشار را نشان داد.

واژه های کلیدی: سیستم تلفیقی عصبی-فازی، الگوریتم ژنتیک-شبکه عصبی، پاپایا

1- استادیار، گروه مهندسی شیمی، دانشکده فنی و مهندسی دانشگاه بناب، بناب، ایران
(*- نویسنده مسئول : Email: a_yousefi@bonabu.ac.ir)

مندرجات

نشریه پژوهش های علوم و صنایع غذایی ایران

با شماره پروانه 124/847 و درجه علمی – پژوهشی شماره 3/11/810 88/5/10 از وزارت علوم، تحقیقات و فناوری

جلد 12 شماره 6 بهمن- اسفند 1395

درجه علمی- پژوهشی این نشریه طی نامه 3/11/47673 90/4/14 از وزارت علوم، تحقیقات و فناوری تا سال 1393 تمدید شده است.

ناشر:گروه علوم و صنایع غذایی دانشکده کشاورزی، دانشگاه فردوسی مشهد **چاپ:** مؤسسه چاپ و انتشارات دانشگاه فردوسی مشـهد

شمارگان: 250 نسخه **قیمت**: 5000 ریال (دانشجویان 2500 ریال)

نشانی: مشهد- کد پستی 91775 صندوق پستی 1163

دانشگاه فردوسی مشهد، دانشکده کشاورزی - گروه علوم وصنایع غذایی - دفتر نشریه پژوهش های علوم وصنایع غذایی ایران.

تلفن: 20-8795618 داخلی 321 نمابر: 8787430

این نشریه درپایگاههای زیر نمایه شده است:

پایگاه استنادی علوم ایران(ISC)، پایگاه اطلاعات علمی جهاد دانشگاهی(SID)، بانک اطلاعات نشریات کشور (MAGIRAN)

پست الکترونیکی: ifstrj@um.ac.ir

این نشریه در سایت http://jm.um.ac.ir/index.php/food_tech/index به صورت مقاله کامل نمایه شده است.

نشریه علمی - پژوهشی

پژوهشهای علوم و صنایع غذایی ایران

جلد۱۲ شماره ۶

سال ۱۳۹۵

(شماره پیاپی: ۴۲)

شاپا: ۴۱۶۱-۱۷۳۵

عنوان مقالات

نشریه علمی- پژوهشی پژوهشهای علوم و صنایع غذایی ایران جلد ۱۲ شماره ۶ سال ۱۳۹۶ 2017 Vol.12 No.6 Iranian Food Science and Technology Research Journal